ROLE OF ATM AND ATR KINASES IN REGULATING GENE EXPRESSION AND CELLULAR SURVIVAL AFTER GENOTOXIC STRESS

by

Sujatha Kumar

A dissertation submitted in partial fulfillment of

the requirements for the degree of

Doctor of Philosophy

(Molecular and Cellular Pharmacology)

at the

UNIVERSITY OF WISCONSIN-MADISON

2006

ROLE OF ATM AND ATR KINASES IN REGULATING GENE EXPRESSION AND CELLULAR SURVIVAL AFTER GENOTOXIC STRESS

Sujatha Kumar

Under the supervision of Assistant Professor Randal S. Tibbetts

at the University of Wisconsin-Madison

ATM (Ataxia-telangiectasia mutated) and ATR (ATM and Rad-3 related) are structurally homologous, functionally non-redundant large molecular weight nuclear protein kinases that belong to the PIKK gene superfamily. ATM/ATR have been implicated as critical regulators of cellular responses to genotoxic stress including the coordination of cell cycle checkpoints, DNA repair, gene expression and induction of apoptosis. Although ATM/ATR-dependent pathways that regulate activation of cell cycle checkpoints are well understood, the identities of the relevant factors that mediate ATM/ATR-dependent changes in gene expression and cell survival remain largely undetermined. We delineated a novel stress-induced signal transduction pathway directly linking ATM to the Ca^{2+}/cAMP response element-binding protein, CREB, a transcription factor that regulates cell growth, homeostasis, and survival. ATM phosphorylated CREB *in vitro* and *in vivo* in response to ionizing radiation (IR) and oxidative stress. IR-induced phosphorylation of CREB correlated with a decrease in CREB trans-activation potential and reduced interaction between CREB and its transcriptional co-activator, CBP. To establish the CREB target genes that may be regulated by

the ATM-CREB pathway, we performed a comparative gene expression microarray analysis. This analysis identified homeobox transcription factor HOXB13, as a potential downstream target repressed by the ATM-CREB pathway. Given that HOXB13 is implicated as an anti-proliferative and pro-apoptotic factor in cells, we propose that ATM-CREB pathway functions in pro-survival capacity by altering the expression of HOXB13. Parallely, we studied the role of ATR in replication stress-induced apoptosis in hydroxyurea (HU)-hypersensitive ML-1 cells. HU is a competitive inhibitor of the enzyme ribonucleotide reducatse that is required for DNA synthesis. Exposure of ML-1 cells to HU caused rapid cell death that correlated well with ATR-dependent accumulation of transcription factor p53 and pro-apoptotic p53 target gene PUMA. In addition, microtubule inhibitor nocodazole suppressed HU-induced p53 accumulation in ML-1 cells suggesting that a microtubule-dependent event is also required for apoptosis in ML-1 cells. Our findings outline a HU-induced cell death pathway and suggest that activation of the ATR is necessary, but not sufficient, for stabilization of p53 in response to DNA replication stress.

Dedication

To my husband Anuj for his unfailing love, support and encouragement throughout this endeavor and others.

For always being there for me, no matter what!

Acknowledgements

I am deeply indebted to my thesis mentor Dr.Randal Tibbetts for his support and guidance throughout the course of my graduate study. I thank him profoundly for spending his valuable time in training me during my initial years in the lab. I am also very grateful to him for providing me the opportunity to work on several projects in his lab.

I convey my special thanks to the current and ex-members of the Tibbetts' Lab (aka Genome Surveillance Research Institute) - Dr. Yuling Shi, Joel Puchalski, Gerald Dodson, Barbara Kraatz-Fortini, Partha Mukhopadhyay, Naval Shanware, Anthony Trinh, Pete Seebart, Eva Zoellner, and Leah Williams for their helpful discussions and support.

I thank members of my thesis committee – Dr. Richard Anderson, Dr. Christopher Bradfield, Dr. Shigeki Miyamoto and Dr. David Wassarman for their valuable advice and suggestions throughout the course of my graduate research. I thank the American Heart Association for support through a Pre-doctoral fellowship.

I thank the following people for helping me with various techniques : Rebecca Katzenberger from the Wassarman Lab for Real Time PCR, Dr.Chunhua Song from the Anderson Lab for help with analyzing microarray data, Rebecca Kirkland

from the Franklin Lab for mice cerebellar granule neuron isolation, and members of the Miyamoto lab for several reagents. I also thank the members of the nuclear signaling group for their helpful discussions and suggestions.

I thank Kathy, Pam, Joanne and Joel for their help at the UW Flow Cytometry facility. I acknowledge Sandra Splinter-Bondurant and Wayne Davis at the UW Gene Expression Center for their help with Gene Chip Arrays. My special thanks are due to Lynn Squire, Terry Hanlon and Karen Wipperfurth for all their help.

Lastly, and most importantly, I thank my husband Anuj, for sharing every minute of this experience with me and making life so wonderful for me. I would also like to thank my entire family for all their support.

Table of Contents

List of Figures

Chapter 1

Chapter 2

Chapter 3

Chapter 4

Chapter 5

List of Tables

Chapter 1

Chapter 3

Abbreviations

A-T	Ataxia telangiectasia
ATM	Ataxia telangiectasia mutated
ATR	ATM and Rad3-related
CBP	CREB binding protein
CGN	Cerebellar granule neurons
CHK1	Checkpoint Kinase 1
CHK2	Checkpoint Kinase 2
CREB	Cyclic AMP response element binding protein
DSB	DNA double strand break
HOXB13	Homeobox gene B13
HU	Hydroxyurea
IR	Ionizing Radiation
KID	Kinase Inducible domain
KIX	KID interacting domain
MEF	Mouse embryonic Fibroblast
ML-1	Myeloid Leukemia-1
qRT-PCR	Quantitative Real Time Polymerase Chain Reaction
RNAi	RNA Interference
Ser	Serine
siRNA	Small interfering RNA
Thr	Threonine

CHAPTER 1

INTRODUCTION

1.1. Ataxia telangiectasia (A-T)

Ataxia-telangectasia (A-T) is a rare chromosmal instability syndrome characterized by radiation sensitivity, cerebellar degeneration, cancer susceptibility, and immunodeficiency (1). A-T is an autosomal recessive disease that affects 1 in every 40,000 live births. A-T manifests in infants between the ages of 1 and 2. Children affected by A-T have motor defects and are confined to a wheel chair by the age of 10. In addition, A-T is also characterized by telangiectasias which cause swelling of blood vessels in eye that cause difficulty in initiating voluntary eye movements. The clinical phenotype of this disease also includes slurred speech, drooling, tremors and mild mental retardation. Since A-T kids are immunodeficient they are susceptible to secondary infections especially of the respiratory tract (reviewed in 36).

One of the hallmark features of cells derived from A-T patients (A-T cells) is hypersensitivity to ionizing radiation (IR) and other agents that induce DNA double strand breaks (DSBs) (1). The radiation sensitivity of A-T cells is a consequence of defects in cell cycle checkpoint control and subtle defects in DNA repair (3). A-T cells are characteristically defective in the G1/S and G2/M cell cycle checkpoints and display radioresistant DNA synthesis (RDS), which represents the failure to transiently downregulate DNA replication in response to DNA damage (3). A-T cells also display a slightly elevated fraction of residual DNA damage that is indicative of a DNA repair defect (3). Cytogenetic analysis

revealed that A-T cells have increased frequency of spontaneous breaks and rearrangements in the chromosomes (3). Combined defects in cell cycle checkpoint activation and DNA repair is believed to contribute to the acquisition of genetic instability and the 100-fold enhanced risk of cancer observed in this disease. Far less is known regarding the mechanism of cerebellar degeneration in A-T. A-T is caused by inactivating mutations in a single gene product called ATM (Ataxia-telangiectasia mutated) (2).

1.2. ATM Protein Kinase

The ATM gene encodes a large molecular mass nuclear protein kinase that belongs to phosphoinositide 3-kinase (PI3K)-related kinase (PIKK) gene superfamily (2) (Fig.1.1). Members of the PIKK family share a highly conserved C-terminal kinase domain that is structurally similar to PI3K (2). The kinase domain of the PIKK's are flanked by two loosely conserved domains termed FAT (FRAP/ATM/TRRAP) and FATC (FAT C-terminal), which are generally expressed in pairs and have presumed functions in kinase activation (38). The N-terminus of the PIKK's have multiple helical HEAT domains which are thought to play a role in scaffolding these kinases into macromolecular signaling complexes (37). Other members of the PIKK family include the ATM homolog ATR (ATM and Rad3-related), DNA repair protein kinase DNAPK, mammalian target of rapamycin mTOR and ATX, a kinase involved in nonsense-mediated mRNA decay (39).

Within this large superfamily of kinases, ATM, ATR and their orthologs in other species form a subgroup of kinases that participate in DNA damage response pathways (3). ATM and ATR are Ser/Thr-Gln directed kinases (40) that phosphorylate a panel of overlapping, as well as distinct substrates involved in cell cycle checkpoint activation, apoptosis regulation, gene expression and DNA repair (3). Even though ATM and ATR have similar substrate specificities (58), they participate in functionally non-redundant pathways. This is exemplified by the fact that ATM is a non-essential gene (4) and ATR is an essential gene (41) in mammalian cells and mice. Another major distinguishing factor between ATM and ATR is the nature of the stimuli they respond to. While ATM is activated primarily by agents that induce DSBs, ATR responds to stimuli that induce replication stress (Hydroxyurea) and bulky DNA lesions (ultraviolet radiation). Mutation of the ATR gene was identified in individuals with Seckel Syndrome, a rare autosomal recessive disorder characterized by dwarfism, microcephaly and mental retardation (42).

1.2.a. Mechanisms of ATM Activation

The mechanism of ATM activation was recently elucidated (43). In the resting state, ATM is held inactive in cells as dimers or higher order multimers with the kinase domain of one ATM molecule bound to the FAT domain of the other ATM molecule. DNA damage induced by irradiation induces rapid intermolecular autophosphorylation of Ser-1981 that contributes to dimer dissociation and a

subsequent increase in ATM catalytic activity. The release of active ATM monomers allows for downstream response pathways to be initiated by increasing accessibility of ATM to its substrates. In addition, Ser-1981 can also be phosphorylated in response to agents that alter chromatin structure including a histone deacetylase inhibitor TSA, chloroquine and hypotonic conditions. Based on these data it has been suggested that DSB induced changes in chromatin structure contribute to ATM activation.

A role for the evolutionarily conserved MRN complex (Mre11/ Rad50 / Nbs1) in ATM activation has been recently demonstrated (44,45,48). This trimeric complex is heavily implicated in maintaining genomic stability and possesses DNA binding activity (Nbs1) as well as nuclease (Mre11) and ATPase (Rad50) activity and can also function as an adaptor to recruit proteins to sites of DNA damage. These functions of the MRN complex have been previously shown to be important in the initial processing of DSBs. In addition, the MRN complex has documented roles in DSB repair through both the homologous recombination and non-homologous end joining pathways. The loss of function mutations of MRN complex in mice result in embryonic lethality, emphasizing the role for this complex in organismal viability.

Recent *in vitro* studies have shown that MRN complex acts as a double strand sensor that recruits ATM to broken DNA ends which results in increase in ATM kinase activity (44). In addition, *in vitro* data also suggest that addition of MRN to

ATM increased the phosphorylation of its downstream substrates many fold (45). ATM has been shown to be in a complex with MR or NBS1 alone, and the physical composition of the complexes contributes to different affinities towards downstream substrates (46). Consistent with these findings, ATM activation as well as downstream substrate phosphorylation is severely compromised in cells lacking functional Mre11 and NBS1, and this defect can be reversed by reconstituting the cells with functional MRN complex. In this regard, the MRN complex is required for both upstream activation and downstream signaling functions of ATM. The current model posits that the MRN complex contributes to cellular responses to DSBs by integrating DNA repair with the activation of checkpoint signaling by inducing a conformational change in ATM that increases its affinity for its downstream substrates.

Consistent with the roles of the MRN complex in ATM activation, hypomorphic mutations in MRN complex results in genome instability syndromes that are also characterized by radiation hypersensitivity and increased cancer susceptibility. For example, missense mutations as well as C-terminal truncations of Mre11 cause AT-LD (A-T Like Disease), a late onset variant of A-T (47). Hypomorphic mutations in NBS1 result in NBS (Nijmegen Breakage Syndrome), which is characterized by microencephaly, mental retardation, and cancer predisposition, but lacks a strong cerebellar degeneration phenotype (49). A variant of this disease is also caused by Rad50 mutations. Given the role for MRN complex in ATM function, it is no surprise that cells derived from AT-LD and NBS patients

display impaired ATM activation and phosphorylation of its downstream substrates following radiation (46).

While ATM is activated in an MRN-dependent manner under low doses, the MRN complex is dispensable for ATM activation at high doses of radiation. In addition, while MRN complex is required for ATM activation in response to IR, it is expendable for replication stress dependent activation of ATM suggesting the possibility for additional mechanisms of ATM activation. Recent data suggest that Tip60 histone acetyl transferase forms a constitutive stable complex with the FATC domain of ATM and induces rapid acetylation of ATM in response to DNA damage (52). DNA damage induces an increase in Tip60 HAT activity independent of ATM catalytic activity. Suppression of Tip60 protein levels by RNA interference blocks IR-induced ATM activation and targeting to nuclear foci as well as downstream phosphorylation of substrates p53 and CHK2.

Recent evidence divulged a role for the members of the Phosphoprotein Phosphatases (PP) family including PP2A and PP5 in ATM activation. PP5 has been shown to associate with ATM in a damage-inducible manner (55). Expression of catalytically inactive form of PP5 results in attenuation of ATM activation and signaling functions (51). In contrast, PP2A and ATM associate constitutively in undamaged cells, and IR induces dissociation of PP2A and ATM (53). Cumulatively, these reports present a strong case for a role for protein phosphatases in activation of ATM.

ATR has been implicated in cellular responses to hypoxia, stalled replication forks induced by DNA replication inhibitors like hydroxyurea (HU) as well as agents that introduce bulky DNA lesions such as UV and alkylating agents (32). The mechanism by which ATR is activated in response to stress stimuli remains unresolved. Several groups have failed to detect an increase in ATR kinase activity after treatment with genotoxic agents such as UV and IR. However, immunostaining analysis revealed that ATR responded to DNA damage by undergoing a dramatic change in intranuclear localization (54,55). While ATR presents a diffused nuclear staining at resting conditions, it localizes to distinct nuclear foci in response to replication stress. It is at these foci that ATR is thought to gain access to its downstream substrates. ATR interacting protein (ATRIP) and single strand DNA binding protein Replication protein A (RPA) have been shown to play important roles in ATR localization and function (54,55).

Some proteins involved in ATM activation have been recently implicated in ATR activation. PP5 has also been shown to form a stress-inducible complex with ATR and is proposed to play a role in modulating the activity of ATR towards its substrates (50). Recent data demonstrate a role for the MRN complex on the ATR-mediated phosphorylation of SMC1 (Structural Maintanence of Chromosomes 1), in response to replication stress (59). However, there is evidence that some ATR-dependent responses do not require the MRN complex. A recent report from the Jackson lab argues for a role for ATM in IR-dependent activation of ATR (56). According to their model, IR-induced ATM activation and

nuclease activity of Mre11 are required for processing of DSBs to generate RPA-coated ssDNA, which is required for recruitment of ATR to nuclear foci and activation of its downstream substrate Checkpoint Kinase 1 (CHK1).

1.2.b. Genome Surveillance functions of the ATM/ATR Kinases: Roles in regulation of Cell Cycle, Apoptosis and Gene Transcription

Upon activation, ATM and ATR kinases orchestrate DNA damage responses via phosphorylation of diverse array of signaling molecules including DNA repair factors (MRN, Breast Cancer Susceptibility genes BRCA1 and BRCA2), transcription factors (Tumor suppressor p53, Nuclear Factor Kappa B (NF αB), cAMP Response Element Binding protein (CREB), Activating Transcription Factor 2 (ATF2)), cell cycle regulators (CHK1, CHK2, Proliferating Cell Nuclear Antigen (PCNA), RPA), and proteins involved in determining cellular fate (p53, NFαB) (reviewed in 32). ATM/ATR-dependent phosphorylation events have been shown to either regulate localization of the protein to sites of DNA damage, modify conformation of target substrate, generate protein-protein interaction motifs and/or modulate stability. The regulation of such a wide array of substrates allows for ATM and ATR to participate in many cellular processes including cell cycle checkpoint activation, DNA repair, gene transcription and apoptosis (reviewed in 3, 32, 57) (Table 1.1).

Key mediators of ATM and ATR checkpoint functions are the checkpoint effector kinases, CHK1 and CHK2. In response to various stress stimuli, ATM/ATR phosphorylates CHK2 and CHK1 respectively, which in turn phosphorylates and inactivates its downstream substrate CDC25 phosphatase (60,62,63). Inactivation of CDC25 phosphatase contributes to inactivation of cyclin-dependent kinases, which in turn results in cell cycle arrest at G1/S and G2/M boundaries (60,62). This mechanism of checkpoint activation is rather rapid and delays G1/S or G2/M transition only for a few hours. Additional programs are activated for sustaining the arrest of cells in these cell cycle boundaries.

Additional ways in which ATM and ATR activate G1/S and G2/M checkpoint is by modulating p53 function through direct and indirect mechanisms (reviewed in 64). ATM/ATR phopshorylates p53 at Ser-15 and promotes p53 accumulation (31). The ubiquitin ligase MDM2 that functions as a negative regulator of p53 is also targeted by ATM/ATR. Phosphorylation of MDM2 by ATM/ATR prevents the interaction of MDM2 with p53 and results in p53 accumulation in cells (65). In addition, ATM/ATR-dependent activation of CHK2/CHK1 targets p53 at Thr-18 and Ser-20 respectively, which prevents interaction of MDM2 with p53 (64). The modifications on p53 and MDM2 contribute to stabilization of p53 levels in cells and results in an increase in its transcriptional activity. The net result of induction of p53 is the activation of p53 target genes including p21/CIP1/WAF1 (cyclin-dependent kinase inhibitor) that is required for both the G1/S and G2/M

checkpoint activation (61). ATM/ATR-dependent phosphorylation of the RFC (Replication Factor C)–related protein Rad17 at Ser-635 and Ser-645 has been shown to be important in activation of G2/M checkpoint (30). In addition, p53-dependent induction of 14-3-3 sigma gene, which mediates the nuclear exclusion of cyclinB-CDC2 complexes also prevents initiation of mitotic events (64). The ATM/ATR-dependent regulation of p53 tumor suppressor constitutes the major pathway for cell cycle checkpoint activation. It is interesting to note that the deregulation of p53 is very common in human cancers.

ATM also phosphorylates NBS1 on Ser-343 and other residues which have been shown to be necessary for S-phase checkpoint activation and survival after IR exposure (66). In addition, phosphorylation of NBS1 at Ser-343 is also required for ATM-mediated phosphorylation of substrates such as Chk2, SMC1 and Fanconi Anemia D 2 (FANCD2) *in vivo*. ATM/ATR-mediated phosphorylation of BRCA1 at several residues contributes to activation of S-phase DNA damage checkpoint (67). While the function of these modifications are not fully understood, it is proposed that they aid in nucleating ATM signaling complexes at sites of DNA damage. Thus the coordinated phosphorylation of several proteins is required for the proper activation of the various cell cycle checkpoints.

Several proteins have been implicated in facilitating the interactions of ATM and ATR with their substrates through the assembly of multiprotein complexes at the sites of DNA damage. These include MDC1 (Mediator of DNA damage

Checkpoint 1), 53BP1 (p53 Binding Protein 1) as well as BRCT (BRCA1 C-Terminal) domain containing proteins (68-69). Mammalian cells that lack expression of these proteins show impaired cell cycle checkpoint mechanisms and enhanced sensitivity to DNA damaging agents. ATR-mediated phosphorylation of CHK1 has been shown to require Claspin, a protein that selectively interacts with chromatin structures created by stalled replication forks (70). ***Given that the ATM-CHK2 and ATR-CHK1 pathway share many common effector proteins, it is striking that ATM and CHK2 are dispensable for development, whereas ATR and CHK1 are essential genes.*** This supports a role for ATR and CHK1 in cell cycle progression, possibly in DNA replication.

Upregulation of p53 in response to stress signals also provides a crucial link between ATM/ATR and the p53-dependent apoptosis program (reviewed in 71). IR-induced p53 accumulation results in activation of pro-apoptotic p53 target genes including BAX, NOXA and PUMA. In addition a series of p53-inducible genes (PIGs) are rapidly upregulated in response to DNA damage and promote the execution of mitochondrial death pathways. ATM may also upregulate pro-survival pathways through direct activation of transcription factor NFαB that has been implicated to function as an anti-apoptotic factor (72). Since ATM activates both pro-apoptotic and anti-apoptotic pathways in response to IR, the ultimate fate of the DNA-damaged cell will depend on the relative balance of ATM-regulated death and survival pathways. Thus whether ATM activation promotes or inhibits apoptosis is cell-context dependent. For instance, while retinas from

ATM-/- mice undergo apoptosis in response to IR, neurons from these mice are resistant to killing by same stimuli (6). Given that ATM regulates the function of several tumor suppressors, it comes as no surprise that ATM deficiency is associated with increased cancer predisposition.

1.2.c. ATM and Neurodegeneration

Far less is known about the neuronal functions of ATM and the mechanisms by which ATM-deficiency causes cerebellar degeneration are largely unexplored. Brains from A-T patients display no gross abnormality at birth, but undergo neurodegeneration during the course of life (73). This suggests that ATM may be required for differentiation of neural progenitor cells in the adult brain. ATM-/- mice display many characteristic features of human A-T including radiation sensitivity, but fail to show a strong neurodegenerative phenotype (4-5). Purkinje and granule neurons, which are most severely affected in human A-T, are not grossly abnormal in *ATM*$^{-/-}$ mice. However, brains from *ATM*$^{-/-}$ mice display subtle developmental defects and are abnormally resistant to IR-induced apoptosis (6-7). It has been proposed that neurodegeneration in human A-T is due to the developmental escape of genomically-damaged neurons, which are destined to degenerate. A second hypothesis posits that neurodegeneration occurs as the result of increased oxidative stress. In support of this hypothesis, brains from ATM-/- mice, especially cerebellum, display markers of increased oxidative stress, including elevated levels of nitrotyrosine, Manganese Superoxide

Dismutase (MnSOD) and Heme Oxgenase 1 (HO-1) (8-9). Elevated levels of Reactive Oxygen Species (ROS), including hydrogen peroxide (H_2O_2) and superoxide anion (O_2^-) are demonstrable in $ATM^{-/-}$ mice (10,11,13). It has been suggested that neurodegeneration in A-T is a consequence of oxidative damage associated with the loss of ATM (9,12). Consistent with a role in mediating responses to oxidative stress, the catalytic activity of ATM is upregulated in response to H_2O_2 (14). Identification of ATM-dependent signaling pathways that regulate neuron homeostasis or survival is imperative for understanding the neurodegenerative process in A-T. ***Given that CREB (Cyclic AMP response element binding protein) is a critical mediator of neuronal survival and mediates gene expression in response to DNA damage and oxidative stress, we hypothesized that the neuronal functions of ATM may be, in part, mediated through its regulation of CREB function.***

1.3. Cyclic AMP Response Element Binding protein (CREB)

CREB is a 341 amino acid (~43kD) protein that belongs to the bZip superfamily of transcription factors (reviewed in 17). The transcription functions of CREB are carried out through binding of a CREB dimer to an 8-bp (TGACGTCA) palindrome called the Cyclic AMP Responsive Element (CRE) in the promoters of target genes. CREB can also bind DNA to a 5 bp (TGACG) sequence called half-CRE with lower affinity. The domain structure of CREB (Fig 1.2) reveals a centrally located 60 amino acid region called the Kinase Inducible Domain (KID)

flanked by two glutamine rich domains Q1 and Q2. At the C-terminal end of the protein is the basic region and leucine zipper required for dimerization and DNA binding respectively (reviewed in 17). The CREB gene is alternatively spliced to produce N-terminally or C-terminally truncated polypeptides with distinct activator and repressor properties (21). Other members of the CREB family include Activating transcription factor 1-3 (ATF1-3) and cAMP response element modulator (CREM) (16). CREB is ubiquitously expressed and lies at the intersection of a multitude of signaling pathways that regulate homeostasis, cell growth, differentiation and survival (16,20). CREB is also heavily implicated in learning and memory (74). CREB-deficient mice are fully formed, but die at birth due to respiratory distress secondary to pulmonary atelectasis (28-29).

CREB-dependent gene expression is induced in response to multiple stimuli including cAMP, growth factors, hypoxia and Calcium (16). DNA-damaging stimuli, including hydrogen peroxide (H_2O_2), UV light, and DNA alkylating agents also modulate CREB-dependent transactivation (20). To date, well over 100 CREB-regulated genes have been identified (Table 1.2) including, but not limited to, cell cycle regulators (Cyclin A, Cyclin D, PCNA and Cyclin Dependent Kinase 5 (CDK5)), DNA repair factors (DNA Polymerase beta, BRCA1), anti-apoptotic genes (Bcl-2, Myeloid Cell Leukemia 1 (MCL1)), Inhibitors of Apoptotic Proteins (IAPs), anti-oxidant enzymes (MnSOD, HO-1), neurotransmitters (Somatostatin Receptor 2(SSTR2), Beta1 Adrenergic Receptor), Immunological regulators (Interleukin 2 and 6 (IL-2, IL-6), T Cell receptor alpha) and transcription factors

(c-Fos, JunD, ATF) (reviewed in 17). Genome wide search for CRE's revealed that approximately 10,000 genes contain a CRE in their promoter. Global analysis of CREB occupancy of CRE's using in vivo promoter microarray showed that CREB occupied CRE of approximately 3000 genes, which accounts for about 20% of all coding genes (75).

1.3.a. Mechanisms of CREB activation

CREB protein mediates basal and stimulus-inducible transcription of target genes in variety of cell types. CREB transactivation domain is bipartite, with the constitutive activity mediated primarily by C-terminal Activation Domain (CAD) and the stimulus-inducible activity contributed by KID domain (76). However, there is evidence for a concerted mechanism for CREB transactivation whereby both the CAD and KID stimulate sequential steps in transcription initiation. CREB stimulates basal transcription of CRE-containing genes through a CAD domain that recruits Transcription Factor II D (TFIID) via interaction with TATA-binding-protein-associated Factor (TAF) proteins (77). Mutations in the CREB-TAF interaction domain have been shown to decrease basal CREB-mediated transactivation. The canonical inducible CREB activation pathway (Fig 1.3) involves cAMP-induced phosphorylation of CREB on Ser-133 by Protein Kinase A (PKA) (18). The phosphorylation of Ser-133 promotes an interaction between KID domain of CREB and the KIX domain of the transcriptional co-activator CBP/p300 (CREB binding protein) (19,25), which further facilitates the interaction

with the basal transcriptional machinery to mediate CREB-dependent gene expression (22). The structure of KIX domain of CBP bound to Ser-133-phosphorylated KID of CREB has been solved using NMR spectroscopy (34). In the absence of phosphorylation at Ser-133, the KID conforms a highly disordered structure. However, upon phopshorylation at Ser-133, the KID domain undergoes a folding transition on binding KIX, forming two alpha helices that kink close to the Ser-133 site. CREB activity is attenuated within a few hours after stimulation, owing to the dephosphorylation of Ser-133 by the Serine/Threonine phosphatase PP1 and PP2A (78).

Additional Ser-133 kinases phosphorylate CREB in response to growth and stress stimuli. These include Mitogen Activated Protein Kinase (MAPK), Calmodulin-Dependent Kinase II and IV (CaMKII, CaMKIV), Protein Kinase B (PKB), and Mitogen and Stress-activated Kinase 1 (MSK-1) (reviewed in 17). In addition to Ser-133, CREB is also phosphorylated on several other Ser/Thr and Tyr residues in the KID. This region, within KID, that encompasses all these phopshorylation sites is referred as the Phopshorylation box (P-Box). For instance, CaMK II and IV phosphorylate Ser-142 that is shown to negatively regulate CREB transactivation by altering CREB-CBP interaction (24). Phosphorylation sites for Casein kinases I and II, as well as glycogen synthase kinase-3 have also been identified in the P-box (33). These additional modifications may modulate CREB-CBP interactions and/or dictate the specificity of CREB-dependent gene expression, perhaps by recruiting distinct

transcriptional coactivators and corepressors. ***One provocative hypothesis in the field is that phosphorylation of these additional residues by stimulus-specific kinases regulate distinct programs of gene expression under different conditions.***

CREB can also be activated inducibly in a Ser-133 phosphorylation-independent manner. The transcriptional co-activator TORC (Transducer Of Regulated CREB activity) binds to the bZIP DNA binding/ dimerization domain of CREB and enhances CREB-mediated transactivation by facilitating the association of CREB with TAFII130 component of TFIID transcriptional complex (79). In addition, the tissue-specific co-activators ACT (Activator of CREM in Testis) and FHL (Four and a Half Lim) are also implicated in facilitating CREB-mediated transactivation through the KID domain in a Ser-133 independent manner (reviewed in 17). CREB can also be post-translationally modified by ubiquitination and SUMOylation, and these modifications have been shown to affect the stability of CREB protein in response to hypoxia (80).

Considering that CREB can be induced in response to diverse stimuli, there is ample interest in the field to determine the factors that contribute to signal discrimination by CREB. The differential ability of CREB to recruit CBP in response to stimuli has been shown to contribute to stimulus-dependent differences in CREB transactivation (24). CREB binding to CRE is highly tissue-specific suggesting that the repertoire of genes regulated by CREB is distinct in

different cell types (81). There is evidence that suggests that the occupancy of CREB on CRE sites may be regulated by DNA methylation and the ability of flanking sequences to recruit co-factors (75). In vivo evidence from the Montminy Lab shows that CREB only occupies unmethylated CREs (75). A recent publication from the Goodman group also argues for the role of epigenetic modification in CREB regulation (81). The ability of CREB to bind DNA and mediate the expression of a particular target gene correlated with methylation of histone H3 at Lysine 4 (81). Differential regulation of CREB target genes may also depend on core promoter configuration (35). For instance, TATA-box containing CREB target genes are induced by cAMP, whereas TATA-less promoters are non-responsive to cAMP, even though CREB binds both promoters with equal affinity.

1.3.b. CREB and Cancer

The positioning of CREB at the intersection of growth and DNA damage-induced pathways suggests that dysregulation of CREB may contribute to neoplastic growth and malignant transformation (82). Constitutive activation of the cAMP-CREB pathway has been observed in endocrine tumors (83) and invasive melanomas, whereas overexpression of a dominant-negative mutant of CREB decreased the tumorigenicity of melanoma cells (84). Furthermore, CRE "decoy" oligonucleotides that sequester CREB transcriptional complexes inhibit the growth of cancer cells, but not normal cells, *in vitro* (85). Recent studies have

shown that CREB is overexpressed in bone marrow of patients with Acute Myeloid Leukemia (AML) (86). In addition, the elevated CREB expression levels in these patients were associated with greater incidence of relapse and poor clinical outcome. CREB dysfunction in AML is proposed to promote tumor formation by improper regulation of cell cycle target genes that contributes to aberrant cellular proliferation (87). Cells from transgenic mice overexpressing CREB under a myeloid specific promoter exhibited properties of transformed cells including growth-factor-independent cell proliferation. Although CREB acts as a proto-oncogene, overexpression of CREB in mice was insufficient to induce leukemogenesis, suggesting additional factors are required to promote tumor formation in mice. CREB has also been implicated in genesis of lymphomas. Interestingly, several CREB target genes such as Cyclin A and Cyclin D are frequently overexpressed in cancers (88). The role of CREB as a proto-oncogene is likely to be a rich area of study in the future.

1.3.c. Neuronal Functions of CREB

CREB is a critical regulator of responses to neuronal stimuli including neurotrophins, neuronal growth factors and mitogens (reviewed in 15). CREB-dependent gene expression in neurons is implicated in processes of learning, memory, neuronal plasticity, circadian rhythm and neurogenesis (15). Several pieces of evidence strongly support a role for CREB as a neuroprotectant (29). CREB-mediated gene expression has been shown to be necessary for nerve

growth factor-dependent survival of sympathetic and cerebellar granule neurons (26). Genetic studies using CREB-deficient mice demonstrate a requirement for CREB in survival of both dorsal root ganglia and sensory neurons in vivo (28). CREB-deficient mice also display axonal growth defects (28). Overexpression of a CREB Ser-133A mutant showed increased apoptosis of sympathetic and cerebellar neurons that could be rescued by overexpression of anti-apoptotic CREB target gene B-Cell Lymphoma 2 (BCL-2) (26). Based on these results it is suggested that the pro-survival effects of CREB is mediated, in part, through the transcription of its anti-apoptotic target gene BCL-2. Overexpression of CREB Ser-133A transgene in pituitary is associated with dwarfism (89). Collectively, these data suggest a role for CREB in cell proliferation and cellular survival. The survival functions of CREB in neurons are partially redundant with those carried out by CREM, which is upregulated in the absence of CREB. The absence of CREB (29) and CREM in developing brain results in generalized cell death, whereas postnatal disruption of transcription mediated through CREB or CREM triggers selective and progressive neurodegeneration due to increased apoptosis (27). ***Given that both the loss of ATM and CREB results in neurodegenerative phenotype, and knowing that CREB regulates neuronal survival and oxidative stress responses, we hypothesized that neuronal functions of ATM may be mediated through regulation of CREB function.***

We have delineated a novel DNA damage-induced signaling link between ATM and CREB (detailed in Chapter 2) (90). We showed that ATM phopshorylated CREB in vitro and in vivo in response to genotoxic stimuli. ATM-mediated phosphorylation of CREB inhibited CREB transactivation by altering CREB-CBP interaction. To gain insight into the transcriptional function of the ATM-CREB pathway, we performed comparative gene expression array analysis. Our preliminary findings suggest that homeobox gene HOXB13 is one downstream CREB target gene regulated by the ATM-CREB pathway (detailed in Chapter 3).

1.4. Homeobox Gene Superfamily

Homeobox genes, originally identified in Drosophila, encode transcription factors that play important roles in development in vertebrates (reviewed in 103). Members of the homeobox superfamily of genes contain a highly conserved C-terminal 61-amino acid sequence known as homeodomain (HD) which is required for recognition and binding to sequence specific DNA motifs (109). In majority of the cases, HD can bind with high affinity to a short DNA sequence containing the ATTA motif, however they can also bind to a TAAT core motif. To date more than 200 vertebrate homeobox genes have been identified that are divided into subfamilies – HOX, MSX, PAX, SIX and LIM - based on similarity of HD and diversity in sequences that flank the HD which confers distinct functional properties. For instance, a hexapeptide sequence close to the HD in HOX family

supports interaction of HOX proteins with PBX homeoproteins. Post-transcriptional and post-translational modifications, sub-cellular localization, and binding to HD-containing co-factors are some ways in which the homeobox-dependent gene expression is regulated (reviewed in 110).

Relatively few *bona fide* cellular targets have been identified for specific homeobox genes *in vivo*. Among the genes identified are extracellular matrix proteins, adhesion molecules, growth factors and cell cycle regulators (reviewed in 105,110). Since homeobox genes function in cellular proliferation and differentiation, it comes as no surprise that deregulation of this family is implicated in several cancers including kidney, prostrate, breast and colon (97). However the mechanism by which homeobox gene alterations cause cancer is not fully understood.

1.4.a. HOX Gene Superfamily

The largest subgroup of homeobox genes is the HOX genes that play crucial roles in embryogenesis (reviewed in 112). So far 39 vertebrate HOX genes have been identified which are organized into 4 chromosomal clusters – A, B, C and D – which have arisen by duplication and divergence of a primordial HOX gene (102). Each cluster has 9 to 11 members that are placed in 13 paralogous groups based on homeobox sequence similarity. An association exists between the arrangement of HOX genes in a cluster and their order of expression during development. For instance, the expression of 3' genes (groups 1-4) occurs early

in development and is restricted to the anterior regions, while the expression of 5' genes (groups 9-13) is delayed and limited to the posterior. Consistent with its major roles in development, it is no surprise that HOX genes are highly conserved among different species. *Cis*-regulatory elements, autoregulation by paralogues and cross regulation by neighboring genes are proposed to contribute to regulation of HOX genes (reviewed in 101).

Loss of function analyses in mice has implicated the HOX genes in development of axial-skeletal vertebrae, limb skeletal elements, neuronal structures and internal organs such as lung (reviewed in 111). In keeping with the role for HOX genes in limb and skeletal development, mutations in certain HOX family members result in conditions such as synpolydactyly, hypodactyly and brachydactyly. The involvement of HOX genes in lineage determination during early hematopoiesis has been proposed (100). Misexpression of HOX genes that occur as a result of chromosomal translocations, involving upstream regulators such as MLL (Mixed Lineage Leukemia), has been implicated in leukemogenesis (104).

HOX genes typically function in assigning cell fate, proliferation, differentiation and patterning embryonic structures. The proliferative functions of HOX genes are mediated through its effects on cell cycle machinery. Bromleigh et al., demonstrated that HOXA10 can directly bind to the p21 promoter and activate p21 transcription which results in cell cycle arrest and differentiation (106). The

cell cycle regulator geminin, which controls DNA replication, has been shown to directly interact with the HD of HOX genes and inhibit its transcriptional function (108). In addition, HOX11 functions are also implicated in activation of G2/M checkpoint via its interaction with protein phosphatases PP1 and PP2A (99).

Deregulation of HOX gene expression and function has been implicated in oncogenesis (reviewed in 98). HOX genes that are normally only active during embryogenesis are re-expressed in neoplastic cells. HOX gene re-expression has been recently identified in SCLC (Small Cell Lung Cancer) and cancers of kidney, brain and mammary glands and is associated with increased tumor vascularization and metastasis (113). In contrast, epigenetic silencing of certain HOX genes is also implicated in the genesis of tumors of renal and colorectal origins (91). Since over expression and suppression of HOX genes have been implicated in tumorigenesis, HOX genes are referred to as "tumor modulators", rather than tumor suppressors or oncogenes.

1.4.b. HOXB13: An anti-proliferative pro-apoptotic HOX gene

HOXB13, the most 5' gene in the HOXB cluster and the last identified member of the HOX family (96), is a non-essential gene in mice, probably owing to the functional redundancy of other HOX isoforms (95). The mouse and human homologs of HOXB13 share 100% amino acid identity in HD and ~91% identity in the remainder of the gene. Mouse HOXB13 is generally expressed in the

posterior regions of the developing embryo, particularly in the caudal extent of spinal cord, tail bud and urogenital sinus. Consistent with its expression pattern, HOXB13 deficient mice display overgrowth of major structures derived from the tail bud, including secondary neural tube (SNT), the caudal spinal ganglia and caudal vertebrae (95). HOXB13 deficient mice are viable and fertile, and the only distinguishing phenotypic characteristic is a long and thick tail. The overgrowth phenotype observed in HOXB13 deficient animals is attributed to increased cell proliferation and decreased apoptosis, emphasizing the role for HOXB13 as a pro-apoptotic and anti-proliferative factor (95). Although the mouse HOXB13 gene is only expressed in prostrate and colorectal tissues, expression of human HOXB13 is also detected in kidney, muscle, brain, testis, uterus, placenta and thymus.

HOXB13 is unique among HOX genes, in that, while most loss of function mutations in HOX genes are associated with loss of various structures, HOXB13 deficiency causes overgrowth of neural elements (95). This finding emphasizes the role of HOXB13 in growth repression and apoptotic induction that contribute to the final stages of developmental patterning. This function of HOXB13 is further exemplified when frozen sections of SNT from HOXB13-proficient and deficient mice were compared by immunostaining with phospho Histone H3 (mitosis marker) and TUNEL (Terminal dUTP-Nick End Labeling) (apoptosis marker). The SNTs from HOXB13-deficient mice displayed decreased staining with mitosis marker and increased reactivity to apoptosis marker, further

suggesting that HOXB13 functions as an inhibitor of neuronal proliferation and an activator of apoptosis in SNT (95). In contrast to several HOX mutants demonstrating increased apoptosis in neural tissues, the hallmark of HOXB13 loss is decreased apoptosis. The anti-proliferative and pro-apoptotic functions of HOXB13 have been observed in several other cell systems, including prostate cancer cell lines (94), primary Renal Cell Carcinomas (RCC) and RCC lines (95), murine caudal spinal cord and epidermal organotypic model system (95). However, the mechanism by which HOXB13 mediates these functions is largely unresolved.

Recent studies by Jung et al., provide one plausible mechanism for HOXB13 mediated growth suppression in prostate cancer cells (94). According to their model, HOXB13 negatively regulates the T-Cell Factor 4 (TCF-4) mediated expression of its target genes c-myc and Cyclin D1 that contributes to arrest of cells in G1 phase of cell cycle (94). The growth suppressive effect of HOXB13 was accompanied by a change in cell morphology, wherein the cells adapt a gigantic cobblestone-like appearance characteristic of cells in a terminally differentiated state. A recent study by the same group also argues for the role of the Androgen Receptor (AR) in mediating HOXB13 induced growth suppression (93). In the context of prostate cancer cells, this group observed that HOXB13 physically interacts with AR and represses hormone-induced AR activity and androgen mediated growth stimulatory signals. HOXB13 induced growth suppression in these cells was relieved by overexpression of hormone-activated

AR. Interestingly, prostate cancer cells that are AR-positive expressed high levels of HOXB13, whereas the AR-negative cells showed diminished HOXB13 expression. A similar correlation between AR and HOXB13 was also observed in tumor xenograft models. Intriguingly, a connection between other HOX13 paralogues and cell cycle progression has also been reported (105). HOXA13 and HOXC13 interact with a DNA replicator sequence within the human Laminin B2 genes. A recent publication from the Maytin lab suggests that HOXB13 can drive differentiation by inducing the enzyme transgluatminase, which is required to assemble differentiation- and cell death-associated structures in cells (92). However the mechanism by which HOXB13 alters transglutaminase activity is not fully understood.

Direct target genes of HOXB13 that may mediate its cellular functions have not yet been identified. While most HOX proteins are presumed transcription factors because of the presence of the DNA binding domain, several HOX proteins have been shown to function as co-activators, repressors or co-factors that function in assembling complexes on DNA. An interesting study by Shen et al., demonstrates a role for HOX proteins in regulation of co-activator CBP/p300 (107). According to their model, HOX proteins, including HOX13 paralogues binds CBP/p300 *in vitro* and *in vivo* through their homeodomains. This interaction prevents HOX genes from binding to DNA and represses the transactivating functions of HOX genes. Conversely, HOX-CBP interaction inhibits histone acetyl

transferase activity of CBP and implicates HOX genes as repressors of transcription.

1.4.c. HOXB13 and Cancer

The HOXB13 gene is methylated in 30% of primary Renal Cell Carcinomas (RCC) and ~73% of human RCC cell lines (91). HOXB13 methylation results in profound loss of its expression and correlates well with the tumor size, grade, stage and invasive capacity. Conversely, re-expression of functional HOXB13 in RCC cells inhibits colony formation and induces apoptosis through caspase 3 activation. It is therefore proposed that hypermethylation and subsequent inactivation of HOXB13 may contribute to RCC tumorigenesis and progression (91). Interestingly, greater than 70% of all colorectal cancers also show loss of HOXB13 expression. In addition, HOXB13 levels are either downregulated or mislocalised in several skin cancers including melanoma, basal cell carcinoma and squamous cell carcinoma (91). In humans loss of heterozygosity of the 17q21 locus, which spans the HOXB cluster is linked to early events of prostate carcinogenesis. Considering the growth suppressive effects of HOXB13, it is conceivable that loss of HOXB13 will provide a survival advantage to the cancer cells. Based on these observations, HOXB13 is proposed to be a candidate tumor suppressor.

1.5. References

1. Becker-Catania,S.G. & Gatti, R. A. (2001) Ataxia-telangiectasia. Adv. Exp. Med.Biol. 495,191-198.

2. Savitsky, K., Bar-Shira, A., Gilad, S., Rotman, G., Ziv, Y., Vanagaite, L., Tagle, D. A., Smith, S., Uziel, T. & Sfez, S. (1995) A single ataxia telangiectasia gene with a product similar to PI-3 kinase. Science. 268, 1749-1753.

3. Shiloh, Y. (2003) ATM and related protein kinases: safeguarding genome integrity. Nat.Rev.Cancer 3, 155-168.

4. Barlow, C., Hirotsune, S., Paylor, R., Liyanage, M., Eckhaus, M., Collins, F., Shiloh, Y., Crawley, J. N., Ried, T., Tagle, D. et al. (1996) Atm-deficient mice: a paradigm of ataxia telangiectasia. Cell 86, 159-171.

5. Xu, Y., Ashley, T., Brainerd, E. E., Bronson, R. T., Meyn, M. S. & Baltimore, D. (1996) Targeted disruption of ATM leads to growth retardation, chromosomal fragmentation during meiosis, immune defects, and thymic lymphoma. Genes Dev. 10, 2411-2422.

6. Herzog, K. H., Chong, M. J., Kapsetaki, M., Morgan, J. I. & McKinnon, P. J. (1998) Requirement for Atm in ionizing radiation-induced cell death in the developing central nervous system. Science 280, 1089-1091.

7. Chong, M. J., Murray, M. R., Gosink, E. C., Russell, H. R., Srinivasan, A., Kapsetaki, M., Korsmeyer, S. J. & McKinnon, P. J. (2000) Atm and Bax cooperate in ionizing radiation-induced apoptosis in the central nervous system. Proc.Natl.Acad.Sci. 97, 889-894.

8. Rotman, G. & Shiloh, Y. (1997) Ataxia-telangiectasia: is ATM a sensor of oxidative damage and stress? Bioessays 19, 911-917.

9. Barzilai, A., Rotman, G. & Shiloh, Y. (2000) ATM deficiency and oxidative stress: a new dimension of defective response to DNA damage. DNA Repair. 1, 3-25.

10. Kamsler, A., Daily, D., Hochman, A., Stern, N., Shiloh, Y., Rotman, G. & Barzilai, A. (2001) Increased oxidative stress in ataxia telangiectasia evidenced by alterations in redox state of brains from Atm-deficient mice. Cancer Res. 61, 1849-1854.

11. Stern, N., Hochman, A., Zemach, N., Weizman, N., Hammel, I., Shiloh, Y., Rotman, G. & Barzilai, A. (2002) Accumulation of DNA damage and

reduced levels of nicotine adenine dinucleotide in the brains of Atm-deficient mice. J.Biol.Chem. 277, 602-608.

12. Barlow, C., Dennery, P. A., Shigenaga, M. K., Smith, M. A., Morrow, J. D., Roberts, L. J., Wynshaw-Boris, A. & Levine, R. L. (1999) Loss of the ataxia-telangiectasia gene product causes oxidative damage in target organs. Proc.Natl.Acad.Sci. 96, 9915-9919.

13. Quick, K. L. & Dugan, L. L. (2001) Superoxide stress identifies neurons at risk in a model of ataxia-telangiectasia. Ann.Neurol. 49, 627-635.

14. Takao, N., Li, Y. & Yamamoto, K. (2000) Protective roles for ATM in cellular response to oxidative stress. FEBS Let. 472, 133-136.

15. Lonze, B. E. & Ginty, D. D. (2002) Function and regulation of CREB family transcription factors in the nervous system.Neuron. 35, 605-623.

16. Shaywitz, A. J. & Greenberg, M. E. (1999) CREB: a stimulus-induced transcription factor activated by a diverse array of extracellular signals. Ann.Rev.Biochem. 68, 821-861.

17. Mayr, B. & Montminy, M. (2001) Transcriptional regulation by the phosphorylation-dependent factor CREB. Nat.Rev.Mol.Cell.Biol..2, 599-609.

18. Gonzalez, G. A. & Montminy, M. R. (1989) Cyclic AMP stimulates somatostatin gene transcription by phosphorylation of CREB at serine 133. Cell. 59, 675-680.

19. Chrivia, J. C., Kwok, R. P., Lamb, N., Hagiwara, M., Montminy, M. R. & Goodman, R. H. (1993) Phosphorylated CREB binds specifically to the nuclear protein CBP. Nature. 365, 855-859.

20. Arias, J., Alberts, A. S., Brindle, P., Claret, F. X., Smeal, T., Karin, M., Feramisco, J. & Montminy, M. (1994) Activation of cAMP and mitogen responsive genes relies on a common nuclear factor. Nature. 370, 226-229.

21. Brindle, P., Linke, S. & Montminy, M. (1993) Protein-kinase-A-dependent activator in transcription factor CREB reveals new role for CREM repressors. Nature. 364, 821-824.

22. Kwok, R. P., Lundblad, J. R., Chrivia, J. C., Richards, J. P., Bachinger, H. P., Brennan, R. G., Roberts, S. G., Green, M. R. & Goodman, R. H. (1994) Nuclear protein CBP is a coactivator for the transcription factor CREB. Nature. 370, 223-226.

23. Kornhauser, J. M., Cowan, C. W., Shaywitz, A. J., Dolmetsch, R. E., Griffith, E. C., Hu, L. S., Haddad, C., Xia, Z. & Greenberg, M. E. (2002) CREB

transcriptional activity in neurons is regulated by multiple, calcium-specific phosphorylation events. Neuron. 34, 221-233.

24. Sun, P., Enslen, H., Myung, P. S. & Maurer, R. A. (1994) Differential activation of CREB by Ca2+/calmodulin-dependent protein kinases type II and type IV involves phosphorylation of a site that negatively regulates activity. GenesDev. 8, 2527-2539.

25. Parker, D., Ferreri, K., Nakajima, T., LaMorte, V. J., Evans, R., Koerber, S. C., Hoeger, C. & Montminy, M. R. (1996) Phosphorylation of CREB at Ser-133 induces complex formation with CREB-binding protein via a direct mechanism. Mol.Cell.Biol. 16, 694-703.

26. Riccio, A., Ahn, S., Davenport, C. M., Blendy, J. A. & Ginty, D. D. (1999) Mediation by a CREB family transcription factor of NGF-dependent survival of sympathetic neurons. Science. 286, 2358-2361.

27. Rudolph, D., Tafuri, A., Gass, P., Hammerling, G. J., Arnold, B. & Schutz, G. (1998) Impaired fetal T cell development and perinatal lethality in mice lacking the cAMP response element binding protein. Proc.Natl.Acad.Sci. 95, 4481-4486.

28. Lonze, B. E., Riccio, A., Cohen, S. & Ginty, D. D. (2002) Apoptosis, axonal growth defects, and degeneration of peripheral neurons in mice lacking CREB. Neuron. 34, 371-385.

29. Mantamadiotis, T., Lemberger, T., Bleckmann, S. C., Kern, H., Kretz, O., Martin, V., Tronche, F., Kellendonk, C., Gau, D., Kapfhammer, J. et al. (2002) Disruption of CREB function in brain leads to neurodegeneration.Nature Genet. 31, 47-54.

30. Bao, S., Tibbetts, R. S., Brumbaugh, K. M., Fang, Y., Richardson, D. A., Ali, A., Chen, S. M., Abraham, R. T. & Wang, X. F. (2001) ATR/ATM-mediated phosphorylation of human Rad17 is required for genotoxic stress responses. Nature 411, 969-974.

31. Tibbetts, R. S., Brumbaugh, K. M., Williams, J. M., Sarkaria, J. N., Cliby, W. A., Shieh, S. Y., Taya, Y., Prives, C. & Abraham, R. T. (1999) A role for ATR in the DNA damage-induced phosphorylation of p53.Genes Dev. 13, 152-157.

32. Abraham, R. T. (2001) Signaling through the ATM and ATR kinases. Genes Dev. 15, 2177-2196.

33. Meggio, F. & Pinna, L. A. (2003) One-thousand-and-one substrates of protein kinase CK2? FASEB J. 17, 349-368.

34. Radhakrishnan, I., Perez-Alvarado, G. C., Parker, D., Dyson, H. J., Montminy, M. R. & Wright, P. E. (1999) Structural analyses of CREB-CBP transcriptional activator-coactivator complexes by NMR spectroscopy: implications for mapping the boundaries of structural domains.J.Molec.Biol. 287, 859-865

35. Conkright, M. D., Guzman, E., Flechner, L., Su, A. I., Hogenesch, J. B. & Montminy, M. (2003) Genome-wide analysis of CREB target genes reveals a core promoter requirement for cAMP responsiveness. Mol. Cell. 11, 1101-1108.

36. Taylor, AM, Byrd, PJ. Molecular pathology of ataxia telangiectasia. J Clin Pathol. (2005) Oct;58(10):1009-15.

37. Perry, J., and N. Kleckner. (2003) The ATRs, ATMs, and TORs are giant HEAT repeat proteins. Cell 112:151–155.

38. Bosotti, R., Isacchi, A., and Sonnhammer, E.L. (2000) FAT: A novel domain in PIK-related kinases. Trends Biochem. Sci. 25: 225–227.

39. Abraham, RT. (2004) PI 3-kinase related kinases: 'big' players in stress-induced signaling pathways.DNA Repair 3(8-9):883-7. Review.

40. Traven A, Heierhorst J. (2005) SQ/TQ cluster domains: concentrated ATM/ATR kinase phosphorylation site regions in DNA-damage-response proteins. Bioessays. 27(4):397-407. Review.

41. Brown EJ, Baltimore D. Essential and dispensable roles of ATR in cell cycle arrest and genome maintenance. (2003) Genes Dev.17(5):615-28.

42. O'Driscoll M, Ruiz-Perez VL, Woods CG, Jeggo PA, Goodship JA. (2003) A splicing mutation affecting expression of ataxia-telangiectasia and Rad3-related protein (ATR) results in Seckel syndrome Nat Genet. 33(4):497-501.

43. Bakkenist CJ, Kastan MB. (2003)DNA damage activates ATM through intermolecular autophosphorylation and dimer dissociation. Nature. 421(6922):499-506.

44. Paull TT, Lee JH. (2005) The Mre11/Rad50/Nbs1 complex and its role as a DNA double-strand break sensor for ATM.Cell Cycle. 4(6):737-40.

45. Lee JH, Paull TT. (2005) ATM activation by DNA double-strand breaks through the Mre11-Rad50-Nbs1 complex. Science. 308(5721):551-4.

46. Cerosaletti K, Concannon P. (2004) Independent roles for nibrin and Mre11-Rad50 in the activation and function of Atm. J Biol Chem. 279(37):38813-9.

47. Delia D, Piane M, Buscemi G, Savio C, Palmeri S, Lulli P, Carlessi L, Fontanella E, Chessa L. (2004) MRE11 mutations and impaired ATM-dependent responses in an Italian family with ataxia-telangiectasia-like disorder. Hum Mol Genet. 13(18):2155-63.

48. Uziel T, Lerenthal Y, Moyal L, Andegeko Y, Mittelman L, Shiloh Y. (2003) Requirement of the MRN complex for ATM activation by DNA damage. EMBO J. 22(20):5612-21.

49. Shiloh Y. (1997) Ataxia-telangiectasia and the Nijmegen breakage syndrome: related disorders but genes apart. Annu Rev Genet. 31:635-62.

50. Zhang J, Bao S, Furumai R, Kucera KS, Ali A, Dean NM, Wang XF. (2005) Protein phosphatase 5 is required for ATR-mediated checkpoint activation. Mol Cell Biol. 25(22):9910-9.

51. Ali A, Zhang J, Bao S, Liu I, Otterness D, Dean NM, Abraham RT, Wang XF. (2004) Requirement of protein phosphatase 5 in DNA-damage-induced ATM activation. Genes Dev. 18(3):249-54.

52. Sun Y, Jiang X, Chen S, Fernandes N, Price BD. (2005) A role for the Tip60 histone acetyltransferase in the acetylation and activation of ATM.Proc Natl Acad Sci U S A. 102(37):13182-7.

53. Goodarzi AA, Jonnalagadda JC, Douglas P, Young D, Ye R, Moorhead GB, Lees-Miller SP, Khanna KK. (2004) Autophosphorylation of ataxia-telangiectasia mutated is regulated by protein phosphatase 2A. EMBO J. 23(22):4451-61.

54. Dodson GE, Shi Y, Tibbetts RS. (2004) DNA replication defects, spontaneous DNA damage, and ATM-dependent checkpoint activation in replication protein A-deficient cells. J Biol Chem. 279(32):34010-4.

55. Zou L, Elledge SJ. (2003) Sensing DNA damage through ATRIP recognition of RPA-ssDNA complexes. Science. 300(5625):1542-8.

56. Jazayeri A, Falck J, Lukas C, Bartek J, Smith GC, Lukas J, Jackson SP. (2006) ATM- and cell cycle-dependent regulation of ATR in response to DNA double-strand breaks. Nat Cell Biol. 8(1):37-45.

57. Shiloh Y. (2001) ATM and ATR: networking cellular responses to DNA damage. Curr Opin Genet Dev. 11(1):71-7. Review.

58. Kim ST, Lim DS, Canman CE, Kastan MB. (1999) Substrate specificities and identification of putative substrates of ATM kinase family members. J Biol Chem. 274(53):37538-43

59. Zhong H, Bryson A, Eckersdorff M, Ferguson DO. (2005) Rad50 depletion impacts upon ATR-dependent DNA damage responses. Hum Mol Genet. 14(18):2685-93.

60. Sorensen CS, Syljuasen RG, Falck J, Schroeder T, Ronnstrand L, Khanna KK, Zhou BB, Bartek J, Lukas J. (2003) Chk1 regulates the S phase checkpoint by coupling the physiological turnover and ionizing radiation-induced accelerated proteolysis of Cdc25A. Cancer Cell.3(3):247-58.

61. Taylor WR, Stark GR. (2001) Regulation of the G2/M transition by p53. Oncogene. 20(15):1803-15.

62. Falck J, Mailand N, Syljuasen RG, Bartek J, Lukas J.(2001) The ATM-Chk2-Cdc25A checkpoint pathway guards against radioresistant DNA synthesis. Nature. 410(6830):842-7.

63. Zhao H, Piwnica-Worms H.(2001) ATR-mediated checkpoint pathways regulate phosphorylation and activation of human Chk1. Mol Cell Biol. 21(13):4129-39.

64. Caspari T. (2000) How to activate p53. Curr Biol.10(8):R315-7. Review.

65. Maya R, Balass M, Kim ST, Shkedy D, Leal JF, Shifman O, Moas M, Buschmann T, Ronai Z, Shiloh Y, Kastan MB, Katzir E, Oren M. (2001)ATM-dependent phosphorylation of Mdm2 on serine 395: role in p53 activation by DNA damage.Genes Dev. 15(9):1067-77.

66. Gatei M, Young D, Cerosaletti KM, Desai-Mehta A, Spring K, Kozlov S, Lavin MF, Gatti RA, Concannon P, Khanna K. (2000) ATM-dependent phosphorylation of nibrin in response to radiation exposure.Nat Genet. 25(1):115-9.

67. Cortez D, Wang Y, Qin J, Elledge SJ. (1999) Requirement of ATM-dependent phosphorylation of brca1 in the DNA damage response to double-strand breaks. Science. 286(5442):1162-6.

68. Mochan TA, Venere M, DiTullio RA Jr, Halazonetis TD. (2003) 53BP1 and NFBD1/MDC1-Nbs1 function in parallel interacting pathways activating ataxia-telangiectasia mutated (ATM) in response to DNA damage. Cancer Res. 63(24):8586-91.

69. Manke IA, Lowery DM, Nguyen A, Yaffe MB.(2003) BRCT repeats as phosphopeptide-binding modules involved in protein targeting. Science. 302(5645):636-9.

70. Kumagai A, Dunphy WG. (2000) Claspin, a novel protein required for the activation of Chk1 during a DNA replication checkpoint response in Xenopus egg extracts. Mol Cell. 6(4):839-49.

71. Schuler M, Green DR.(2001) Mechanisms of p53-dependent apoptosis. Biochem Soc Trans. 29(Pt 6):684-8. Review.

72. Lee SJ, Dimtchev A, Lavin MF, Dritschilo A, Jung M.(1998) A novel ionizing radiation-induced signaling pathway that activates the transcription factor NF-kappaB.Oncogene. 17(14):1821-6.

73. Allen DM, van Praag H, Ray J, Weaver Z, Winrow CJ, Carter TA, Braquet R, Harrington E, Ried T, Brown KD, Gage FH, Barlow C. (2001) Ataxia telangiectasia mutated is essential during adult neurogenesis. Genes Dev. 15(5):554-66.

74. Frank DA, Greenberg ME. CREB: a mediator of long-term memory from mollusks to mammals. Cell. 1994 Oct 7;79(1):5-8.

75. Zhang X, Odom DT, Koo SH, Conkright MD, Canettieri G, Best J, Chen H, Jenner R, Herbolsheimer E, Jacobsen E, Kadam S, Ecker JR, Emerson B, Hogenesch JB, Unterman T, Young RA, Montminy M. (2005) Genome-wide analysis of cAMP-response element binding protein occupancy, phosphorylation, and target gene activation in human tissues. Proc Natl Acad Sci U S A. 102(12):4459-64.

76. Quinn PG.Mechanisms of basal and kinase-inducible transcription activation by CREB. (2002) Prog Nucleic Acid Res Mol Biol. 72:269-305.

77. Felinski EA, Quinn PG (1999). The CREB constitutive activation domain interacts with TATA-binding protein-associated factor 110 (TAF110) through specific hydrophobic residues in one of the three subdomains required for both activation and TAF110 binding. J Biol Chem. 274(17):11672-8.

78. Wadzinski BE, Wheat WH, Jaspers S, Peruski LF Jr, Lickteig RL, Johnson GL, Klemm DJ.(1993) Nuclear protein phosphatase 2A dephosphorylates protein kinase A-phosphorylated CREB and regulates CREB transcriptional stimulation.Mol Cell Biol. 13(5):2822-34.

79. Conkright MD, Canettieri G, Screaton R, Guzman E, Miraglia L, Hogenesch JB, Montminy M. (2003) TORCs: transducers of regulated CREB activity. Mol Cell. 12(2):413-23.

80. Comerford KM, Leonard MO, Karhausen J, Carey R, Colgan SP, Taylor CT. (2003) Small ubiquitin-related modifier-1 modification mediates resolution of

CREB-dependent responses to hypoxia. Proc Natl Acad Sci U S A. 100(3):986-91

81. Cha-Molstad H, Keller DM, Yochum GS, Impey S, Goodman RH. (2004) Cell-type-specific binding of the transcription factor CREB to the cAMP-response element. Proc Natl Acad Sci U S A. 101(37):13572-7.

82. Conkright MD, Montminy M. (2005) CREB: the unindicted cancer co-conspirator. Trends Cell Biol.15(9):457-9. Review.

83. Rosenberg D, Groussin L, Jullian E, Perlemoine K, Bertagna X, Bertherat J. (2002) Role of the PKA-regulated transcription factor CREB in development and tumorigenesis of endocrine tissues.Ann N Y Acad Sci. 968:65-74. Review.

84. Xie S, Price JE, Luca M, Jean D, Ronai Z, Bar-Eli M. (1997) Dominant-negative CREB inhibits tumor growth and metastasis of human melanoma cells. Oncogene. 15(17):2069-75.

85. Cho-Chung YS, Park YG, Nesterova M, Lee YN, Cho YS. (2000) CRE-decoy oligonucleotide-inhibition of gene expression and tumor growth. Mol Cell Biochem. 212(1-2):29-34.

86. Shankar DB, Cheng JC, Sakamoto KM. (2005) Role of cyclic AMP response element binding protein in human leukemias. Cancer. 2005 104(9):1819-24. Review.

87. Shankar DB, Cheng JC, Kinjo K, Federman N, Moore TB, Gill A, Rao NP, Landaw EM, Sakamoto KM. (2005) The role of CREB as a proto-oncogene in hematopoiesis and in acute myeloid leukemia. Cancer Cell.7(4):351-62.

88. Deshpande A, Sicinski P, Hinds PW.(2005) Cyclins and cdks in development and cancer: a perspective.Oncogene. 24(17):2909-15. Review.

89. Struthers RS, Vale WW, Arias C, Sawchenko PE, Montminy MR. (1991) Somatotroph hypoplasia and dwarfism in transgenic mice expressing a non-phosphorylatable CREB mutant. Nature. 350(6319):622-4.

90. Shi Y, Venkataraman SL, Dodson GE, Mabb AM, LeBlanc S, Tibbetts RS. (2004) Direct regulation of CREB transcriptional activity by ATM in response to genotoxic stress. Proc Natl Acad Sci U S A. 101(16):5898-903.

91. Okuda H, Toyota M, Ishida W, Furihata M, Tsuchiya M, Kamada M, Tokino T, Shuin T (2005) Epigenetic inactivation of the candidate tumor suppressor gene HOXB13 in human renal cell carcinoma. Oncogene. 1-10.

92. Mack JA, Li L, Sato N, Hascall VC, Maytin EV (2005) Hoxb13 up-regulates transglutaminase activity and drives terminal differentiation in an epidermal organotypic model. J Biol Chem.280(33):29904-11.

93. Jung C, Kim RS, Zhang HJ, Lee SJ, Jeng MH. (2004) HOXB13 induces growth suppression of prostate cancer cells as a repressor of hormone-activated androgen receptor signaling. Cancer Res. 64(24):9185-92.

94. Jung C, Kim RS, Lee SJ, Wang C, Jeng MH (2004) HOXB13 homeodomain protein suppresses the growth of prostate cancer cells by the negative regulation of T-cell factor 4. Cancer Res. 64(9):3046-51.

95. Economides KD, Zeltser L, Capecchi MR (2003) Hoxb13 mutations cause overgrowth of caudal spinal cord and tail vertebrae. Dev Biol. 256(2):317-30.

96. Zeltser L, Desplan C, Heintz N. (1996) Hoxb-13: a new Hox gene in a distant region of the HOXB cluster maintains colinearity. Development. 122(8):2475-84.

97. Anbazhagan R, Raman V. (1997) Homeobox genes: molecular link between congenital anomalies and cancer. Eur J Cancer. 33(4):635-7

98. Cillo C. HOX genes in human cancers. Invasion Metastasis. 1994-95;14(1-6):38-49. Review.

99. Kawabe T, Muslin AJ, Korsmeyer SJ. HOX11 interacts with protein phosphatases (1997) PP2A and PP1 and disrupts a G2/M cell-cycle checkpoint. Nature. 385(6615):454-8.

100. Lawrence HJ, Sauvageau G, Humphries RK, Largman C. (1996) The role of HOX homeobox genes in normal and leukemic hematopoiesis. Stem Cells. (3):281-91. Review.

101. Maconochie M, Nonchev S, Morrison A, Krumlauf R. (1996) Paralogous Hox genes: function and regulation. Annu Rev Genet. 30:529-56. Review.

102. Hoegg S, Meyer A. (2005) Hox clusters as models for vertebrate genome evolution. Trends Genet. 21(8):421-4. Review.

103. Holland PW, Takahashi T.(2005) The evolution of homeobox genes: Implications for the study of brain development.Brain Res Bull. 66(4-6):484-90. Review.

104. Guenther MG, Jenner RG, Chevalier B, Nakamura T, Croce CM, Canaani E, Young RA. (2005) Global and Hox-specific roles for the MLL1 methyltransferase. Proc Natl Acad Sci U S A. 102(24): 8603-8.

105. Del Bene F, Wittbrodt J. (2005) Cell cycle control by homeobox genes in development and disease. Semin Cell Dev Biol. 16(3):449-60. Review.

106. Bromleigh VC, Freedman LP. (2000) p21 is a transcriptional target of HOXA10 in differentiating myelomonocytic cells.Genes Dev. 14(20):2581-6.

107. Shen WF, Krishnan K, Lawrence HJ, Largman C. (2001) The HOX homeodomain proteins block CBP histone acetyltransferase activity. Mol Cell Biol. 21(21): 7509-22.

108. Luo L, Yang X, Takihara Y, Knoetgen H, Kessel M. (2004) The cell-cycle regulator geminin inhibits Hox function through direct and polycomb-mediated interactions. Nature 427(6976):749-53.

109. Scott MP, Tamkun JW, Hartzell GW 3rd. (1989) The structure and function of the homeodomain. Biochim Biophys Acta. 989(1):25-48. Review.

110. Cillo C, Cantile M, Faiella A, Boncinelli E. (2001) Homeobox genes in normal and malignant cells. J Cell Physiol. 188(2):161-9.

111. Goodman FR. (2002) Limb malformations and the human HOX genes. Am J Med Genet. 112(3):256-65. Review.

112. Mark M, Rijli FM, Chambon P.(1997) Homeobox genes in embryogenesis and pathogenesis. Pediatr Res. 42(4):421-9.

113. Tiberio C, Barba P, Magli MC, Arvelo F, Le Chevalier T, Poupon MF, Cillo C. (1994) HOX gene expression in human small-cell lung cancers xenografted into nude mice. Int J Cancer. 58(4):608-15.

1.6. Figures

Figure 1.1. PIKK Gene Superfamily. The domain structure of the various PIKK family members is shown here. Within this large superfamily, ATM/ATR and their orthologs form a subfamily of kinases implicated in DNA damage responses.

Kinase Domain ■ FATC Domain FAT Domain

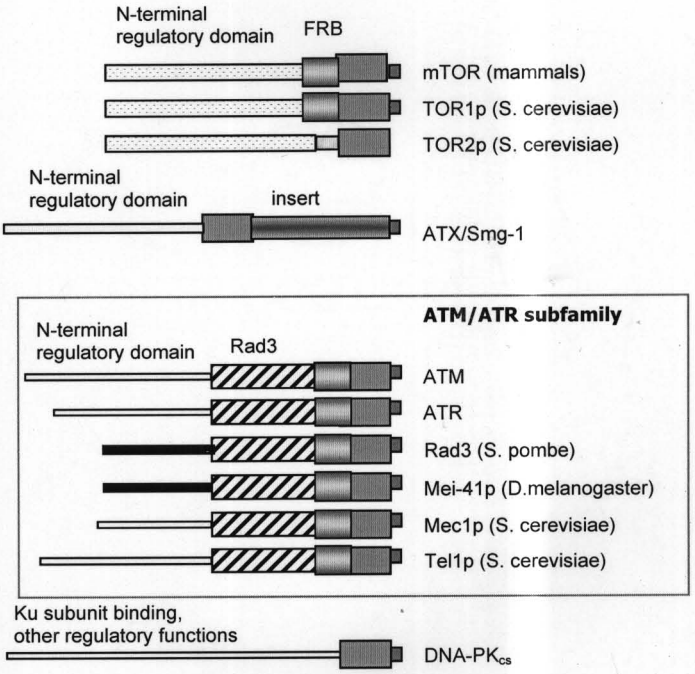
N-terminal
regulatory domain
FRB
mTOR (mammals)
TOR1p (S. cerevisiae)
TOR2p (S. cerevisiae)
N-terminal
regulatory domain
insert
ATX/Smg-1
ATM/ATR subfamily
N-terminal
regulatory domain
Rad3
ATM
ATR
Rad3 (S. pombe)
Mei-41p (D.melanogaster)
Mec1p (S. cerevisiae)
Tel1p (S. cerevisiae)
Ku subunit binding,
other regulatory functions
DNA-PKcs

Table 1.1. Substrates and Functions of ATM and ATR Kinases. Summary of the various ATM and ATR substrates and their biological functions.

Substrates	Functions
p53, CHK1, CHK2, MDM2	G1/S Checkpoint Activation
CHK1, RPA, NBS1, SMC1, Mre11, FANCD2, BRCA1	Intra S Checkpoint Activation
BLM, CHK2, BRCA1, Rad17	G2/M Checkpoint Activation
p53, CREB, NFαB,NEMO	Cell Fate Determination
CHK2, c-Abl, E2F1	DNA Repair
p53, NFαB, c-Jun, CREB	Gene Expression

Figure 1.2. Cyclic AMP response Element Binding Protein (CREB). The domain structure of CREB protein is shown here. A centrally located Kinase Inducible Domain (KID) is flanked by two glutamine rich regions Q1 and Q2. The C-terminal end of the protein contains the bZIP domain (basic region + Leucine Zipper) which is required for DNA binding and dimerization. CAD - C-terminal Activation Domain, NLS - Nuclear Localization Sequence.


Q1
α
KID
Q2/CAD
bZip/NLS

Figure 1.3. Mechanisms of CREB Activation. The canonical inducible CREB activation pathway involves cAMP-induced phosphorylation of CREB on Ser-133 by Protein Kinase A (PKA). The phosphorylation of Ser-133 promotes the interaction between CREB and its transcriptional co-activator CBP/p300, which further facilitates the interaction with the basal transcriptional machinery to mediate CREB-dependent gene expression. In addition to PKA, several other protein kinases, including Mitogen Activated Protein Kinase (MAPK), Calmodulin-Dependent Kinase II and IV (CaMKII, CaMKIV), Protein Kinase B (PKB), and Mitogen and Stress-activated Kinase 1 (MSK-1) phosphorylate the Ser-133 site *in vitro,* and *in vivo* in response to a variety of cellular stimuli.

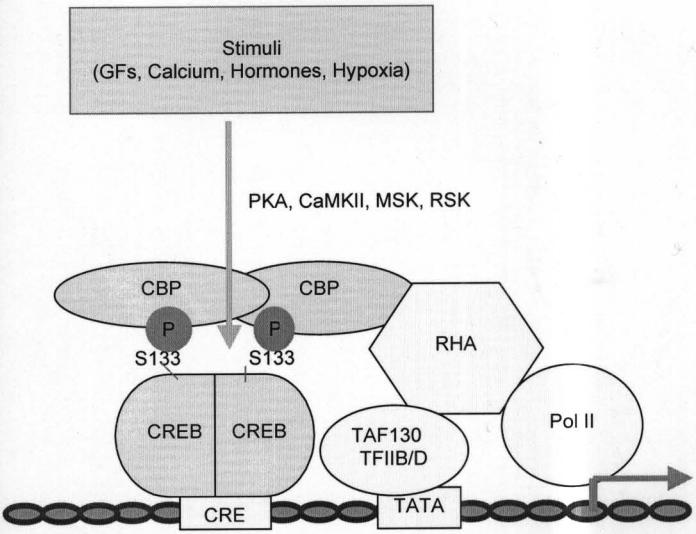
Stimuli
(GFs, Calcium, Hormones, Hypoxia)
PKA, CaMKII, MSK, RSK
CBP
CBP
P
P
S133
S133
RHA
CREB
CREB
TAF130
TFIIB/D
Pol II
CRE
TATA

Table 1.2. CREB-dependent Gene Expression. The table summarizes a subset of CREB-dependent genes. Through the regulation of a large array of genes, CREB participates in a variety of cellular functions.

Target Gene	Functions
BCL-2, MCL-1, IAPs	Cell Survival
PCNA, CDK5, Cyclin A, Cyclin D1	Cell Cycle
SSRT2, beta1 AR, TH, VIP, i NOS	Neurotransmission
DNA Pol beta, BRCA1	DNA repair
c-fos, JunD, NURR1, ICER	Transcription
MnSOD, HO-1	Oxidative Stress Regulation
BDNF, FGF6, TNF alpha	Growth Factors
PPAR gamma, Insulin, Glucagon, LDH, HMG CoA Synthase	Metabolism
IL-2, IL-6, TCR alpha	Immune Regulation

CHAPTER 2

Direct regulation of CREB transcriptional activity by ATM in response genotoxic stress

*Sujatha L. Venkataraman, *Yuling Shi, Gerald E. Dodson, Angela M. Mabb, Scott LeBlanc, and Randal S. Tibbetts

*These authors contributed equally to this work

A version of this Chapter was published in 2004 in *Proc. Natl. Acad. Sci.* 101(16): 5898-5903.

2.1. Abstract

Ataxia-telangiectasia (A-T) is a syndrome of cancer susceptibility, immune dysfunction, and neurodegeneration that is caused by mutations in the ataxia-telangiectasia-mutated (*ATM)* gene. ATM has been implicated as a critical regulator of cellular responses to DNA damage including the activation of cell cycle checkpoints and induction of apoptosis. Although defective cell cycle checkpoint regulation and associated genomic instability presumptively contribute to cancer susceptibility in A-T, the mechanism of neurodegeneration in A-T is not well understood. In addition, although ATM is required for the induction of the p53 transcriptional program in response to DNA damage, the identities of the relevant transcription factors that mediate ATM-dependent changes in gene expression remain largely undetermined. In this report we describe a signal transduction pathway directly linking ATM to the Ca^{2+}/cAMP response element-binding protein, CREB, a transcription factor that regulates cell growth, homeostasis, and survival. ATM phosphorylated CREB *in vitro* and *in vivo* in response to ionizing radiation (IR) and H_2O_2 on a stress-inducible domain. IR-induced phosphorylation of CREB correlated with a decrease in CREB trans-activation potential and reduced interaction between CREB and its transcriptional co-activator, CBP. A CREB mutant containing alanine substitutions at ATM phosphorylation sites displayed enhanced trans-activation potential, resistance to inhibition by IR, and increased binding to CBP. We propose that ATM-mediated phosphorylation of CREB in response to DNA damage modulates CREB-

dependent gene expression and that dysregulation of the ATM-CREB pathway may contribute to neurodegeneration in A-T.

2.2. Introduction

Ataxia-telangiectasia (A-T) is a recessive genetic syndrome characterized by immune deficiency, cancer susceptibility, and cerebellar degeneration (1). A-T is caused by mutations in *ATM*, which encodes a protein kinase belonging to the phosphoinositide 3-kinase-related kinase gene superfamily (2). At the cellular level, ATM-deficient cells grow poorly in culture, are genetically unstable and display exquisite sensitivity to ionizing radiation (IR) and radiomimetic drugs (1). A-T cells are also characteristically defective in the G_1/S, intra-S, and G_2/M cell cycle checkpoints following β-irradiation (3), which is believed to contribute to genomic instability and cancer susceptibility.

The checkpoint-signaling functions of ATM are achieved through the coordinated phosphorylation of polypeptide substrates, including p53, BRCA1, NBS1, and CHK2, which transmit signals to the DNA repair, apoptosis, and cell cycle machinery (3). Far less is known regarding the mechanism of cerebellar degeneration in A-T. Purkinje and granule neurons, which are most severely affected in human A-T, are not grossly abnormal in $ATM^{-/-}$ mice (4, 5). However, brains from $ATM^{-/-}$ mice display subtle developmental defects and are abnormally resistant to IR-induced apoptosis (6,7). It has been proposed that neurodegeneration in human A-T is due to the developmental escape of genomically-damaged neurons, which are destined to degenerate (6). A second hypothesis posits that neurodegeneration occurs as the result of increased

oxidative stress (8, 9). In support of this hypothesis, brains from *ATM*$^{-/-}$ mice display markers of oxidative stress including increased levels of heme oxygenase, thioredoxin, and reactive oxygen species (ROS) (10-14). The basis for enhanced oxidative stress in the absence of ATM has not been determined, but may be a consequence of persistent DNA damage (11).

Identification of ATM-dependent signaling pathways that regulate neuron homeostasis or survival is imperative for understanding the neurodegenerative process in A-T. One relatively well-characterized stress-response and neuron-survival factor is the Ca^{2+}/cyclic AMP response element-binding protein, CREB. CREB is a bZIP family transcription factor that plays key roles in neuronal development, function, and survival (15). CREB transcriptional activity is upregulated in response to a wide variety of cellular stimuli, including cAMP, Ca^{2+}, hypoxia, UV light, and growth factors (16, 17). The canonical CREB activation pathway involves stimulus-induced phosphorylation of CREB on Ser-133 by protein kinase A (PKA) or other Ser-133 kinases (18). The phosphorylation of Ser-133 promotes an interaction between the kinase-inducible domain (KID) of CREB and the transcriptional co-activator CREB-binding protein (CBP), which potentiates the expression of CREB target genes (19-22). CREB activity is also subject to negative regulation. Phosphorylation of Ser-142 by Calmodulin kinase II (CaMKII) or CK2 inhibits CREB transcriptional activity and destabilizes the interaction between the KID and CBP (23-25).

CREB is a *bona fide* neuron survival factor. Overexpression of dominant-negative CREB mutants causes death of cultured neurons and genetic disruption of *CREB* in mice results in axonal growth defects and perinatal lethality (26-28). Furthermore, conditional disruption of *CREB* and the *CREB*-related factor, *CREM*, causes apoptosis of post-mitotic neurons (29). The anti-apoptosis functions of CREB are attributable to CREB-dependent transcription of pro-survival genes such as Bcl-2 and neuron growth factors (26, 30, 31).

Despite an extensive body of literature investigating CREB activation, little is known regarding the regulation of CREB in response to overt DNA-damaging stimuli. Given that genetic inactivation of *CREB* and *ATM* yield neuronal phenotypes, we were intrigued by the possibility that ATM functions upstream of CREB in a DNA damage-induced signaling pathway. We now present evidence that ATM directly regulates CREB phosphorylation and trans-activation potential in response to IR and oxidative stress through a novel, Ser-133 phosphorylation-independent, mechanism. These findings have implications for understanding how ATM modulates gene expression in response to stress stimuli and may provide a link between CREB dysregulation and neurodegeneration in A-T.

2.3. Materials and Methods

Cell culture and antisera. K562 and HEK 293T cells were maintained in RPMI-1640 media and DMEM containing 10% FCS, respectively. G-361 osteosarcoma

cells and L-40, and AT59 lymphoblasts were provided by Dr. Yosef Shiloh (Tel Aviv University). C3ABR, AT1, and AT3 lymphoblasts were provided by Dr. Martin Lavin (Queensland Institute of Medical Research). All lymphoblast cultures were maintained in RPMI-10% FCS. For the generation of β-pS-121 antisera, rabbits were immunized with a KLH-conjugated CREB phosphopeptide (CSVTDpSQKRR) derived from amino acids 117-125 of human CREB. The resulting antiserum was affinity-purified as described previously (32). Other antibodies used in this study include a-CREB (Cell Signaling), β-pS-133 (Upstate Biotechnology), β-ATM (Ab-3, Calbiochem), and β-GST (Sigma).

Plasmid constructs. The CREB:pSPORT6 plasmid was obtained through the IMAGE EST sequencing consortium (Invitrogen). GST-KIX was a gift of Dr. Jennifer Nyborg (Colorado State University) and was expressed and purified as described (33). FLAG-CBP was kindly provided by Dr. Pang Yao (Duke University). HIS-CREB was generated by subcloning a full-length human CREB cDNA into the *Sal*I-*Hind*III sites of pET 28a (Novagen). The HIS-CREB proteins were purified by nickel chromatography as described by the manufacturer. Transient transfection of HEK 293T cells was performed using calcium phosphate DNA precipitation.

Protein analysis and kinase assays. ATM kinase assays were performed as described (34). Extracts were immunoprecipitated with 1 mg of control IgG or β-ATM at 4° C for 1 h. The immunoprecipitates were washed and incubated with 1

μg of HIS-CREB substrate per reaction. GST-KIX pull-down assays were performed as described (33). Briefly, HEK 293T cell extracts were prepared using lysis buffer (35) and 100 μg of extract was incubated with 20 μg of GST-KIX immobilized on glutathione agarose beads in 1 ml of PBS containing 0.1% NP-40 and protease inhibitors (5 μg/ml leupeptin, 10 μg/ml pepstatin, 5 μg/ml aprotinin) at 4° C for 4 h. The beads were washed three times with PBS containing 0.5% NP-40 and eluted by boiling in 2X SDS sample loading buffer. For CREB-CBP co-immunoprecipitations, HEK 293T cells were co-transfected with FLAG-CBP (4 μg) and CREB (0.4 μg) expression plasmids. Twenty-four hours later, cells were exposed to 20 Gy of IR or mock irradiated and harvested 1 h later in Co-IP buffer (50 mM Tris (pH, 7.5), 100 mM NaCl, 0.5% Tween-20, 0.2% NP-40) with protease inhibitors. Extracts were immunoprecipitated using FLAG M2-agarose affinity gel (Sigma), washed in Co-IP buffer containing 200 mM NaCl, and analyzed by SDS-PAGE and immunoblotting with β-CREB and β-FLAG antibodies.

Luciferase Assays. Gal4-CREB luciferase assays were performed using the PathDetect *trans*-Reporting System (Stratagene). The Gal4-CREB plasmid (pFA2-CREB) expresses the amino-terminal 280 amino acids of CREB fused to the Gal4 DNA binding domain. HEK 293T cells were co-transfected with 50 ng of wild-type or mutant Gal4-CREB expression vectors and 1 μg of GAL4-LUC. Twenty-four hours later, the cells were exposed to IR (20 Gy) or mock irradiated. Luciferase activity was measured 1 h later using a Pharmingen Moonlight

luminometer. Presented results were normalized for β-galactosidase expression and represent the averaged values of at least three independent experiments.

2.4. Results

CREB is phosphorylated in response to ionizing radiation and H_2O_2. To explore the potential relationship between ATM and CREB we initially tested whether CREB was phosphorylated on Ser-133 after exposure to IR, an archetypal ATM-activating stimulus (3). K562 cell extracts were prepared at various times after exposure to 20 Gy of IR and subjected to immunoblot analysis using an antibody specific for Ser-133-phosphorylated CREB (β-pS-133). CREB from untreated cell extracts migrated as a major species of approximately 40 kDa and a minor species of 42 kDa on SDS-PAGE gels (Figure 2.1.A). Following exposure to IR, a greater fraction of CREB migrated as the slow-mobility form, though the overall band intensities did not change. The induction of the electrophoretic mobility shift was maximal by 30 min post IR and declined to unstimulated levels by 24 h. The IR-induced electrophoretic mobility shift was also revealed using a β-CREB antibody (Figure 2.1.A, bottom panel), was detectable with IR doses as low as 2 Gy (Figure 2.6.A), and was fully reversed upon phosphatase treatment of the cell extracts, indicating that the observed mobility shift was a consequence of phosphorylation (Figure 2.1.B). H_2O_2 also induced the time- and dose-dependent phosphorylation of CREB (Figure 2.1.C).

Based on these results, we conclude that CREB is phosphorylated on a site distinct from Ser-133 in K562 cells following IR or H_2O_2 treatment.

We next examined the ATM dependence of IR-induced CREB phosphorylation. In contrast to cell lines expressing wild-type ATM (L-40, C3ABR), the IR-induced electrophoretic mobility shift of CREB was absent in the ATM-deficient cell lines AT59 and AT3 (Figure 2.1.D). In AT59 cells, a fraction of CREB migrated as the slow-mobility form in the absence of IR. However, the abundance of this species did not increase after IR exposure, indicating that ATM is required for the inducible component of CREB phosphorylation. The A-T cell lines also displayed a complete defect in H_2O_2-induced CREB phosphorylation (Figure 2.6.B). Finally, both IR and H_2O_2-induced CREB phosphorylation were inhibited by the ATM inhibitor caffeine (Figure 2.6.C). These findings strongly suggest that functional ATM is required for the phosphorylation of CREB in response to IR and oxidative stress.

ATM phosphorylates CREB *in vitro*. CREB contains six Ser/Thr-Gln (SQ/TQ) motifs that may serve as phospho-acceptor sites for ATM/ATR kinase family members (Figure 2.2.A). Three of these residues (Thr-100, Ser-111, and Ser-121) are located near the amino terminal boundary of the KID, which spans amino acids 100-160 of CREB (21). To determine whether CREB is phosphorylated by ATM *in vitro*, we used a histidine-tagged CREB (HIS-CREB) fusion protein substrate in ATM kinase assays. HIS-CREB was phosphorylated

upon incubation with β-ATM immunoprecipitates (IPs), but not IPs prepared using control IgG (Figure 2.2.B). Experiments using ectopically expressed, HA-tagged wild-type and kinase-inactive ATM revealed that a functional ATM kinase domain was essential for *in vitro* phosphorylation of CREB (Figure 2.7.). Individual Ala substitutions at Thr-100, Ser-111, or Ser-121 inhibited ATM-catalyzed phosphate incorporation, and the mutation of Ser-111 had a particularly strong inhibitory effect, reducing HIS-CREB phosphorylation by approximately 70% (Figure 2.2.B). Mutation of Thr-100, Ser-111, and Ser-121 in combination reduced HIS-CREB phosphorylation to near background levels, whereas mutation of Thr-186, Thr-215, and Thr-256 individually (not shown) or in combination (Figure 2,2.B) had little effect. We conclude that ATM phosphorylates CREB on Thr-100, Ser-111, and Ser-121, and that Ser-111 represents the major *in vitro* phosphorylation site.

CREB is phosphorylated on Ser-111 and Ser-121 in intact cells. To initially examine whether CREB is phosphorylated on one or more ATM phosphorylation sites *in vivo*, we transfected HEK 293T cells with plasmids encoding wild-type CREB ($CREB^{WT}$) or CREB containing individual or combination Ala substitutions at Thr-100, Ser-111, or Ser-121, and then examined the H_2O_2-induced electrophoretic mobility shift of the overexpressed proteins. The majority of overexpressed $CREB^{WT}$ migrated as the hyper-phosphorylated form on SDS-PAGE gels and exposure to H_2O_2 caused a further increase in the phosphorylated fraction (Figure 2.2.C). Ala substitutions at Thr-100 ($CREB^{100A}$)

and Ser-121 ($CREB^{121A}$) partially suppressed the basal level of hyper-phosphorylated CREB, but had no effect on the H_2O_2-induced mobility shift (Figure2.2.C). In contrast, a Ser-111 Ala mutation abolished the H_2O_2-induced mobility shift and this effect was recapitulated using a $CREB^{3A}$ mutant containing Ala substitutions at all three phosphorylation sites. These findings suggest that CREB is phosphorylated on Thr-100, Ser-111, and Ser-121 *in vivo*, and that phosphorylation of Ser-111 is required for the H_2O_2-induced mobility shift.

ATM phosphorylation sites antagonize CREB-CBP complex formation. The three ATM phosphorylation sites in CREB lie within the KID, which binds to CBP through a 94 amino acid region termed the KIX domain, in a Ser-133 phosphorylation-dependent manner (25). To determine whether the ATM sites modulate CREB-CBP interactions, we employed a GST-KIX "pull-down" assay that measures the binding of soluble CREB proteins to GST-KIX immobilized on glutathione-agarose beads (25). HEK 293T cells were transfected with $CREB^{WT}$, $CREB^{3A}$ or $CREB^{133A}$ expression plasmids and exposed to IR or mock irradiated. Cell extracts were then incubated with GST-KIX-beads and the bound proteins analyzed by SDS-PAGE and immunoblotting with β-CREB. The GST-KIX pull-down assay revealed that $CREB^{WT}$ bound to GST-KIX, whereas $CREB^{133A}$ containing an Ala substitution at Ser-133 showed reduced affinity (Figure 2.3.A). In contrast, the KIX-binding capacity of $CREB^{3A}$ was elevated 4-5-fold relative to $CREB^{WT}$ (Figure 2.3.A and data not shown). The $CREB^{WT}$ and $CREB^{3A}$ proteins exhibited comparable reactivity with the β-pS-133 antibody, suggesting that

differential binding to GST-KIX was not a consequence of differences in Ser-133 phosphorylation (data not shown).

The effects of IR on the CREB-KIX interaction were also examined. IR exposure inhibited the interaction between $CREB^{WT}$ and GST-KIX, but had no effect on the binding of the $CREB^{3A}$ mutant (Figure 2.3.A). During these experiments we noted that, in comparison to $CREB^{WT}$, the binding of $CREB^{133A}$ to GST-KIX was more strongly inhibited by IR (Figure 2.3.A). This finding suggested that ATM-mediated phosphorylation of $CREB^{133A}$ disrupted a low affinity $CREB^{133A}$-KIX interaction. Consistent with this possibility, the KIX-binding activity of a $CREB^{3A/133A}$ mutant, containing Ala substitutions at Ser-133 and all three ATM sites, was resistant to IR (Figure2.3.B). IR also inhibited the interaction between endogenous CREB and GST-KIX, and the observed inhibition was reversed by the ATM inhibitor, wortmannin (Figure2.3.C). The combined findings imply that ATM phosphorylation sites antagonize CREB-KIX interactions and that phosphorylation of Ser-133 counteracts the inhibitory effects of these residues.

Further experiments were performed to confirm that ATM phosphorylation sites modulate CREB-CBP interactions in intact cells. HEK 293T cells were co-transfected with $CREB^{WT}$ or $CREB^{3A}$ and full-length FLAG-CBP expression plasmids. Cells were exposed to 20 Gy of IR or mock irradiated and cell extracts immunoprecipitated with a-FLAG. Immunoblot analysis using a-CREB revealed that IR inhibited the co-immunoprecipitation of $CREB^{WT}$ with FLAG-CBP. In

contrast, $CREB^{3A}$ demonstrated enhanced co-immunoprecipitation with CBP that was resistant to inhibition by IR (Figure 2.3.D). These results confirm the GST-KIX binding data and suggest that ATM phosphorylation sites antagonize CREB-CBP complex formation *in vivo*.

Effects of ATM phosphorylation site mutations on CREB trans-activation potential. The CBP-binding results described above suggested that ATM phosphorylation sites may impact CREB trans-activation potential. To test this possibility, we employed a reporter gene assay in which the DNA binding domain of yeast Gal4 is fused to the amino-terminal 280 amino acids of CREB (see Materials and Methods). HEK 293T cells were co-transfected with a luciferase construct containing tandem GAL4 binding sites (GAL4-Luc) and plasmids encoding Gal4-$CREB^{WT}$, Gal4-$CREB^{3A}$, or Gal4-$CREB^{133A}$. The transfected cells were then exposed to IR or mock irradiated and luciferase assays performed 1 h later. This assay revealed that the transcriptional activity of Gal4-$CREB^{3A}$ was consistently two-fold higher than the activity of Gal4-$CREB^{WT}$ in the absence of stimulus (Figure 2.4.A). Exposure to IR inhibited the basal activity of Gal4-$CREB^{WT}$, but only marginally affected the activity of Gal4-$CREB^{3A}$. The inhibition of Gal4-$CREB^{WT}$ was modest, ranging from 30-50% in multiple experiments. The activating effects of ATM phosphorylation site mutations on CREB trans-activation potential were also observed using a 5X-CRE-luciferase reporter and full-length CREB constructs, and could be recapitulated by single amino acid substitutions at Ser-111 or Ser-121 (Figure 2.4.B and 2.8.B). In addition, cellular

exposure to the ATM inhibitors wortmannin (20 mM) or caffeine (5 mM) had a slight enhancing effect on CREB trans-activation potential (Figure 2.8.A). These data suggest that ATM-mediated phosphorylation antagonizes CREB trans-activation potential.

Mutation of the three ATM phosphorylation sites activated CREB, whereas mutation of the PKA site at Ser-133 inhibited CREB activity. Therefore, we tested whether the $CREB^{3A}$ mutation could rescue the activation defect of the $CREB^{133A}$ mutant. The trans-activation potential of Gal4-$CREB^{3A/133A}$ mutant containing Ala substitutions at Thr-100, Ser-111, Ser-121, and Ser-133 was comparable to that of Gal4-$CREB^{133A}$, indicating that Ala substitutions at ATM sites are insufficient to activate Gal4-CREB independently of the Ser-133 phosphorylation site (Figure 2.8.B). In addition, IR pre-exposure did not attenuate forskolin-induced CREB activation, suggesting that the canonical phospho-Ser-133-dependent activation pathway is dominant to the ATM pathway in this assay (data not shown). In summary, the combined data suggest that ATM phosphorylation sites negatively regulate CREB trans-activation potential, and are congruent with the CBP-binding results.

Ser-121 is a highly inducible ATM phosphorylation site. The above results strongly suggested ATM phosphorylates CREB in response to DNA damage and that the putative ATM phosphorylation sites at Thr-100, Ser-111, and Ser-121 negatively regulate CREB trans-activation potential and binding to CBP. To

unequivocally prove that Thr-100, Ser-111, and Ser-121 are *bona fide* ATM phosphorylation sites, we attempted to generate phospho-specific antibodies that recognize each residue. We successfully generated an antibody that recognizes phosphorylated Ser-121 (β-pS-121). β-pS-121 demonstrated robust and phosphatase-sensitive reactivity with CREB following cellular exposure to H_2O_2 (Figure 2.5.A and 2.9.A). As a specificity control, we demonstrated that β-pS-121 recognized ectopically expressed $CREB^{WT}$, but not $CREB^{121A}$ (Figure 2.9.B). Phosphorylation of CREB on Ser-121 was defective in the ATM-deficient cell lines AT59 and AT1, indicating that ATM is responsible for phosphorylation of this site *in vivo* (Figure 2.5.A). As expected, IR strongly induced the phosphorylation of Ser-121 (Figure 2.5.B). UV light, aphidicolin, and the hypoxia-mimetic drug deferioxamine mesylate also induced Ser-121 phosphorylation, but with delayed kinetics and lower magnitude in comparison to IR or H_2O_2 (Figure 2.10. and data not shown). From these findings we conclude that the phosphorylation of CREB on Ser-121 represents a general response to cellular stress.

The phosphorylation of endogenous CREB on Ser-121 was highly inducible by IR, yet a fraction of CREB was phosphorylated on Ser-111 in the absence of DNA damage, as evidenced by the presence of the slow mobility form on SDS-PAGE gels (Figure 2.1.A and 2.2.C). We therefore postulated that Ser-111 phosphorylation is required for phosphorylation of Ser-121. Consistent with this possibility, a Ser-111 Ala substitution completely blocked the H_2O_2-induced

phosphorylation of Ser-121 (Figure 2.10.C). These data are consistent with a model whereby the phosphorylation of Ser-111 primes the inducible phosphorylation of Ser-121 in response to stress stimuli.

CREB has been implicated as a positive regulator of neuron survival, whereas ATM promotes apoptosis of neurons in response to DNA damage (7,15). Therefore, the neuronal functions of ATM and CREB may be linked. As a first step toward establishing this possibility, we tested whether CREB was phosphorylated on Ser-121 in cerebellar granule neurons (CGNs) isolated from seven-day old mice. Exposure of CGNs to IR resulted in Ser-121 phosphorylation that was maximal 1-2 post-IR and was suppressed by wortmannin (Figuer 2.5.C). From this result we conclude that the ATM-CREB pathway is activated by DNA damage in primary neurons.

2.5. Discussion

We have delineated an ATM-CREB signaling pathway linking the genome surveillance apparatus to a key regulator of gene expression and cell survival (Figure 2.11.). Our findings indicate that ATM regulates CREB via a non-canonical, Ser-133 phosphorylation-independent mechanism involving the direct phosphorylation of three closely-spaced amino acids (Thr-100, Ser-111, and Ser-121) located with the KID of CREB. Given that the ATM phosphorylation sites are clustered, and that phosphorylation of at least two of the sites (Ser-111 and Ser-

121) is induced by a wide variety of stress stimuli, we collectively refer to Thr-100/Ser-111/Ser-121 as a stress-inducible domain (SID). ATM is required for both IR and H_2O_2-induced CREB phosphorylation. However, CREB was also phosphorylated on Ser-121 in response to UV light, aphidicolin, and hypoxia, which are stimuli that activate the ATM-related kinase, ATR (36). It is therefore likely that ATM and ATR collectively regulate CREB phosphorylation in response to stress stimuli. Our findings further suggest that the phosphorylation of Ser-111 is required for the DNA damage-inducible phosphorylation of Ser-121 (Figure 2.10.C). Interestingly, Ser-111, which is a preferred ATM phosphorylation site *in vitro*, also conforms to a consensus CK2 site. CK2 displays high basal activity *in vivo* and has previously been implicated as a CREB kinase (37, 38). It is therefore conceivable that CK2 plays a role in priming the damage-inducible phosphorylation of Ser-121.

Although the functional implications of the ATM-CREB pathway remain to be fully elucidated, our findings suggest that one outcome of ATM-mediated CREB phosphorylation is the inhibition of CBP binding. Combination or single ATM phosphorylation site mutations enhanced the CBP-binding affinity of CREB 4-5 fold, whereas IR inhibited the binding of both endogenous CREB and transiently-transfected CREB to CBP. Relative to endogenous CREB, the CBP-binding of overexpressed $CREB^{WT}$ was generally less sensitive to IR. We suspect that the difference is caused by the strong constitutive phosphorylation of transiently-transfected CREB on Ser-111 (Figure 2.2.C), which may blunt the IR-inducible

component of the response. The enhanced CBP-binding activity of $CREB^{3A}$ relative to $CREB^{WT}$, even in the absence of IR, supports this hypothesis (Figure 2.3.A). Notably, the 4-5-fold increased CBP-binding capacity of $CREB^{3A}$ translated into an approximately two-fold enhancement of CREB trans-activation potential. The modest activating effects of ATM phosphorylation site mutations on CREB activity are reminiscent of findings that examined the impact of Ala substitutions at the inhibitory CaMKII phosphorylation site at Ser-142 (23, 24). However, the non-linearity between the CBP binding and trans-activation parameters suggests that the impact of the ATM phosphorylation sites on CREB transcriptional functions may not be adequately modeled by generic CREB reporter assays, but instead may be gene and promoter context dependent.

Precisely how ATM phosphorylation sites modulate the CREB-KIX interaction is not known. The Ser-111 and Ser-121 phosphorylation sites lie within a-helix A of the KID, which does not directly contact the KIX domain (39). We propose that ATM-mediated phosphorylation induces a conformational change in the KID that attenuates binding to KIX. Consistent with this possibility, an Ala substitution at Ser-111 grossly altered CREB electrophoretic mobility (Figure 2.2.C), suggesting that phosphorylation of this residue may impact CREB conformation. Our results further suggest that the phospho-Ser-133-dependent binding of CREB to the KIX domain is dominant over the inhibitory effects of the ATM phosphorylation sites. Specifically, the $CREB^{133A}$ mutant, which displays weak CBP-binding affinity, unmasked a strong inhibitory effect of IR on the CREB-KIX interaction that was

reversed when the ATM phosphorylation sites were mutated (Figure 2.3.B). This finding suggests that the phosphorylation of $CREB^{WT}$ on Ser-133 opposes the antagonistic effects of ATM phosphorylation sites on CREB-KIX complex formation.

The broad implications of the ATM pathway for CREB-dependent gene expression are presently unclear. It is conceivable that, by modulating CBP binding affinity, ATM alters the repertoire of CREB-dependent gene expression. Given that the PKA pathway preferentially activates CRE-containing promoters which possess a TATA box (40), it is possible that ATM principally affects the expression of TATA-less CREB targets, which include DNA repair factors and cell cycle regulators (40). Further studies are needed to comprehensively examine the impact of the ATM-CREB pathway on basal and stress-induced expression of CREB target genes. Finally, given that CREB is a neuron survival factor, it is attractive to speculate that ATM-CREB pathway regulates neuron homeostasis and/or apoptosis. Consistent with a neuronal function for the ATM-CREB pathway, we found that ATM phosphorylated CREB in CGNs exposed to IR (Figure 2.5.C). Future studies will be needed to determine the function of the ATM-CREB pathway in neurons and to ascertain whether dysregulation of the ATM-CREB pathway contributes to neuropathogenesis in A-T.

2.6. References

1. Becker-Catania,S.G. & Gatti,R.A. (2001) Ataxia-telangiectasia. *Adv. Exp. Med. Biol.* 495,191-198.

2. Savitsky, K., Bar-Shira, A., Gilad, S., Rotman, G., Ziv, Y., Vanagaite, L., Tagle, D. A., Smith, S., Uziel, T. & Sfez, S. (1995) A single ataxia telangiectasia gene with a product similar to PI-3 kinase. *Science* 268, 1749-1753.

3. Shiloh, Y. (2003) ATM and related protein kinases: safeguarding genome integrity. *Nat.Rev.Cancer* 3,155-168.

4. Barlow, C., Hirotsune, S., Paylor, R., Liyanage, M., Eckhaus, M., Collins, F., Shiloh, Y., Crawley, J. N., Ried, T., Tagle, D. *et al.* (1996) Atm-deficient mice: a paradigm of ataxia telangiectasia. *Cell* 86, 159-171.

5. Xu, Y., Ashley, T., Brainerd, E. E., Bronson, R. T., Meyn, M. S. & Baltimore, D. (1996) Targeted disruption of ATM leads to growth retardation, chromosomal fragmentation during meiosis, immune defects, and thymic lymphoma. *Genes Dev.* 10, 2411-2422.

6. Herzog, K. H., Chong, M. J., Kapsetaki, M., Morgan, J. I. & McKinnon, P. J. (1998) Requirement for Atm in ionizing radiation-induced cell death in the developing central nervous system. *Science* 280, 1089-1091.

7. Chong, M. J., Murray, M. R., Gosink, E. C., Russell, H. R., Srinivasan, A., Kapsetaki, M., Korsmeyer, S. J. & McKinnon, P. J. (2000) Atm and Bax cooperate in ionizing radiation-induced apoptosis in the central nervous system. *Proc.Natl.Acad.Sci.* 97, 889-894.

8. Rotman, G. & Shiloh, Y. (1997) Ataxia-telangiectasia: is ATM a sensor of oxidative damage and stress? *Bioessays* 19, 911-917.

9. Barzilai, A., Rotman, G. & Shiloh, Y. (2002)ATM deficiency and oxidative stress: a new dimension of defective DNA damage response. *DNA Repair.* 1, 3-25.

10. Kamsler, A., Daily, D., Hochman, A., Stern, N., Shiloh, Y., Rotman, G. & Barzilai, A. (2001) Increased oxidative stress in ataxia telangiectasia evidenced by alterations in redox state of brains from Atm-deficient mice. *Cancer Res.* 61, 1849-1854.

11. Stern, N., Hochman, A., Zemach, N., Weizman, N., Hammel, I., Shiloh, Y., Rotman, G. & Barzilai, A. (2002) Accumulation of DNA damage and

reduced levels of nicotine adenine dinucleotide in the brains of Atm-deficient mice. *J.Biol.Chem.* 277, 602-608.

12. Barlow, C., Dennery, P. A., Shigenaga, M. K., Smith, M. A., Morrow, J. D., Roberts, L. J., Wynshaw-Boris, A. & Levine, R. L. (1999) Loss of the ataxia-telangiectasia gene product causes oxidative damage in target organs. *Proc.Natl.Acad.Sci.* 96, 9915-9919.

13. Quick, K. L. & Dugan, L. L. (2001) Superoxide stress identifies neurons at risk in a model of ataxia-telangiectasia. *Ann.Neurol.* 49, 627-635.

14. Takao, N., Li, Y. & Yamamoto, K. (2000) Protective roles for ATM in cellular response to oxidative stress. *FEBS Let.* 472, 133-136.

15. Lonze, B. E. & Ginty, D. D. (2002) Function and regulation of CREB family transcription factors in the nervous system.*Neuron.* 35, 605-623.

16. Shaywitz, A. J. & Greenberg, M. E. (1999) CREB: a stimulus-induced transcription factor activated by a diverse array of extracellular signals. *Ann.Rev.Biochem.* 68, 821-861.

17. Mayr, B. & Montminy, M. (2001) Transcriptional regulation by the phosphorylation-dependent factor CREB. *Nat.Rev.Mol.Cell.Biol.*. 2, 599-609.

18. Gonzalez, G. A. & Montminy, M. R. (1989) Cyclic AMP stimulates somatostatin gene transcription by phosphorylation of CREB at serine 133. *Cell.* 59, 675-680.

19. Chrivia, J. C., Kwok, R. P., Lamb, N., Hagiwara, M., Montminy, M. R. & Goodman, R. H. (1993) Phosphorylated CREB binds specifically to the nuclear protein CBP. *Nature.* 365, 855-859.

20. Arias, J., Alberts, A. S., Brindle, P., Claret, F. X., Smeal, T., Karin, M., Feramisco, J. & Montminy, M. (1994) Activation of cAMP and mitogen responsive genes relies on a common nuclear factor. *Nature.* 370, 226-229.

21. Brindle, P., Linke, S. & Montminy, M. (1993) Protein-kinase-A-dependent activator in transcription factor CREB reveals new role for CREM repressors. *Nature.* 364, 821-824.

22. Kwok, R. P., Lundblad, J. R., Chrivia, J. C., Richards, J. P., Bachinger, H. P., Brennan, R. G., Roberts, S. G., Green, M. R. & Goodman, R. H. (1994) Nuclear protein CBP is a coactivator for the transcription factor CREB. *Nature.* 370, 223-226.

23. Kornhauser, J. M., Cowan, C. W., Shaywitz, A. J., Dolmetsch, R. E., Griffith, E. C., Hu, L. S., Haddad, C., Xia, Z. & Greenberg, M. E. (2002) CREB transcriptional activity in neurons is regulated by multiple, calcium-specific phosphorylation events. *Neuron.* 34, 221-233.

24. Sun, P., Enslen, H., Myung, P. S. & Maurer, R. A. (1994) Differential activation of CREB by Ca2+/calmodulin-dependent protein kinases type II and type IV involves phosphorylation of a site that negatively regulates activity. *Genes Dev.* 8, 2527-2539.

25. Parker, D., Ferreri, K., Nakajima, T., LaMorte, V. J., Evans, R., Koerber, S. C., Hoeger, C. & Montminy, M. R. (1996) Phosphorylation of CREB at Ser-133 induces complex formation with CREB-binding protein via a direct mechanism. *Mol.Cell.Biol.* 16, 694-703.

26. Riccio, A., Ahn, S., Davenport, C. M., Blendy, J. A. & Ginty, D. D. (1999) Mediation by a CREB family transcription factor of NGF-dependent survival of sympathetic neurons.*Science.* 286, 2358-2361.

27. Rudolph, D., Tafuri, A., Gass, P., Hammerling, G. J., Arnold, B. & Schutz, G. (1998) Impaired fetal T cell development and perinatal lethality in mice lacking the cAMP response element binding protein. *Proc.Natl.Acad.Sci.* 95, 4481-4486.

28. Lonze, B. E., Riccio, A., Cohen, S. & Ginty, D. D. (2002) Apoptosis, axonal growth defects, and degeneration of peripheral neurons in mice lacking CREB. *Neuron.* 34, 371-385.

29. Mantamadiotis, T., Lemberger, T., Bleckmann, S. C., Kern, H., Kretz, O., Martin, V., Tronche, F., Kellendonk, C., Gau, D., Kapfhammer, J. *et al.* (2002) Disruption of CREB function in brain leads to neurodegeneration.*Nature Genet.* 31, 47-54.

30. Shieh, P. B., Hu, S. C., Bobb, K., Timmusk, T. & Ghosh, A. (1998) Identification of a signaling pathway involved in calcium regulation of BDNF expression. *Neuron.* 20, 727-740.

31. Tao, X., Finkbeiner, S., Arnold, D. B., Shaywitz, A. J. & Greenberg, M. E. (1998) Ca2+ influx regulates BDNF transcription by a CREB family transcription factor-dependent mechanism. *Neuron.* 20, 709-726.

32. Bao, S., Tibbetts, R. S., Brumbaugh, K. M., Fang, Y., Richardson, D. A., Ali, A., Chen, S. M., Abraham, R. T. & Wang, X. F. (2001) ATR/ATM-mediated phosphorylation of human Rad17 is required for genotoxic stress responses. *Nature* 411, 969-974.

33. Van Orden, K. Giebler, H. A., Lemasson, I., Gonzales, M. & Nyborg, J. K. (1999) Binding of p53 to the KIX domain of CREB binding protein. A potential link to human T-cell leukemia virus, type I-associated leukemogenesis. *J.Biol.Chem.* 274, 26321-26328.

34. Sarkaria, J. N., Tibbetts, R. S., Busby, E. C., Kennedy, A. P., Hill, D. E. & Abraham, R. T. (1998) Inhibition of phosphoinositide 3-kinase related kinases by the radiosensitizing agent wortmannin. *Cancer Res.* 58, 4375-4382.

35. Tibbetts, R. S., Brumbaugh, K. M., Williams, J. M., Sarkaria, J. N., Cliby, W. A., Shieh, S. Y., Taya, Y., Prives, C. & Abraham, R. T. (1999) A role for ATR in the DNA damage-induced phosphorylation of p53.*Genes Dev.* 13, 152-157.

36. Abraham, R. T. (2001) Cell cycle checkpoint signaling through the ATM and ATR kinases.*Genes Dev.* 15, 2177-2196.

37. Meggio, F. & Pinna, L. A. (2003) One-thousand-and-one substrates of protein kinase CK2? *FASEB J.* 17, 349-368.

38. Saeki, K., Yuo, A. & Takaku, F. (1999) Cell-cycle-regulated phosphorylation of cAMP response element-binding protein: identification of novel phosphorylation sites. *Biochem. J.* 338, 49-54.

39. Radhakrishnan, I., Perez-Alvarado, G. C., Parker, D., Dyson, H. J., Montminy, M. R. & Wright, P. E. (1999) Structural analyses of CREB-CBP transcriptional activator-coactivator complexes by NMR spectroscopy: implications for mapping the boundaries of structural domains.*J. Molec. Biol.* 287, 859-865.

40. Conkright, M. D., Guzman, E., Flechner, L., Su, A. I., Hogenesch, J. B. & Montminy, M. (2003) Genome-wide analysis of CREB target genes reveals a core promoter requirement for cAMP responsiveness. *Mol. Cell.* 11, 1101-1108.

2.7. Figure Legends

Figure 2.1. ATM-dependent phosphorylation of CREB in response to IR and oxidative stress. (**A**) K562 cells were exposed to 20 Gy of IR and then harvested at the indicated times. Cell extracts were analyzed by SDS-PAGE and immunoblotting using an antibody specific for the Ser-133 phosphorylation site of CREB (β-pS-133, top panel) or β-CREB (bottom panel). (**B**) IR-induced CREB electrophoretic mobility shift is abolished by phosphatase treatment. Cell extracts prepared from unirradiated or β-irradiated K562 cells were treated with lambda phosphatase (PPase) or sham treated and then analyzed by immunoblotting with a-CREB. (**C**) Phosphorylation of CREB in response to H_2O_2. K562 cells were treated with increasing concentrations of H_2O_2 for the indicated time. Cell extracts were prepared and analyzed by immunoblotting with β-CREB. (**D**) Phosphorylation of CREB in ATM deficient lymphoblasts. Cells expressing wild-type ATM (L-40, C3ABR) or mutant ATM (AT59, AT3) were left untreated or exposed to 10 Gy of IR. One hour later, cell extracts were prepared and analyzed by SDS-PAGE and immunoblotting with β-CREB.

FIGURE 2.1

A

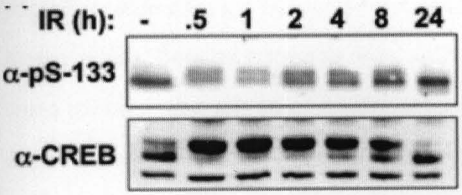

B

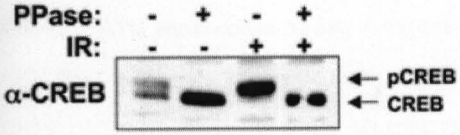

C

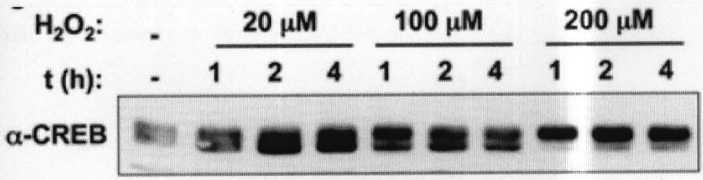

D

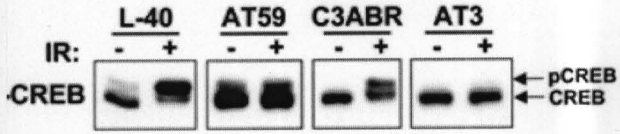

Figure 2.2. ATM phosphorylates CREB *in vitro*. (**A**) Primary amino acid sequence and schematic depiction of CREB. Locations of potential ATM phosphorylation sites are highlighted in bold and denoted by asterisks. (**B**) ATM kinase assay. Detergent extracts from G-361 cells were immunoprecipitated using control rabbit IgG (-) or β-ATM antibodies (+). The immunoprecipitates were incubated with either a wild-type HIS-CREB fusion protein substrate (WT) or a HIS-CREB substrate containing the indicated single or combination Ala substitutions. Kinase reactions were performed in the presence of g-^{32}P-ATP and the reaction products were analyzed by SDS-PAGE and autoradiography. (**C**) Effects of ATM phosphorylation site mutations on CREB electrophoretic mobility. HEK 293T cells were transfected with expression plasmids encoding wild-type CREB (WT), CREB bearing single Ala substitutions at Thr-100, Ser-111, or Ser-121, or a CREB^{3A} mutant containing Ala substitutions at all three sites. Twenty-four hours after transfection, the cells were treated with H_2O_2 or vehicle for 1 h. Cell extracts were then immunoblotted with β -CREB.

FIGURE 2.2

A

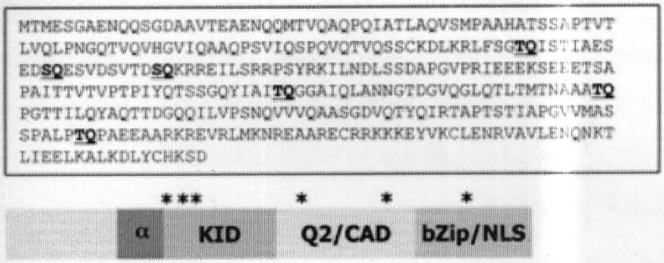

B

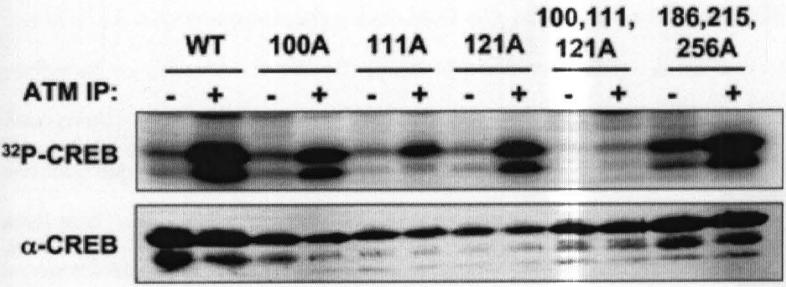

C

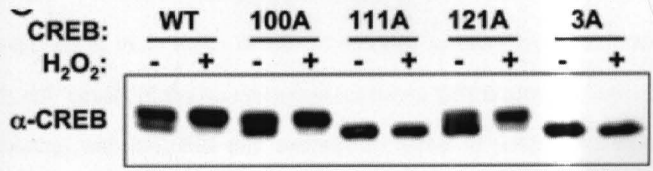

Figure 2.3. ATM phosphorylation sites antagonize CREB-CBP complex formation. (A) Analysis of CREB-KIX interactions by GST-KIX pull-down assay. HEK 293T cells were transfected with vector, $CREB^{WT}$, $CREB^{3A}$, or $CREB^{133A}$ expression plasmids. Equal amounts of cell extracts from irradiated (20 Gy, 1 h) or unirradiated cells were incubated with GST-KIX-agarose beads. Bound proteins were eluted and analyzed by immunoblotting with β-CREB. Short and long exposures of the film are shown. Expression levels of the transfected CREB proteins are shown in the bottom panel. (**B**) IR-dependent inhibition of $CREB^{133A}$-KIX interactions requires intact ATM phosphorylation sites. HEK 293T cells were transfected with $CREB^{133A}$ or $CREB^{3A/133A}$ containing Ala substitutions at Ser-133 and all three ATM phosphorylation sites. GST-KIX pull-down assays were then performed as described in (A). (**C**) Effect of wortmannin (Wm) on CREB-KIX interactions. HEK 293T cells were exposed to 20 mM Wm or vehicle for 30 min and then exposed to IR (20 Gy) or mock irradiated. After 1 h, cell extracts were incubated with GST-KIX and the levels of bound CREB determined by immunoblotting. (**D**) $CREB^{3A}$ shows enhanced co-immunoprecipitation with full-length CBP. HEK 293T cells were co-transfected with FLAG-CBP and either $CREB^{WT}$ or $CREB^{3A}$ expression vectors. Twenty-four hours later, cells were exposed to IR or mock irradiated and cell extracts immunoprecipitated with β-FLAG. Levels of the co-immunoprecipitated CREB proteins were determined by blotting with β-CREB and expression levels of CREB and FLAG-CBP were assessed by blotting with β-CREB and β-FLAG, respectively.

FIGURE 2.3.

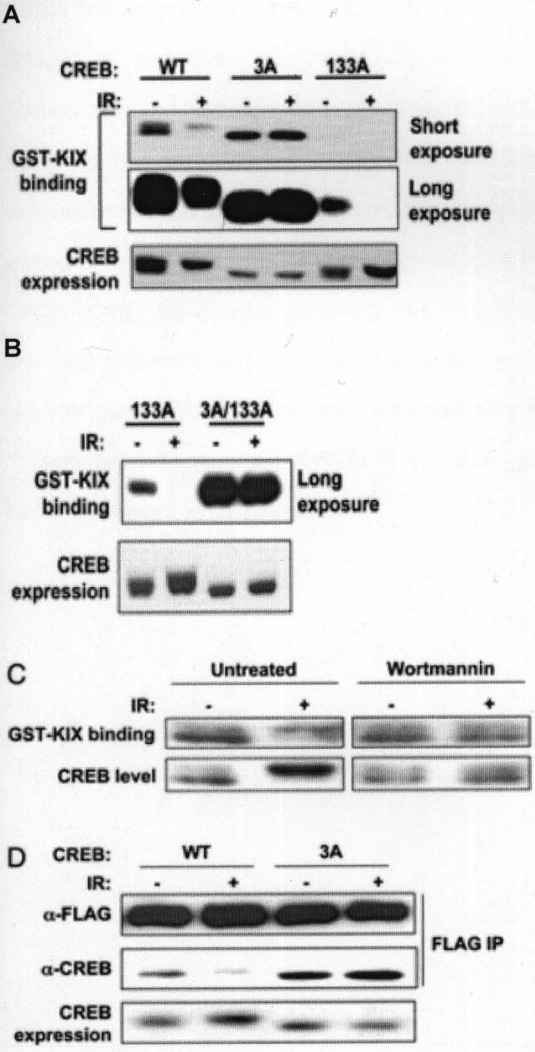
A
CREB:
WT
3A
133A
IR:
- + - + - +
GST-KIX binding
Short exposure
Long exposure
CREB expression
B
133A
3A/133A
IR:
- + - +
GST-KIX binding
Long exposure
CREB expression
C
Untreated
Wortmannin
IR:
- + - +
GST-KIX binding
CREB level
D
CREB:
WT
3A
IR:
- + - +
α-FLAG
α-CREB
FLAG IP
CREB expression

Figure 2.4. Alanine substitutions at ATM phosphorylation sites enhance CREB transcriptional activity. (**A**) HEK 293T cells were co-transfected with GAL4-Luc, and either Gal4-CREB^{WT}, Gal4-CREB^{3A} or Gal4-CREB^{133A}. Transfected cells were exposed to IR (20 Gy) or mock irradiated and harvested 1 h later for luciferase assays. The data were normalized for co-transfected β-Gal expression and are plotted as relative luciferase activity. The data represent the averaged results of at least three experiments (n=5 for Gal4-CREB^{WT} and Gal4-CREB^{3A}). (**B**) Transcriptional activity of full-length CREB toward a CRE-Luc promoter construct. HEK 293T cells were co-transfected with a 5X-CRE-Luc reporter construct and expression plasmids encoding CREB^{WT} or CREB^{3A}. Transfected cells were exposed to IR or mock irradiated and processed for luciferase assays as described in (A).

FIGURE 2.4.

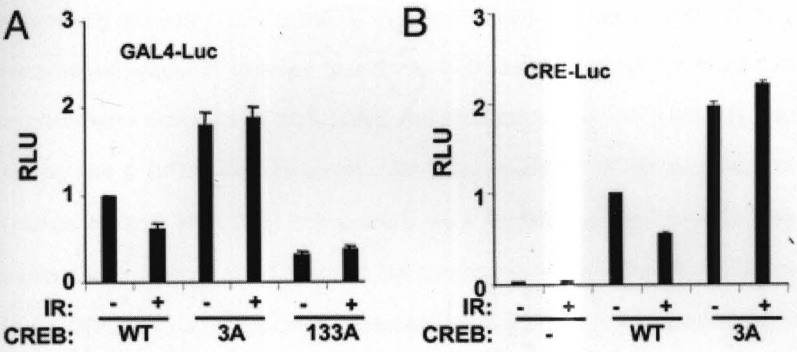
A
GAL4-Luc
RLU
3
2
1
0
IR: - + - + - +
CREB: WT 3A 133A
B
CRE-Luc
RLU
3
2
1
0
IR: - + - + - +
CREB: - WT 3A

Figure 2.5. Stress-induced phosphorylation of CREB on Ser-121. (A) H_2O_2-induced phosphorylation of CREB on Ser-121 is ATM dependent. Cells expressing wild-type ATM (K562, L-40) or ATM deficient cells (AT59, AT1BI) were left untreated or exposed to 200 mM H_2O_2 and harvested 1 h later. Cell extracts were analyzed by SDS-PAGE and immunoblotting with β-pS-121 (top panel) and β-CREB (bottom panel). (**B**) Time course of IR-induced Ser-121 phosphorylation. HEK 293T cell extracts were prepared at the indicated time points after irradiation with 10 Gy and analyzed by immunoblotting with β-pS-121 and β-CREB. (**C**) ATM-mediated phosphorylation of CREB in cerebellar granule neurons (CGNs). Mouse CGNs were exposed to 10 Gy of IR or mock irradiated. Cell extracts were prepared at the indicated times and analyzed by immunoblotting with β-pS-121 and β-CREB. Where indicated, the samples were treated Wmn (20 μM) 15 min prior to irradiation.

FIGURE 2.5.

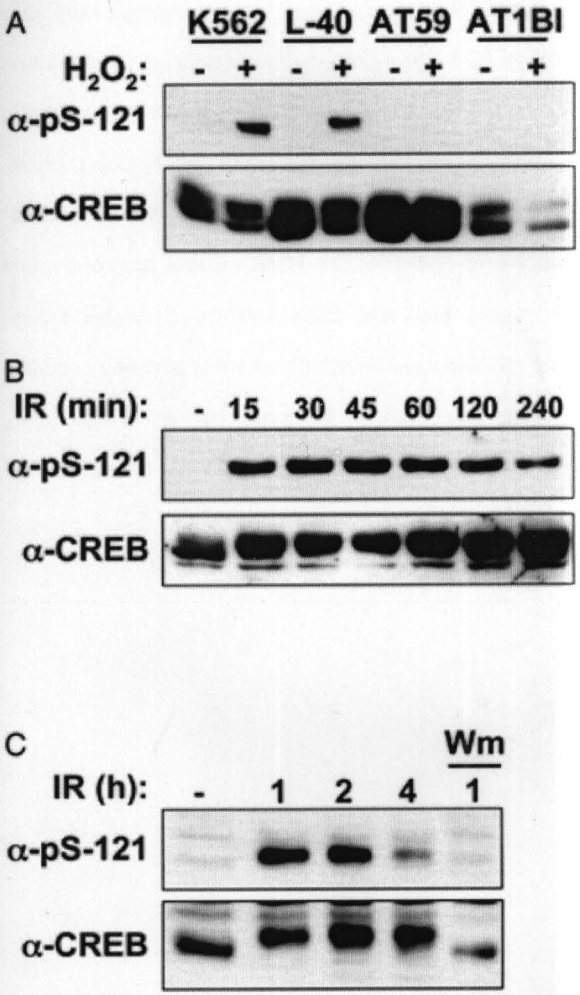
A
K562
L-40
AT59
AT1BI
H_2O_2:
- + - + - + - +
α-pS-121
α-CREB
B
IR (min):
- 15 30 45 60 120 240
α-pS-121
α-CREB
C
Wm
IR (h):
- 1 2 4 1
α-pS-121
α-CREB

FIGURE 2.6. Analysis of stress-induced CREB phosphorylation. (*A*) Dose–response of ionizing radiation (IR)-induced CREB phosphorylation. K562 cells were exposed to the indicated doses of IR. Extracts were prepared 1 h later and analyzed by blotting with β-CREB. **(*B*)** ATM dependence of H_2O_2-induced CREB phosphorylation. Cells expressing wild-type ATM (K562, L-40) or ATM deficient cells (AT59, AT3) were left untreated or exposed to 200 m M H_2O_2 and harvested 1 h later. Cell extracts were analyzed by SDS/PAGE and immunoblotting with β -CREB. **(*C*)** Inhibition of IR- and H_2O_2-induced CREB phosphorylation by caffeine. K562 cells were cultured in the presence of 5 mM caffeine or vehicle alone for 15 min before exposure to IR (20 Gy) or H_2O_2 (200 μM). Cells were then harvested 1 h later and analyzed by SDS/PAGE and immunoblotting with β-CREB.

FIGURE 2.6.

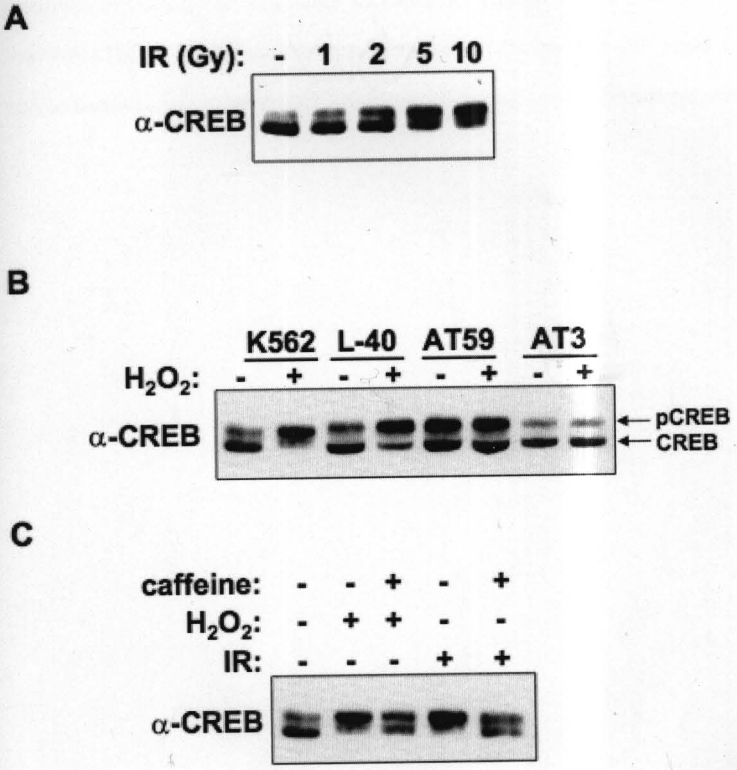
A
IR (Gy): - 1 2 5 10
α-CREB
B
K562 L-40 AT59 AT3
H2O2: - + - + - + - +
α-CREB
pCREB
CREB
C
caffeine: - - + - +
H2O2: - + + - -
IR: - - - + +
α-CREB

FIGURE 2.7. Recombinant ATM phosphorylates CREB *in vitro*. Human embryonic kidney (HEK) 293T cells were transfected with control vector or plasmids encoding hemagglutinin (HA)-tagged wild-type ATM (WT) or kinase-inactive ATM (KI). ATM was immunoprecipitated by using β -HA antibody, and kinase assays were carried out by using a HIS-CREB fusion protein substrate.

FIGURE 2.7.

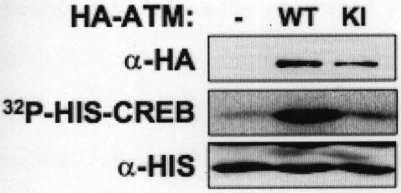

FIGURE 2.8. Effects of ATM inhibitors and ATM phosphorylation site mutations on CREB transactivation potential. (*A*) Enhancement of CREB transactivation potential by wortmannin and caffeine. Human embryonic kidney (HEK) 293T cells were cotransfected with GAL4-Luc and either Gal4-CREB^{WT} or Gal4-CREB^{3A}. Transfected cells were exposed to ionizing radiation (IR) or mock irradiated in the absence or presence of wortmannin (Wm, 20 μ M) or caffeine (5 mM). Cells were harvested 1 h later and assayed for luciferase activity. The data are normalized for β -Gal expression and reflect the averaged results of three experiments. **(*B*)** Single phosphorylation-site substitutions at Ser-111 or Ser-121 enhance CREB transactivation potential. HEK 293T cells were transfected with Gal4-Luc and either Gal4-CREBWT, Gal4-CREB3A, Gal4-CREB^{133A}, Gal4-CREB$^{3A/133A}$, Gal4-CREB^{111A}, or Gal4-CREB^{121A}. Reporter assays were performed as described in *A*. The Gal4-CREB$^{3A/133A}$ mutant contains Ala substitutions at Thr-100, Ser-111, Ser-121, and Ser-133. The activity of Gal4-CREB^{mut} containing a DNA binding domain mutation and Gal4-CREB^{WT} cotransfected with a PKA expression plasmid were used as negative and positive controls, respectively.

FIGURE 2.8.

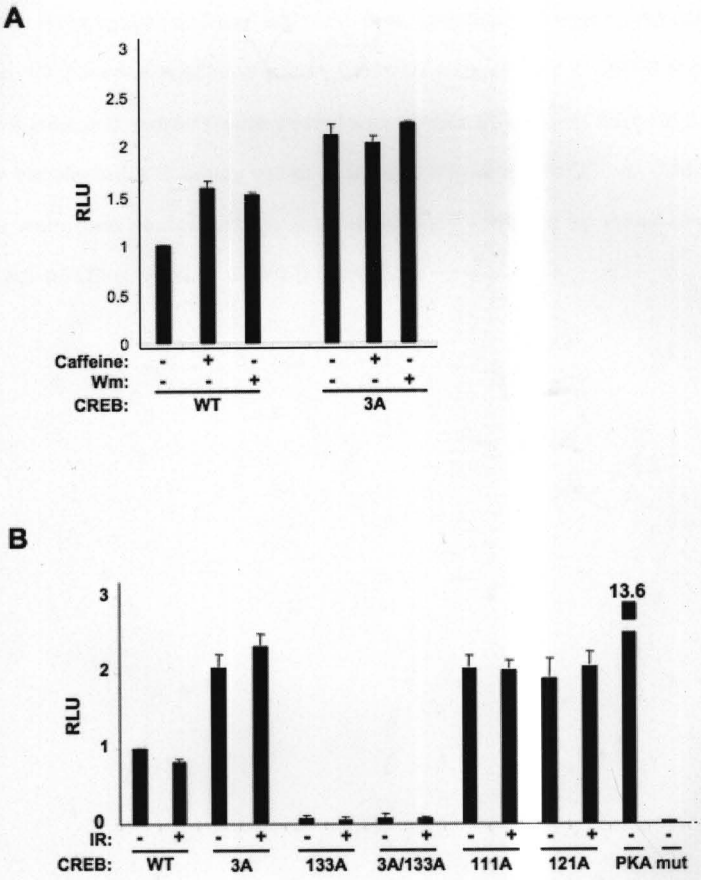
A
RLU
3
2.5
2
1.5
1
0.5
0
Caffeine: - + - - + -
Wm: - - + - - +
CREB: WT 3A
B
RLU
3
2
1
0
13.6
IR: - + - + - + - + - + - + - -
CREB: WT 3A 133A 3A/133A 111A 121A PKA mut

FIGURE 2.9. Characterization of a CREB Ser-121 phospho-specific antibody. (***A***) Human embryonic kidney (HEK) 293T cells were treated with H_2O_2 (200 m M) or vehicle and harvested 1 h later. Cell extracts were immunoblotted using the phospho-specific β-pS121 antibody (*Upper*) and β -CREB (*Lower*). Where indicated, extracts were treated with lambda PPase. (***B***) HEK 293T cells were transfected with empty vector or vectors encoding $CREB^{WT}$ or $CREB^{121A}$. Cells were then treated with H_2O_2 or vehicle and analyzed by immunoblotting with a β-pS121 (*Upper*) or β-CREB (*Lower*).

FIGURE 2.9.

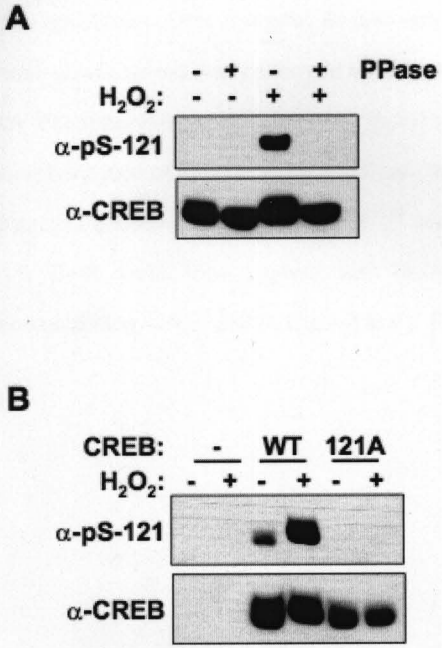

FIGURE 2.10. Stress-induced phosphorylation of CREB on Ser-121. Human embryonic kidney (HEK) 293T cells were exposed to UV light (50 J/m^2, ***A***) or aphidicolin (APH, 5 m g/ml, ***B***) and harvested at the indicated time points. Immunoblot analysis was performed by using β -pS121 and β -CREB antibodies. (***C***) Phosphorylation of CREB on Ser-111 is required for H_2O_2-induced phosphorylation of Ser-121. HEK 293T cells were transfected with empty vector or vectors encoding $CREB^{WT}$ or $CREB^{111A}$ containing an Ala substitution at Ser-111. Cells were then treated with H_2O_2 or vehicle and analyzed by immunoblotting with β -pS121 (*Upper*) and β -CREB (*Lower*).

FIGURE 2.10.

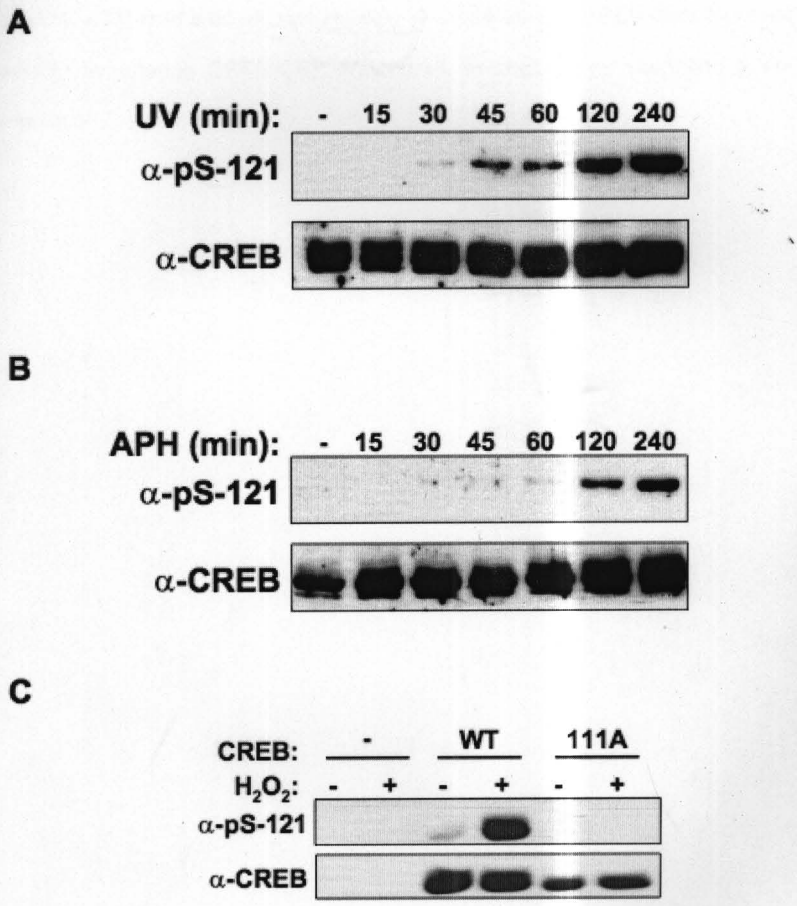
A
UV (min): - 15 30 45 60 120 240
α-pS-121
α-CREB
B
APH (min): - 15 30 45 60 120 240
α-pS-121
α-CREB
C
CREB: - WT 111A
H2O2: - + - + - +
α-pS-121
α-CREB

FIGURE 2.11. A novel stress-induced ATM-CREB pathway. In response to DNA damaging stimuli, ATM phosphorylates CREB at Thr100, Ser111 and Ser121. ATM-mediated phosphorylation of CREB inhibits CREB transcriptional activity by altering CREB-CBP interaction, or possibly by recruiting a co-repressor.

FIGURE 2.11.

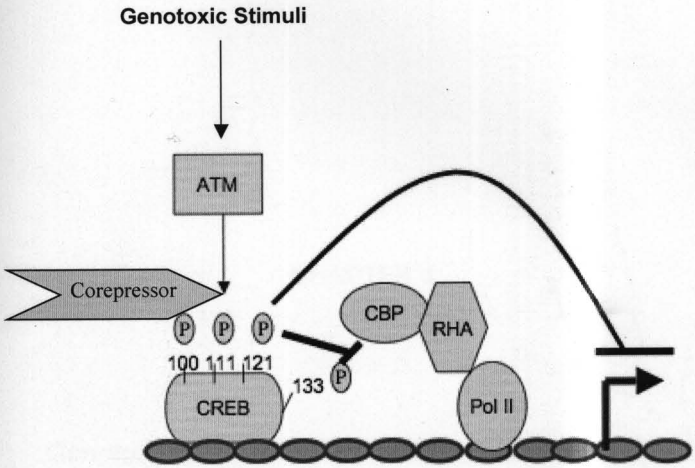
Genotoxic Stimuli
ATM
Corepressor
P
P
P
100 111 121
133
P
CREB
CBP
RHA
Pol II

CHAPTER 3

Genotoxic stimuli-induced HOXB13 transcriptional repression may be mediated by the ATM-CREB pathway

3.1. Abstract

The cyclic AMP response element binding protein (CREB) is a bZip family transcription factor that plays key roles in cell growth and survival. Previous work from our lab showed that the tumor suppressor protein kinase ATM (Ataxia-telangiectasia Mutated) phosphorylated CREB both *in vitro* and *in vivo* on a Ser/Thr-cluster domain. ATM-mediated phosphorylation of CREB inhibited CREB transcriptional activity by altering CREB's affinity for its transcriptional co-activator CBP (CREB Binding Protein). To establish the CREB target genes that may be regulated by the ATM-CREB pathway, we performed a comparative gene expression microarray analysis. This analysis identified homeobox transcription factor HOXB13, as a downstream target repressed by the ATM-CREB pathway. HOXB13 mRNA is downregulated upon exposure to ionizing radiation (IR). Using RNA interference (RNAi) we show that the IR-induced HOXB13 repression was dependent on both ATM and CREB, suggesting that the DNA-damage dependent regulation of HOXB13 may be mediated through the ATM-CREB pathway. Given that HOXB13 is implicated as an anti-proliferative and pro-apoptotic factor in cells, we propose that ATM-mediated phosphorylation of CREB may promote cellular survival by repressing the functions of HOXB13.

3.2. Introduction

We had previously shown that in response to genotoxic stress, ATM phosphorylated CREB *in vitro* and *in vivo* on at least two serine residues proximal to the KID (1). ATM-mediated phosphorylation of CREB inhibited CREB transcriptional activity by altering CREB-CBP interaction (1). To establish the CREB target genes that may be regulated by the ATM-CREB pathway, we performed comparative gene expression microarray analysis. We identified HOXB13, a member of homeobox gene superfamily, as one of the potential targets regulated by the ATM-CREB pathway.

Homeobox genes encode transcription factors that play important roles in development in vertebrates (2). Members of the homeobox superfamily of genes contain a highly conserved C-terminal 61-amino acid sequence known as HomeoDomain (HD) that is required for binding to sequence specific DNA motifs (3). Relatively few *bona fide* cellular targets have been identified for specific homeobox genes *in vivo*. Among the genes identified are extracellular matrix proteins, adhesion molecules, growth factors and cell cycle regulators (4,5). To date more than 200 vertebrate homeobox genes have been identified which are divided into six subfamilies.

The largest subfamily of homeobox genes is the HOX genes that play crucial roles in embryogenesis (6). So far 39 vertebrate HOX genes have been identified

which are organized into 4 chromosomal clusters – A, B, C and D – which have arisen by duplication and divergence of a primordial HOX gene (7). Each cluster has 9 to 11 members that are placed in 13 paralogous groups based on homeobox sequence similarity. An association exists between the arrangement of HOX genes in a cluster and their order of expression during development. For instance, the expression of 3' genes (groups 1-4) occurs early in development and is restricted to the anterior regions, while the expression of 5' genes (groups 9-13) is delayed and limited to the posterior.

HOXB13, the most 5' gene in the HOXB cluster and the last identified member of the HOX family (8), is a non-essential gene, probably owing to the functional redundancy of other HOX isoforms (9). The mouse and human homologs of HOXB13 share 100% amino acid identity in HD and ~91% identity in the remainder of the gene. HOXB13 deficient mice are viable and fertile, and the only distinguishing phenotypic characteristic is a long and thick tail. The overgrowth phenotype observed in HOXB13 deficient animals is attributed to increased cell proliferation and decreased apoptosis, emphasizing the role for HOXB13 as an anti-proliferative and pro-apoptotic factor (9). The direct target genes of HOXB13 that may mediate its cellular functions have not yet been identified. The function of HOXB13 as a tumor suppressor is underscored by the fact that this gene is often lost in a variety of cancers including those of renal, skin and prostrate (10).

In this report we show that HOXB13 mRNA is downregulated upon exposure to IR. Using RNA interference (RNAi) we show that the IR-induced HOXB13 repression is dependent on both ATM and CREB, suggesting that the DNA damage-dependent regulation of HOXB13 may be mediated through the ATM-CREB pathway. Given that HOXB13 is implicated as an anti-proliferative and pro-apoptotic factor in cells, we propose that ATM-mediated phosphorylation of CREB may promote cellular survival by repressing the functions of HOXB13.

3.3. Materials and Methods

Cell Culture and Antisera. HEK293T cells and CREB-deficient Mouse Embryonic Fibroblasts (CREB-/- MEFs) were maintained in DMEM supplemented with 10% Fetal Calf Serum (FCS). CEM T cells were grown in RPMI-1640 media containing 10% FCS and 10mM HEPES. Antibody suppliers included Genetex (κ-ATM) and Upstate Cell Signaling Solutions (κ-CREB and κ-Tubulin).

Transfections. $1x10^6$ HEK293T cells were transiently transfected with 3μg scrambled control siRNA (Scri) or siRNA targeted specifically towards ATM (ATMi) or CREB (CREBi) using standard calcium phosphate precipitation procedure. The ATMi and CREBi was provided as a SmartPool mixture of four annealed oligonucleotides (Dharmacon). A significant reduction in protein levels was apparent 48 hours post-siRNA transfection. For DNA transfections, 2-4ug of

plasmid DNA was transfected into 293T cells and CREB-/- MEFs using calcium phosphate precipitation procedure and Fugene 6 transfection reagent (Roche) respectively.

Protein Analysis. Cell extracts were prepared using lysis buffer containing 25mM HEPES, 300mM NaCl, 0.5% NP-40 and protease inhibitors (5 μg/ml leupeptin, 10 μg/ml pepstatin, 5 μg/ml aprotinin). 75μg of the extracts were boiled at 100°C for 10 minutes in 2X SDS sample loading buffer. The samples were separated on 10% SDS-PAGE gels and transferred to Immobilon-P PVDF membranes (Millipore). Membranes were blocked in Tris-buffered saline containing 0.2% Tween-20 (TBS-T) and 5% dried milk and incubated with the indicated primary antibodies diluted in blocking solution. After washing with TBS-T, the membranes were incubated with HRP-conjugated sheep anti-mouse or goat anti-rabbit secondary antibodies (Jackson) and developed using Supersignal Chemiluminescent Substrate (Pierce).

RNA Isolation and Quantitative Real Time PCR (qRT-PCR). Total RNA was isolated from HEK293T cells using the RNeasy Kit (Qiagen) according to manufacturer's instructions. Concentration of the isolated RNA was determined using BECKMAN DU-50 UV spectrophotometer. 1ug of total RNA was reverse transcribed to generate cDNA using iScript cDNA synthesis Kit (BioRad). The resulting cDNAs were amplified using iScript SYBR green PCR Kit (BioRad). Product accumulation was monitored by measuring SYBR green fluroscence in

the MyiQ Single Color Real Time PCR Detection System (BioRad). The cycling program is as follows : Step 1- 95°C for 3 min, Step 2 – 95°C for 0.30 min, 61°C for 0.30 min, 72°C for 0.30 min for 40 cycles, Step 3 - 95°C for 0.30 min and 55°C for 0.30 min. The PCR primers used in this study are as follows : HOXB13 5' aaggatatcgaaggcttgctggga 3', 3' tagttgacagcaggcatcagcgta 5' and GAPDH 5' aggttgtctcctgcgacttcaaca 3', 3' ttgtcattgagagcaatgccagcc 5'. The relative expression levels of each gene was determined from a standard curve obtained from known dilutions of cDNA. All mRNA expression data were normalized to expression of the housekeeping gene GAPDH in the corresponding sample. Duplicate samples from three experiments were utilized to generate the bar graphs.

Microarray Analysis. Total RNA was isolated from HEK293T cells using RNeasy Kit (Qiagen). Double stranded cDNA was generated and *in vitro* transcribed using T7 polymerase and biotinylated CTP and UTP to produce complementary RNA (cRNA). The biotinylated cRNA was purified using RNeasy columns (Qiagen), fragmented, and hybridized to human U133A Plus 2.0 gene chip arrays (Affymetrix, CA). After washing (using Affymetrix fluidics station), the bound cRNA was labeled with phycoerythrin-conjugated streptavidin. The array was scanned using a Affymetrix GeneArray Scanner 3000 which revealed the positions and intensities of fluorescent signals. The resulting data was analyzed using Affymetrix Gene Chip Operating Software v1.4 (GCOSv1.4.).

3.4. Results

Expression of a CREB3A mutant inhibits clonogenic survival. Previous data from our laboratory had shown that ATM phosphorylated CREB *in vivo* in response to genotoxic stimuli (1). As a first step to gaining insight into the function of this pathway, we sought to generate CREB-/- MEFs stably reconstituted with either a zeocin resistant plasmid encoding FLAGCREB wild type ($FLAGCREB^{WT}$) or a CREB mutant with alanine substitutions on all the ATM phosphorylation sites ($FLAGCREB^{3A}$). $1x10^6$ CREB-/- MEFs were transiently transfected with $FLAGCREB^{WT}$ or $FLAGCREB^{3A}$ using Fugene 6 transfection reagent. 24 hours later, the cells were trypsinized and counted using a heamocytometer. The cells were serially diluted in zeocin containing media to a concentration of 10000 cells / plate to 50 cells / plate. The cells were allowed to grow for 7-10 days in selection media. Whereas the $FLAGCREB^{WT}$ transfected cells formed several colonies after 10 days in culture, the $FLAGCREB^{3A}$ transfected cells failed to do so, suggesting that the ATM phosphorylation sites on CREB may be required for clonogenic survival (data not shown). Similar results were obtained upon infection of CREB-/- MEFs with $CREB^{WT}$ or $CREB^{3A}$ retroviruses (data not shown). Based on these data we propose that the ATM phosphorylation sites on CREB may function in pro-survival capacity.

Gene expression microarray analysis reveals ATM and CREB-dependent genes. We had previously shown that in response to genotoxic stimuli ATM

phopshorylated CREB in at least two serine residues (Ser-111 and Ser-121) *in vivo* (1). We hypothesized that this signal-specific phosphorylation event imparted specificity for CREB-dependent gene expression i.e., ATM-CREB pathway altered expression of a specific subset of CREB target genes. To address this hypothesis, HEK293T cells were either transfected with scrambled control siRNA (Scri) or siRNA targeted specifically towards ATM (ATMi) or CREB (CREBi). Western Blotting analysis revealed efficient decrease in ATM and CREB levels in ATMi and CREBi transfected samples respectively, as compared to control samples (data not shown). 48 hours later, the cells were either left untreated or treated with 20Gy IR for 4 hours. To address our hypothesis we employed two approaches – First, a focused approach using Real Time PCR to compare basal and damage-induced mRNA levels of CREB target genes with suspected functions in apoptosis, DNA repair, celll cycle regulation and oxidative stress responses. The list of genes that we examined included cell cycle regulators (PCNA, Cyclin D, Cyclin A, MCM3, RPA), Checkpoint Kinases (CHK1,CHK2), Cell survival regulators (BCL-2, MCL-1), Antioxidant defense enzymes (HO-1, MnSOD), and transcriptional regulators (c-fos and ICER). However this approach was unsuccessful in identifying the downstream target of this pathway. The second more unbiased approach utilized comparative gene expression microarray analysis to more broadly examine the impact of ATM-CREB pathway on global gene expression. This analysis identified approximately 70 genes including transcription factors, cell cycle regulators, extracellular matrix proteins and DNA repair factors that were differentially regulated in response to

IR in an ATM and CREB-dependent manner (Table 3.1.). We validated the results from microarray analysis using Real Time PCR with gene specific primers toward 9 of these genes. This subset included genes that were implicated in DNA replication, transcription and cell cycle including HOXB13, HOXD8, PDGF alpha, HEXIM1, E2F2, E2F7, BCL11A and CCT8 (Figure 3.1.). In this report we focus on a homeobox gene HOXB13 as a potential downstream target gene of the ATM-CREB pathway.

HOXB13 expression is downregulated in response to IR and H_2O_2. To examine if HOXB13 expression was regulated in response to DNA damage, we exposed HEK293T cells to varying doses of IR (0-20Gy) for 4 hours and performed qRT-PCR analysis using primers specific for HOXB13 gene. HOXB13 mRNA levels from each sample was normalized to the amount of GAPDH from the corresponding sample. As shown in Figure 3.2.A, the HOXB13 mRNA levels decreased in response to IR treatment by approximately 50%. The decrease in HOXB13 levels was apparent at doses as low as 2Gy of IR. We then sought to examine the kinetics of the IR-dependent HOXB13 repression. HEK293T cells were exposed to 20Gy IR for varying time points (0-6h) and qRT-PCR analysis was performed. HOXB13 levels decreased in response to IR within 2 hours of treatment and remained low through the entire length of the experiment (Figure 3.2.B). Similar decreases in HOXB13 expression levels was observed using H_2O_2 as stimulus (data not shown). Intriguingly, similar experiments performed with CEMT cells showed a more pronounced, greater than 100-fold decrease in

HOXB13 mRNA (Figure 3.4.). The IR-induced repression in CEMT cells was apparent at doses as low as 1Gy of IR (Figure 3.3.A). Surprisingly, the effects on HOXB13 mRNA are rapid, occurring within an hour of exposure to stress stimuli (Figure 3.3.B). Collectively these data suggest that HOXB13 levels are suppressed in response to genotoxic stimuli.

IR-induced suppression of HOXB13 is ATM and CREB-dependent. To determine if the decrease in HOXB13 mRNA in response to DNA damage required ATM and CREB, HEK293T cells were transiently transfected with either Scri or ATMi or CREBi. 48 hours later, the cells were either left untreated or treated with 20Gy IR for 4 hours. qRT-PCR was performed with primers specific for HOXB13. As shown in Figure 3.3., IR-induced repression of HOXB13 mRNA by ~3 fold in Scri transfected cells. In the absence of any DNA damage, transfection with ATMi or CREBi resulted in slight decrease in levels (~20-30%) of HOXB13, suggesting that ATM and CREB are marginally required for the basal expression of HOXB13. Interestingly, we consistently observed that in response to IR treatment, both the ATMi and CREBi transfected cells failed to repress HOXB13 mRNA. Based on these data we conclude that the IR-induced repression of HOXB13 requires both ATM and CREB, suggesting that the DNA-damage dependent-regulation of HOXB13 may be mediated through the ATM-CREB pathway. Direct examination of the contribution of the ATM phosphorylation sites to IR-induced HOXB13 repression cannot be addressed at

the present time because of our inability to generate surviving $CREB^{3A}$ expressing clones in a CREB-/- background (data not shown).

3.5. Discussion

We had previously reported that in response to stress stimuli, ATM phosphorylated CREB *in vivo* (1). We also showed that ATM-mediated phosphorylation of CREB inhibited CREB transcriptional activity by altering CREB-CBP interaction (1). To establish the CREB target genes that may be regulated by the ATM-CREB pathway, we performed a comparative gene expression microarray analysis. This analysis identified homeobox transcription factor HOXB13, as a downstream target repressed by the ATM-CREB pathway. In this report we show that HOXB13 mRNA is downregulated upon exposure to IR. Using RNA interference we show that the IR-induced HOXB13 repression was dependent on both ATM and CREB, suggesting that the DNA-damage dependent regulation of HOXB13 may be mediated through the ATM-CREB pathway. Given that HOXB13 is implicated as an anti-proliferative and pro-apoptotic factor in cells, we propose that ATM-mediated phosphorylation of CREB may promote cellular survival by repressing the functions of HOXB13.

In the absence of any DNA damage, reducing the levels of CREB in cells using RNA interference resulted in only a slight decrease (~30%) in HOXB13 expression. This suggests that other transcription factors are required for basal

expression of HOXB13. Nevertheless, it is clear from our data that the IR-induced repression of HOXB13 is mediated through both ATM and CREB. The mechanism by which ATM-CREB pathway contributes to HOXB13 repression is presently unclear. One possibility is that ATM-mediated phosphorylation of CREB recruits a co-repressor, which inhibits the expression of HOXB13. For instance, ATM target sites on CREB may recruit a Histone Deacetylase (HDAC) that can cause transcriptional repression. It has been previously shown that CREB can bind to class I HDAC and this interaction required at least one of the two glutamine rich regions (Q1 or Q2) in CREB (11). Another possibility is that upon phosphorylation of ATM sites in CREB, the affinity of CREB to bind the HOXB13 promoter is decreased. Careful examination of HOXB13 promoter region reveals a single half-CRE binding site for CREB. CREB has been shown to occupy half-CRE sites with lower affinity. Our previous unpublished findings using electrophoretic mobility shift assays did not reveal a role for the ATM phosphorylation sites in altering DNA binding activity of CREB. However these experiments utilized a synthetic 3XCRE as probe, which may not recapitulate CREB binding to chromatin. It is fully possible that the genotoxic stress-induced changes in DNA binding activity of CREB may be promoter-context dependent. In the future, chromatin immunoprecipitation assays will be performed to determine if CREB directly binds to the HOXB13 promoter and if this binding is altered by IR treatment.

Previous studies have shown that overexpression of HOXB13 in cancer cells results in decreased cell proliferation and increased apoptosis (12). Conversely, a small interfering RNA targeted specifically towards HOXB13 in cells resulted in increased proliferation and decreased apoptosis in prostrate cancer cells (12). However, the HOXB13 target genes that mediate its functions in cell growth and survival are currently unknown. Our previous studies revealed that a $CREB^{3A}$ mutant was more active than the $CREB^{WT}$ in gene reporter assays. Based on these data, it is conceivable that the inability of CREB3A to form surviving colonies may be a result of increased HOXB13 function in these cells. HOXB13 is implicated as a tumor suppressor in various cancers including renal, prostrate and skin (13,14). Considering that HOXB13 contains a consensus ATM phosphorylation site, it will be interesting to determine if HOXB13 function is also directly regulated by ATM.

The magnitude of the effect of HOXB13 repression upon exposure to stress stimuli varies in different cell lines. Whereas in HEK293T cells, IR induces repression of HOXB13 by 2-fold (Figure 3.2.), in CEMT cells we observe greater than a 100-fold repression (Figure 3.4.). The IR-induced decrease in HOXB13 in CEMT cells occurs at very low doses of IR and within 1 hour of treatment (Figure 3.4.). HOXB13 contains a very long 3' untranslated region that harbors several motifs that may decrease its RNA stability. The magnitude of HOXB13 repression may also be one way to explain differential sensitivities of these cells to IR. For instance, HEK293T are more resistant to killing by IR than CEMT cells. It is also

important to monitor changes in protein levels of HOXB13 in these cell lines in response to genotoxic stimuli. We are unable to address this at the present time due to the unavailability of a commercially available HOXB13 antibody.

In response to genotoxic stimuli, ATM activates transcription factors that are implicated in both pro-apoptotic and anti-apoptotic endpoints. For example, in response to DNA damage, ATM causes stabilization of p53 levels in cells through direct phopshorylation at Ser-15 (15). Stress-induced p53 accumulation results in activation of pro-apoptotic p53 target genes including BAX, NOXA and PUMA (16). In addition a series of p53-inducible genes (PIGs) are rapidly upregulated in response to DNA damage and promote the execution of mitochondrial death pathways (16). In response to the same stimuli, ATM also upregulates pro-survival pathways through direct activation of transcription factor NFκB which has been implicated to function as an anti-apoptotic factor (17). Our findings demonstrate yet another putative pro-survival pathway initiated by ATM through the direct phopshorylation of CREB. We propose that the pro-survival functions of the ATM-CREB pathway may be mediated through the repression of HOXB13. Since cells activate both pro- and anti-apoptotic pathways in response to IR, it is reasonable to suggest that the ultimate fate of the DNA-damaged cell will depend on the relative balance of ATM-regulated death and survival pathways.

3.6. References

1. Shi Y, Venkataraman SL, Dodson GE, Mabb AM, LeBlanc S, Tibbetts RS. (2004) Direct regulation of CREB transcriptional activity by ATM in response to genotoxic stress. Proc Natl Acad Sci U S A. 101(16):5898-903.

2. Holland PW, Takahashi T.(2005) The evolution of homeobox genes: Implications for the study of brain development.Brain Res Bull. 66(4-6):484-90. Review.

3. Scott MP, Tamkun JW, Hartzell GW 3rd. (1989) The structure and function of the homeodomain. Biochem Biophys Acta. 989(1):25-48. Review.

4. Del Bene F, Wittbrodt J. (2005) Cell cycle control by homeobox genes in development and disease.Semin Cell Dev Biol. 16(3):449-60. Review.

5. Cillo C, Cantile M, Faiella A, Boncinelli E. (2001) Homeobox genes in normal and malignant cells. J Cell Physiol. 188(2):161-9.

6. Mark M, Rijli FM, Chambon P.(1997) Homeobox genes in embryogenesis and pathogenesis. Pediatr Res. 42(4):421-9.

7. Hoegg S, Meyer A. (2005) Hox clusters as models for vertebrate genome evolution.Trends Genet. 21(8):421-4. Review.

8. Zeltser L, Desplan C, Heintz N. (1996) Hoxb-13: a new Hox gene in a distant region of the HOXB cluster maintains colinearity. Development. 122(8):2475-84.

9. Economides KD, Zeltser L, Capecchi MR (2003) Hoxb13 mutations cause overgrowth of caudal spinal cord and tail vertebrae. Dev Biol. 256(2):317-30.

10. Okuda H, Toyota M, Ishida W, Furihata M, Tsuchiya M, Kamada M, Tokino T, Shuin T (2005) Epigenetic inactivation of the candidate tumor suppressor gene HOXB13 in human renal cell carcinoma. Oncogene. 1-10.

11. Canettieri G, Morantte I, Guzman E, Asahara H, Herzig S, Anderson SD, Yates JR 3rd, Montminy M. Attenuation of a phosphorylation-dependent activator by an HDAC-PP1 complex. Nat. Struct. Biol. (2003) 10(3):175-81.

12. Jung C, Kim RS, Lee SJ, Wang C, Jeng MH (2004) HOXB13 homeodomain protein suppresses the growth of prostate cancer cells by the negative regulation of T-cell factor 4. Cancer Res. 64(9):3046-51.

13. Anbazhagan R, Raman V. (1997) Homeobox genes: molecular link between congenital anomalies and cancer.Eur J Cancer. 33(4):635-7

14. Cillo C. HOX genes in human cancers.Invasion Metastasis. 1994-95;14(1-6):38-49. Review.

15. Tibbetts, R. S., Brumbaugh, K. M., Williams, J. M., Sarkaria, J. N., Cliby, W. A., Shieh, S. Y., Taya, Y., Prives, C. & Abraham, R. T. (1999) A role for ATR in the DNA damage-induced phosphorylation of p53.Genes Dev. 13, 152-157.

16. Schuler M, Green DR.(2001) Mechanisms of p53-dependent apoptosis. Biochem Soc Trans. 29(Pt 6):684-8. Review.

17. Lee SJ, Dimtchev A, Lavin MF, Dritschilo A, Jung M.(1998) A novel ionizing radiation-induced signaling pathway that activates the transcription factor NF-kappaB.Oncogene. 17(14):1821-6.

3.7. Figure Legends

Table 3.1. Gene Expression Analysis. HEK293T cells were either transfected with scrambled control siRNA (Scri) or siRNA targeted specifically towards ATM (ATMi) or CREB (CREBi). 48 hours later, the cells were either left untreated or treated with 20Gy IR for 4 hours. Total RNA was isolated using RNeasy Kit. Double stranded cDNA was generated and *in vitro* transcribed using T7 polymerase and biotinylated CTP and UTP to produce cRNA. The biotinylated cRNA was purified using RNeasy columns, fragmented, and hybridized to human U133A Plus 2.0 gene chip arrays. The array was scanned using Affymetrix GeneArray Scanner 3000 that revealed the positions and intensities of fluorescent signals. The resulting data was analyzed using Affymetrix Gene Chip Operating Software v1.4 (GCOSv1.4.). The genes that showed greater than 2 fold increase (Table 3.1.A) or decrease (Table 3.1.B) upon IR treatment in an ATM and CREB-dependent manner are tabulated here.

Table 3.1.a. Genes that were upregulated upon exposure to IR in an ATM and CREB dependent manner -

Function	Gene Name
DNA replication Checkpoint	CTD1 --DNA replication factor
ATP hydrolysis	ATAD 2 ATPase
N/A	Loosely resembles two proteins
nucleosome assembly	nucleosome assembly protein 1-like 2--NAPL2--
Ubiquitin assembly	F-box and leucine-rich repeat protein 17--FBXL17
ER Golgi transport	coatomer protein complex, subunit alpha(COPA)
Negative regulator of CDK	hexamethylene bis-acetamide inducible 1--HEXIM1
DNA replication and cell cycle	MCM5 minichromosome maintenance deficient 5, cell division cycle 46
DNA replication and cell cycle	MCM4 minichromosome maintenance deficient 4
protein binding	THUMP domain containing 3--THUMPD3
post-replication repair	WD repeat domain 33(WDR33
Cell cycle/Proliferation/Signaling	E2F1
Steroid signaling	Homo sapiens steroid-5-alpha-reductase (SRD5A2)
N/A	Loosely resembles two proteins
Steroid biosynthesis	Isopentenyl-diphosphate delta isomerase 1(IDI1
Growth Inhibitor	inhibitor of growth family, member 3--ING3
DNA repair and transcription	BTG family, member 2 (BTG2)
Cell cycle/Proliferation/Signaling	E2F transcription factor 2 (E2F2)
N/A	MSTPO23
Actin binding protein	ARP3
Anion transport	Solute carrier family 4, sodium bicarbonate cotransporter
protein binding	Salvador homolog 1 (Drosophila)--SAV1
Cell cycle/Proliferation/Signaling	E2F7

Table 3.1.b. Genes repressed upon IR treatment in an ATM and CREB-dependent manner –

Function	Gene Name
protein folding and cellular metabolism	Chaperonin containing TCP1, subunit 8 (theta) CCT8
Transcription factor	SATB family member 2 (SATB2)
DNA replication	MCM3 minichromosome maintenance deficient 3 associated protein antisense (MCM3PAS)
N/A	chromosome 10 open reading frame 41
Electron Transport	cytochrome P450, family 2, subfamily R, polypeptide 1-CYP2R1
N/A	Transcribed Locus
Transcription factor	Homeobox gene HOXD8
N/A	MDS009- DTW containing domain
N/A	N/A
N/A	Mouse and Zebra Fish/ BAC clones
tRNA processing	dihydrouridine synthase 4-like (S. cerevisiae)-DUS4L
Extracellular matrix protein	Multimerin 2 (MMRN2)
Extracellular matrix protein	Fibronectin type III domain containing 3A
Development	Plexin A2 (PLXNA2)- neuronal
Check	hydrolethalus syndrome 1--HYLS1
Sugar Binding	FLJ44186 protein
Cell cycle/Proliferation/Signaling	PDGF alpha
pyridine nucleotide biosynthesis	chromosome 9 open reading frame 95
Check	Aconitase
cell proliferation, hormone response	RAS-like, estrogen-regulated, growth inhibitor- (RERG)
N/A	Transcribed locus, weakly similar to NP_114018.1 flotillin 2 (Rat)
N/A	Loosely resembles several proteins
Metabolism	Glyceronephosphate O-acyltransferase
Protein Glycosylation	ST6GALNAC3
Transcription	myeloid/lymphoid or mixed-lineage leukemia translocated to, 10
Chromatin assembly and disassembly	ARID4B
hypothetical protein	MGC45438
N/A	loosely resembles couple of proteins in

	C.Elegans
N/A	FAM51A1
N/A	similar to KIAA1503 protein [Homo sapiens]
Cell adhesion	Integrin, alpha V (vitronectin receptor, alpha polypeptide, antigen CD51)
mRNA splicing	LSM10, U7 small nuclear RNA associated
Extracellular matrix protein	Heparan sulfate sulfotransferase (HS3ST3A1)
Negative Regulator of cell cycle and apoptosis	PHD finger protein 17 (PHF17) - chromatin remodeling and prot-prot interactions
Transcription	hepatocyte nuclear factor 4, gamma-HNF4G
N/A	Mostly BACs
Cell cycle and polarity	par-6 partitioning defective 6 homolog beta (C. elegans)--PARD6B
Transcription	B-cell CLL/lymphoma 11A (zinc finger protein)--BCL11A
Transcription, Apoptosis	death associated transcription factor 1 (DATF1)
Transcription	Zinc Finger protein 278
Transcription and Development	Homeobox gene HOX B13
N/A	Trichohyalin and coiled-coil domain containing 18 (CCDC18)
Transcription	Zinc Finger protein 165
ATP hydrolysis	ATPase 6 in mitochondria
Electron Transport	cytochrome P450, family 26, subfamily A, polypeptide 1--CYP26A1
Transcription	Zinc finger protein 99
Negative Regulator of cell cycle and apoptosis	mutated in colorectal cancers--(MCC)
protein transport	Sorting nexin 12 (SNX12)
N/A	Homo sapiens gene for seven transmembrane helix receptor
Ion transport	ATP synthase, H+ transporting, mitochondrial F0 complex, subunit s (factor B)--ATP5S
cAMP hydrolysis	Phosphodiesterase 4A (PDE4A)
GPCR signaling	RHOU (Ras family small GTPase)

FIGURE3.1. Validation of microarray analysis by Real Time PCR. HEK293T cells were transfected with scrambled control siRNA (Scri), or an siRNA targeted specifically towards ATM (ATMi) or CREB (CREBi). 48 hours later, the cells were either left untreated or treated with 20Gy IR for 4 hours. Total cellular RNA was isolated using RNeasy Kit. 1ug of total RNA was reverse transcribed to generate cDNA using iScript cDNA synthesis Kit. The resulting cDNAs were amplified using the iScript SYBR green PCR Kit and Quantitative Real Time PCR with gene-specific primers was performed using MyiQ Single Color Real Time PCR Detection System. All mRNA expression data was normalized to expression of the housekeeping gene GAPDH in the corresponding sample.

FIGURE 3.1.

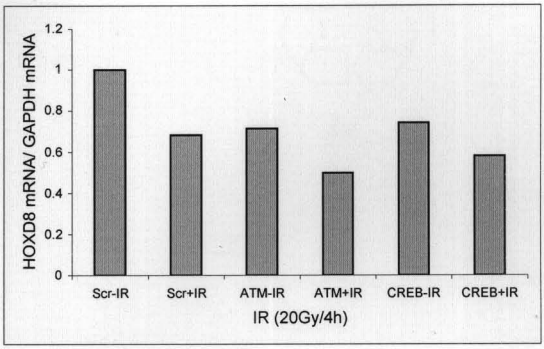
HOXD8 mRNA/ GAPDH mRNA
1.2
1
0.8
0.6
0.4
0.2
0
Scr-IR
Scr+IR
ATM-IR
ATM+IR
CREB-IR
CREB+IR
IR (20Gy/4h)

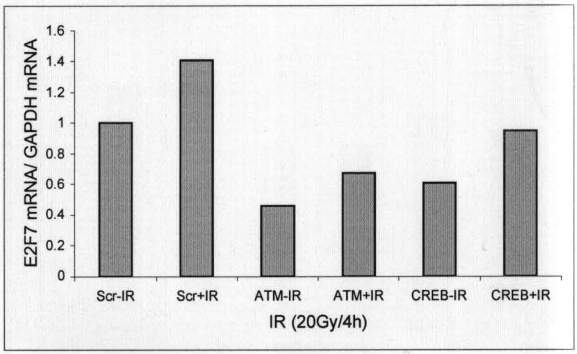
E2F7 mRNA/ GAPDH mRNA
1.6
1.4
1.2
1
0.8
0.6
0.4
0.2
0
Scr-IR
Scr+IR
ATM-IR
ATM+IR
CREB-IR
CREB+IR
IR (20Gy/4h)

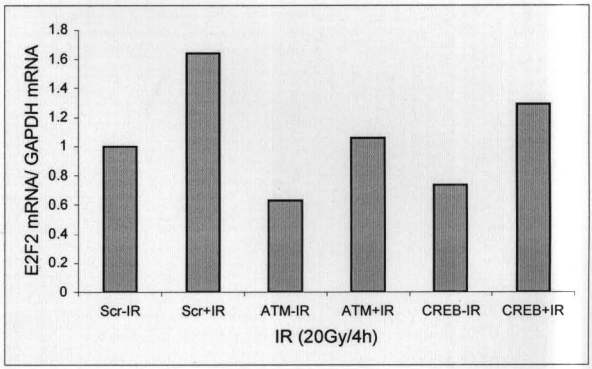
E2F2 mRNA/ GAPDH mRNA
1.8
1.6
1.4
1.2
1
0.8
0.6
0.4
0.2
0
Scr-IR
Scr+IR
ATM-IR
ATM+IR
CREB-IR
CREB+IR
IR (20Gy/4h)

FIGURE 3.1. (Contd.)

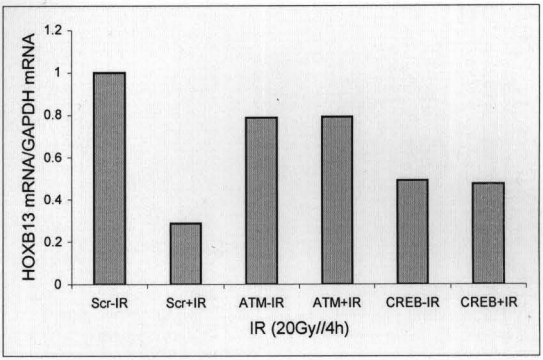

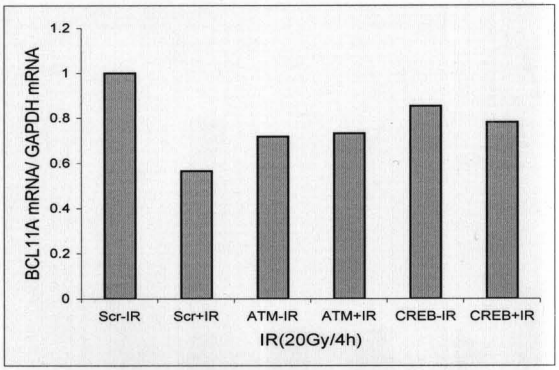

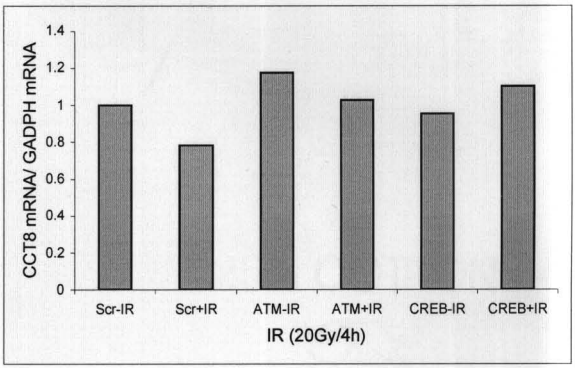

FIGURE 3.1. (Contd.)

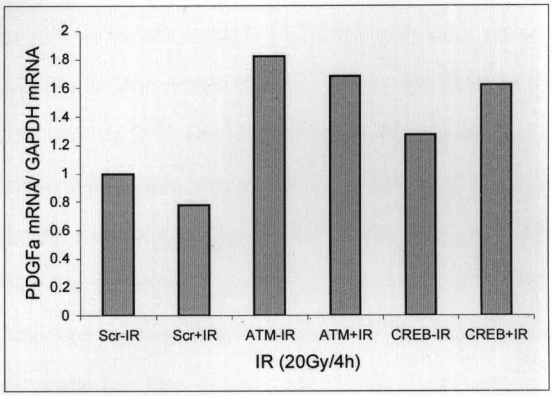

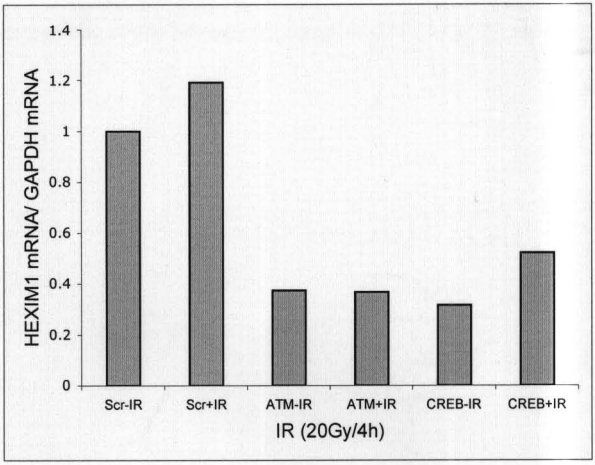

FIGURE 3.2. HOXB13 mRNA is downregulated upon exposure to genotoxic stress stimuli. HEK293T cells were either left untreated or treated with **(A)** varying doses of IR for 4 h, or **(B)** 20Gy of IR for varying time points. Total cellular RNA was isolated using RNeasy Kit. 1ug of total RNA was reverse transcribed to generate cDNA using iScript cDNA synthesis Kit. The resulting cDNAs were amplified using the iScript SYBR green PCR Kit and Quantitative Real Time PCR was performed using the MyiQ Single Color Real Time PCR Detection System. Duplicate samples from three experiments were utilized to generate the bar graphs. All mRNA expression data was normalized to expression of the housekeeping gene GAPDH in the corresponding sample.

FIGURE 3.2.

A

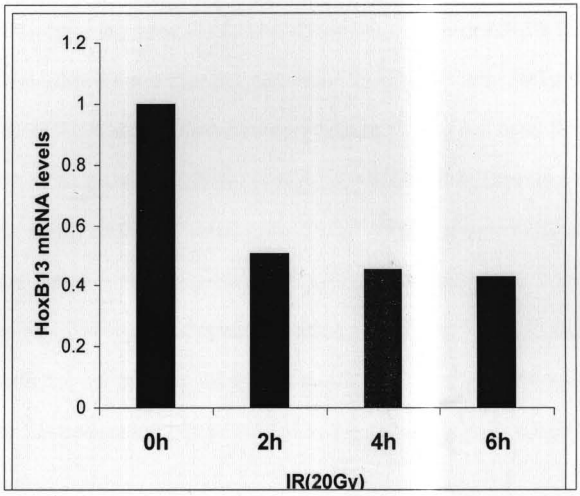
HoxB13 mRNA levels
1.2
1
0.8
0.6
0.4
0.2
0
0h
2h
4h
6h
IR(20Gy)

B

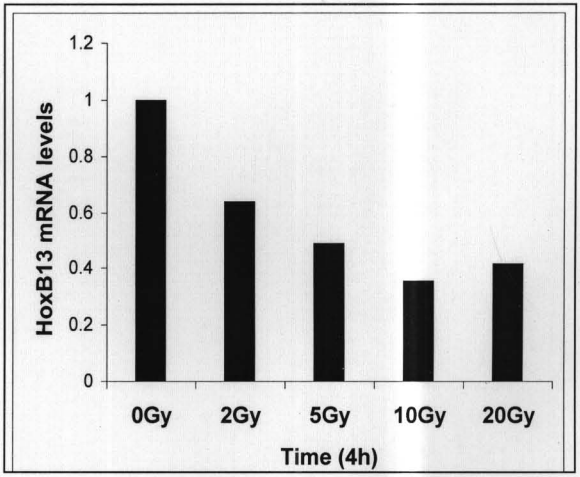
HoxB13 mRNA levels
1.2
1
0.8
0.6
0.4
0.2
0
0Gy
2Gy
5Gy
10Gy
20Gy
Time (4h)

FIGURE 3.3. IR-induced HOXB13 repression is ATM- and CREB-dependent. HEK293T cells were transfected with scrambled control siRNA (Scri), or an siRNA targeted specifically towards ATM (ATMi) or CREB (CREBi). 48 hours later, the cells were either left untreated or treated with 20Gy IR for 4 hours. Total cellular RNA was isolated using RNeasy Kit. 1ug of total RNA was reverse transcribed to generate cDNA using iScript cDNA synthesis Kit. The resulting cDNAs were amplified using the iScript SYBR green PCR Kit and Quantitative Real Time PCR was performed using the MyiQ Single Color Real Time PCR Detection System. Duplicate samples from three experiments were utilized to generate the bar graphs. All mRNA expression data was normalized to expression of the housekeeping gene GAPDH in the corresponding sample.

FIGURE 3.3.

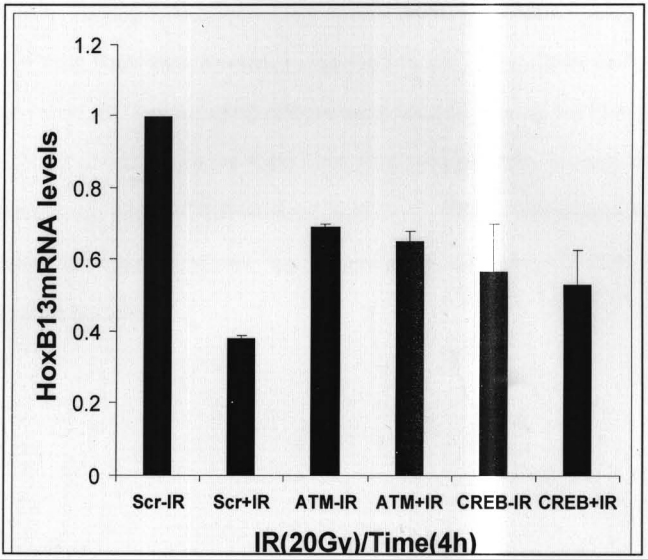
HoxB13mRNA levels
1.2
1
0.8
0.6
0.4
0.2
0
Scr-IR
Scr+IR
ATM-IR
ATM+IR
CREB-IR
CREB+IR
IR(20Gy)/Time(4h)

FIGURE 3.4. IR-induced HOXB13 repression in CEM T cells. CEMT cells were either left untreated or treated with **(A)** varying doses of IR for 4 h, or **(B)** 10Gy of IR for varying time points. Total cellular RNA was isolated using RNeasy Kit. 1ug of total RNA was reverse transcribed to generate cDNA using iScript cDNA synthesis Kit. The resulting cDNAs were amplified using the iScript SYBR green PCR Kit and Quantitative Real Time PCR was performed using the MyiQ Single Color Real Time PCR Detection System. All mRNA expression data was normalized to expression of the housekeeping gene GAPDH in the corresponding sample.

FIGURE 3.4.

A

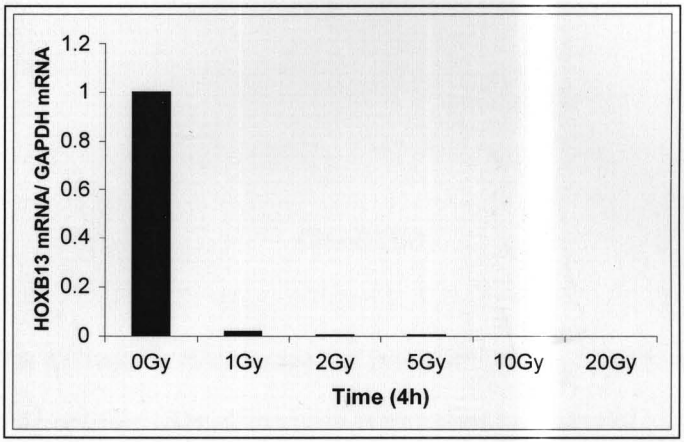
HOXB13 mRNA/ GAPDH mRNA
1.2
1
0.8
0.6
0.4
0.2
0
0Gy
1Gy
2Gy
5Gy
10Gy
20Gy
Time (4h)

B

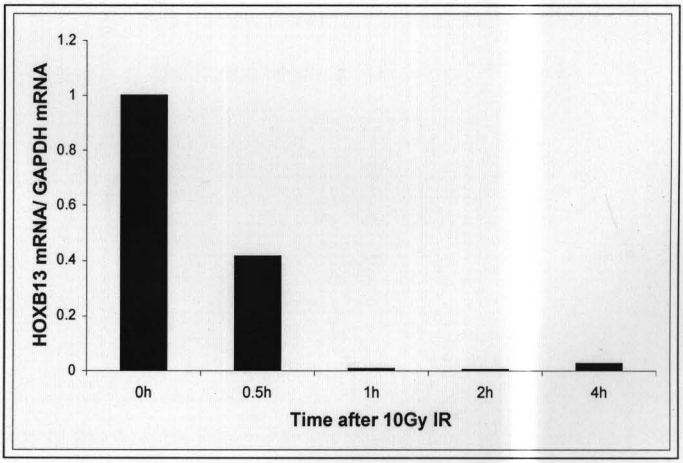
HOXB13 mRNA/ GAPDH mRNA
1.2
1
0.8
0.6
0.4
0.2
0
0h
0.5h
1h
2h
4h
Time after 10Gy IR

CHAPTER 4

ATR Activation Necessary but not Sufficient for p53 Induction and Apoptosis in Hydroxyurea-Hypersensitive Myeloid Leukemia

Sujatha Kumar, Gerald E. Dodson, Anthony Trinh,

Joel R. Puchalski, and Randal S. Tibbetts

A version of this chapter was published in 2005 in *Cell Cycle* 4(11):1665-1672.

4.1. ABSTRACT

Hydroxyurea (HU) is a competitive inhibitor of ribonucleotide reductase that is used for the treatment of myeloproliferative disorders. HU inhibits DNA replication and induces apoptosis in a cell type-dependent manner, yet the relevant pathways that mediate apoptosis in response to this agent are not well characterized. In this study, we employed the human myeloid leukemia 1 (ML-1) cell line as a model to investigate the mechanisms of HU-induced apoptosis. Exposure of ML-1 cells to HU caused rapid cell death that was accompanied by hallmark features of apoptosis, including membrane blebbing, phosphatidylserine translocation, and caspase activation. HU-induced apoptosis required new protein synthesis, was induced by HU exposures as short as 15 min, and correlated with the accumulation of p53 and induction of the p53 target gene PUMA. p53 induction in ML-1 cells was ATR dependent and downregulation of p53 through RNAi delayed HU-induced apoptosis. HU did not induce p53 or induce apoptosis in Molt-3 leukemia cells, even though exposure to HU induced a comparable level of DNA damage and robustly activated the ATR pathway. The microtubule inhibitor nocodazole suppressed HU-induced p53 accumulation in ML-1 cells suggesting that a microtubule-dependent event contributes to p53 induction and apoptosis in this cell line. Our findings outline an HU-induced cell death pathway and suggest that activation of the ATR is necessary, but not sufficient, for stabilization of p53 in response to DNA replication stress.

4.2. INTRODUCTION

The objective of the present study was to examine the role of ATM-related Kinase ATR in regulating cellular survival after replication stress. The ATR protein kinase is a key regulator of cellular responses to HydroxyUrea (HU) and other forms of DNA replication stress. Known substrates for ATR and ATM include tumor suppressors p53 and BRCA1, the downstream effector kinases CHK1 and CHK2, and a host of other proteins that participate in DNA repair and cell cycle checkpoint regulation (19). ATR has been implicated in the G_2/M checkpoint (19-20). However, its most critical functions relate to its role as a regulator of DNA replication. ATR is an essential gene in mice that is also required for viability at the cellular level (20-22). ATR-deficient cells exhibit high levels of spontaneous and replication stress-induced DSBs that lead to loss of viability (20-24). ATR suppresses premature replication origin firing and enforces the S-M checkpoint, which delays mitosis in the presence of unreplicated DNA (25-29). These combined functions define ATR as a critical determinant of cell survival following DNA replication stress.

The S-phase checkpoint functions of ATR are mediated, in part, through phosphorylation and activation of its effector kinase, CHK1 (30-32). CHK1, in turn, phosphorylates the CDC25A phosphatase leading to its ubiquitylation and degradation (33). CHK1-mediated phosphorylation also negatively regulates the CDC25C phosphatase by promoting its association with 14-3-3 proteins and

nuclear export (34-35). Downregulation of CDC25A and CDC25C leads to inhibition of the CDK2 and CDK1 cyclin-dependent kinases, which mediate progression through S phase and mitosis, respectively (36). Thus, CHK1 elicits S-and G_2/M phase arrests, in part, by inactivation of CDK2 and CDK1. CHK1 is also implicated in the DNA damage-induced phosphorylation of p53 on Ser-20, which relieves p53 repression by MDM2 (37). Defects in CHK1 partially phenocopy ATR deficiency and are associated with premature mitosis, premature origin firing, defective homologous recombination, and sensitivity to anti-metabolites (38-45). Finally, a recent study described reduced or undetectable expression of CHK1 in a subset of aggressive leukemias suggesting that downregulation of CHK1 may occur during leukemogenesis (46).

Hydroxyurea (HU) has been used for the treatment of chronic myelogenous leukemia and other myeloproliferative disorders including polycythemia vera and essential thrombocytosis for more than 30 years (1). HU is a competitive inhibitor of ribonucleotide reductase (RNR), a tetrameric enzyme comprised of two regulatory (M-1) and two catalytic (M-2) subunits that catalyzes the rate-limiting step in the production of reduced deoxyribonucleoside triphosphates (dNTPs) (2). HU belongs to the anti-metabolite class of drugs that block key steps in DNA biosynthesis and are widely used to treat cancer. Clinically relevant examples include the nucleoside analogues 5-fluorouracil, an inhibitor of thymidylate synthase, and gemcitabine, which inhibits RNR and DNA polymerase alpha (3,4). Although each of these agents inhibits DNA synthesis, they also have unique

effects on DNA metabolism that contribute to their unique cytotoxicity profiles *in vitro* and anti-cancer properties *in vivo* (5).

Despite its clinical utility and well-characterized biochemical mechanism of action, the pathways through which HU exerts its cytotoxic effects in mammalian cells are less well understood. The p53 tumor suppressor has been implicated as a cell-type-dependent determinant of HU sensitivity. p53 expression was associated with apoptosis in IL-3-dependent bone marrow cells and EBV immortalized lymphoblasts, but other studies have failed to show a cause-and-effect link between p53 status and HU sensitivity (6-9). Interestingly, an earlier report showed that HU induced a transcriptionally inert form of p53 in human RKO colon carcinoma cells, though this may have been a cell-type dependent phenomenon (10,11). Stalled replication forks (RFs) arising secondary to dNTP depletion are a likely source of pro-apoptosis signals in HU-treated cells. Stalled RFs are recombination substrates that can be converted into cytotoxic DNA double-strand breaks (DSBs) (12-14). Studies using bacterial systems have shown that the homologous recombination (HR) pathway of DNA repair is essential for suppression of DSBs and for the reactivation of stalled RFs following exposure to replication inhibitors (15). HR is also important for the maintenance and restart of stalled RFs in mammals; defects in proteins required for HRR, including the RecA ortholog RAD51 are associated with accumulation of spontaneous DSBs during DNA replication (16). Members of the RecQ

helicase family of proteins, including BLM, are also important for recovery from DNA replication stress, perhaps through the suppression of deleterious recombination events (17).

In this report we have explored the cellular response to HU in a myeloid leukemia cell line (ML-1) derived from a patient with acute myelogenous leukemia (47). ML-1 cells express wild-type p53 and have been used as a model for studying DNA damage-induced cell cycle checkpoint activation and for investigating the anti-leukemic potential of nucleoside analogues (48-49). While screening a panel of leukemia cell lines for sensitivity to HU, we made the discovery that ML-1 cells are remarkably sensitive to this drug. Here, we characterize the HU sensitivity of ML-1 cells and explore the mechanism of HU-induced apoptosis. Our study provides evidence that an ATR-p53 pathway functions in a pro-death capacity in response to HU and that activation of ATR is necessary, but not sufficient, for p53 induction in response to DNA replication stress.

4.3. METHODS

Cell culture and antisera. All cell lines used in this study were maintained in RPMI containing 10% FBS and 10 mM HEPES. ML-1 cells were obtained from Dr. Scott Kaufmann (Mayo Clinic). HPB-ALL and Karpas 45 cell lines were kindly provided by Dr. Shigeki Miyamoto (University of Wisconsin-Madison).

Antibody suppliers included: Oncogene Research (κ-RPA32), Santa Cruz Biotechnology (κ-CHK1 (G-4), κ-p53 (DO-1)), Upstate Cell Signaling Solutions (κ-tubulin, κ-PARP, κ-PUMA), and R&D Systems (κ-CHK1-pS317, κ-p53-pS20). The ATR antibody has been previously published (50). Zeocin (Invitrogen) was used at a concentration of 0.5 μg/ml. Nocodazole (Sigma) was made as a 0.5 mg/ml stock in DMSO and added to a final concentration of 0.5 μg/ml 30-60 min prior to HU addition.

Protein analysis. A number of ML-1 nuclear proteins, including ATR, CHK1, RPA32, and p53 were resistant to extraction with our standard cell lysis buffer containing 25 mM HEPES, 300 mM NaCl, and 0.5% NP-40. Therefore, all extracts were prepared by boiling in SDS-PAGE sample loading buffer as follows: the cells were washed once in PBS and resuspended to a density of 1 x 10^7 cells/ml in PBS. An equal volume of 4X sample loading buffer (100 mM Tris-HCl pH 6.8, 8% SDS, 40% glycerol, 20% κ-mercaptoethanol, 0.008% bromophenol blue) was added and the samples were heated at 100°C for 10 min. One hundred microliters of each sample were separated on 10% SDS-PAGE gels and transferred to Immobilon-P PVDF membranes (Millipore). Membranes were blocked in Tris-buffered saline containing 0.2% Tween-20 (TBS-T) and 5% dried milk and incubated overnight at 4° C with the indicated primary antibodies diluted in blocking solution. After washing with TBS-T, the blots were incubated with HRP-conjugated sheep anti-mouse or goat anti-rabbit secondary antibodies

(Jackson) and developed using SuperSignal chemilluminescent substrate (Pierce).

Cell cycle analysis and apoptosis assays. For propidium iodide (PI) staining, 1 x 10^6 ML-1 cells were resuspended in 300 μl of PBS. The cells were fixed by the addition of 700 μl of ice-cold 100% ethanol while vortexing. The fixed cells were resuspended in PBS containing 20 μg/ml PI, 50 μg/ml RNAse A, and 0.2% Tween-20 and analyzed by flow cytometry. The data were plotted using the WinMDI shareware package (Stanford University). Annexin V staining was performed using the ApoAlert system (Clontech) according to the manufacturer's conditions. The caspase inhibitor cocktail used in this study contained 50 μM each of zVAD-FMK, YVAD-FMK, and DEVD-FMK (Bachem Bioscience), which were added 1 h prior to HU exposure.

Microscopy. For the phospho-H2AX analysis, ML-1 cells were treated with buffer or 3 mM HU and collected 1 h or 4 h later. The cells were cytospun onto glass slides and, fixed with 4% paraformaldehyde-PBS, and permeabilized in PBS containing 0.2% Triton-X 100 (PBS-T) for 10 min. The cells were then washed with PBS and blocked for 30 min in PBS containing 3% BSA and 2% goat serum prior to immunostaining overnight at 4° C with 2 μg/ml of κ-phospho-H2AX antibody diluted in blocking solution. The cells were washed three times in PBS-T and incubated for 1 h at room temperature with 0.4μg/ml FITC-conjugated

goat anti-mouse IgG (Caltag). The cells were washed twice with PBS-T, once in PBS, and mounted using SlowFade reagent (Invitrogen). A Carl Zeiss Axiovert 200 fluorescence microscope was used to visualize the samples.

RNA interference. Approximately 2 x 10^6 ML-1 cells were electroporated with 20 μl of 20 μM scrambled control siRNA or siRNA targeted to ATR or p53 (51). The p53 siRNA was provided as a SmartPool mixture of four annealed oligonucleotides (Dharmacon). Electroporation was carried out with a single 325V, 10 ms pulse using an ECM 80 Electro Square Porator (BTX). The cells were transferred to growth medium and allowed to recover for 48 h prior to drug treatment and analysis.

4.4. RESULTS

ML-1 cells are highly sensitive to HU. ML-1 is a p53-positive human myeloid leukemia cell line that has been used as a model to study apoptosis and cell cycle checkpoint induction by genotoxic stress (52-53). To examine whether ML-1 cells undergo apoptosis in response to HU, we exposed the cells to the drug for 2-8 h and then stained the cells with annexin V-FITC. Flow cytometric analysis revealed that ML-1 cells underwent extensive apoptosis in response to HU. Apoptosis was detectable by 4 h after treatment and was maximal by 6 h post-HU exposure, when approximately 40% of the cells stained positive for annexin V

(Figure 4.1.A). HU-induced apoptosis manifested as an accumulation of cells exhibiting a hypodiploid DNA content and a corresponding decrease in the S phase population, which is consistent with the mechanism of HU as an S-phase-specific cytotoxic agent (Figure 4.1.B). Bright field and fluorescence microscopy of HU-treated ML-1 cells revealed highly characteristic signs of apoptosis, including membrane blebbing and nuclear fragmentation (Figure 4.1.C). The DNA replication inhibitor aphidicolin also induced apoptosis in ML-1 cells with kinetics that were nearly indistinguishable from HU (data not shown).

We next compared the HU sensitivity of ML-1 to other leukemic cell lines. For this analysis we employed p53-deficient (K562, Jurkat) and p53 wild-type (Molt-3) cell lines. Each cell line was exposed to 3 mM HU for 6 h and apoptosis induction measured by annexin V staining and flow cytometry. ML-1 cells were more sensitive to HU than either of the p53-deficient cell lines, which failed to undergo appreciable apoptosis during the 6 h time course of the experiment (Figure 4.2.A). Although Molt-3 cells were susceptible to HU, they were quantitatively less sensitive than ML-1 cells; the viability of ML-1 cells decreased by 27% during the experiment, whereas the viability of Molt-3 cells decreased by 7%. Similar results were obtained when hypodiploid DNA content was used as a parameter of HU-induced apoptosis. A 4 h treatment with HU induced hypodiploid DNA in 32% of ML-1 cells, but only 4% of Molt-3 cells (Figure 4.2.B). The virtual absence of apoptosis in the p53-deficient K562 and Jurkat cell lines

following HU exposure is consistent with a key role for p53 in this process. However, the fact that p53-wild-type ML-1 and Molt-3 cells exhibit differential survival in response to HU indicates that p53 functional status is not the sole determinant of sensitivity to this drug.

The HU sensitivity of ML-1 cells could reflect a general hypersensitivity of this cell line to genotoxic stimuli. To test this hypothesis, we compared the apoptosis profiles of ML-1 and Molt-3 cells exposed to IR. In comparison to HU, 10 Gy of IR was a relatively weak inducer of apoptosis in ML-1 cells. Whereas HU induced apoptosis within 4 h, IR-induced apoptosis was not observed until 6-8 h after exposure, at which time approximately 25% of the cells were annexin V-positive (Figure 4.2.C and data not shown). The fraction of irradiated cells undergoing apoptosis remained nearly constant over the next 8 h. IR was a much stronger stimulus of apoptosis in Molt-3 cells. Molt-3 viability decreased from 82% to 29% 8 h after exposure to 10 Gy of IR, and further declined to 2% after 16 h (Figure 4.2.C). These results suggest that ML-1 cells are not generally hypersensitive to genotoxic stress, but instead may harbor specific defects that confer susceptibility to DNA replication inhibitors.

Characterization of HU-induced apoptosis in ML-1 cells. Given the rapidity of HU-induced apoptosis, we were interested in determining the minimum length of drug exposure required to induce cell death. Remarkably, exposure to HU for as

little as 15 min was sufficient to increase the fraction of annexin V-positive cells after 4 h (Figure 4.3.A). Increasing the HU exposure time to 1 h led to a corresponding increase in the apoptotic fraction, whereas longer exposures did not further augment cell death. This result indicates that the commitment phase of apoptosis in ML-1 cells occurs within 1 h of HU exposure and that ML-1 cells are unable to recover from a transient DNA replication block.

To further characterize HU-induced apoptosis in ML-1 cells, we measured the caspase-mediated cleavage of poly(ADP-ribose) polymerase (PARP), which serves as a reliable marker for genotoxin-induced apoptosis (54). Using antibodies that recognize full-length PARP and its major caspase cleavage product, we observed that the majority of PARP migrated as the full-length, non-cleaved form in asynchronously growing ML-1 cells (Figure 4.3.B). Exposure to HU resulted in PARP cleavage that was detectable at the 4 h time point. Both PARP cleavage and cell blebbing were blocked by pan-specific caspase inhibitors (Figure 4.3.C and data not shown), indicating that HU-induced caspase activation is causal for apoptosis.

Insight into the mechanism of apoptosis can be gleaned from assessing the requirement for *de novo* protein synthesis. To determine whether protein synthesis was required for HU-induced apoptosis, ML-1 cells were preincubated with the protein synthesis inhibitor cycloheximide (CHX, 5 μg/ml) for 30 min prior to the addition of HU. Cells were then incubated for an additional 4 h and stained

with annexin V-FITC and PI. The percentage of annexin V-positive cells increased from 2% to 9% following exposure to CHX alone, indicating that CHX is mildly toxic to ML-1 cells (Figure 4.4.A). However, CHX clearly antagonized HU-induced apoptosis. The annexin V-positive fraction declined from 29% in cells treated with HU, to 11% in cells treated with CHX and HU, which is similar to the level of apoptosis in cells treated with CHX alone. New protein synthesis is therefore required for HU-induced cell death in ML-1 cells.

HU-induced apoptosis correlates with p53 induction. The p53 tumor suppressor plays a critical role in apoptosis induction by genotoxic stimuli by facilitating the expression of pro-apoptosis genes including *BAX*, *PUMA*, *NOXA*, and factors that promote oxidative cellular damage (55). We therefore sought to determine whether induction of p53 correlated with apoptosis in HU-treated ML-1 cells. ML-1 or Molt-3 cells were mock treated or exposed to HU over a 4 h time course and cell extracts analyzed by SDS-PAGE and immunoblotting with a a-p53 antibody. Exposure of ML-1 cells to HU resulted in the induction of p53 that was detectable within 2 h of drug treatment and was maximal by the 4 h time point, at which time the cells demonstrated features of apoptosis (Figure 4.4.B). The level of p53 induction by HU was slightly lower than the level obtained following exposure to 10 Gy of IR. However, when one considers that the effects of HU are restricted to the 30-40% of ML-1 cells in S phase, the relative potencies of the two agents as inducers of p53 are comparable. In contrast, the

induction of p53 in HU-treated Molt-3 cells was weak, even though p53 was strongly induced by IR in this cell line (Figure 4.4.B). Thus, the induced levels of p53 in ML-1 and Molt-3 cells correlate with the relative sensitivities of these cell lines to HU. We also examined the expression of the p53-dependent target gene PUMA following HU exposure. PUMA protein levels exhibited transient induction 1 h after exposure to HU, suggesting its enhanced expression may precipitate apoptosis in ML-1 cells (Figure 4.4.C).

ATR-dependent induction of p53 is required for HU-induced apoptosis. The degree of p53 induction in ML-1 and Molt-3 cells correlated with their relative sensitivities to HU; ML-1 cells strongly induced p53 and were sensitive to HU, whereas Molt-3 cells weakly induced p53 and were comparatively resistant to HU. We therefore sought to directly test the importance of p53 for apoptosis induction and to establish the upstream requirements for p53 induction. To test whether p53 contributed to HU-induced apoptosis, we electroporated ML-1 cells with control siRNA or p53-specific siRNA and then challenged the cells with HU or vehicle 48 h later. Immunoblotting using κ-p53 and κ-PARP antibodies demonstrated that the basal and HU-induced levels of p53 were efficiently suppressed by the p53 siRNA (Figure 4.5.A). In contrast, the p53 siRNA did not block the expression or HU-induced phosphorylation of the 32 kDa subunit of replication protein A (RPA32). The suppression of p53 correlated with a dramatic

reduction in the amount of cleaved PARP at the 4 h time point, which strongly suggests that p53 is required for apoptosis induction.[141]

The upregulation and activation of p53 in response to genotoxic stress is promoted by ATM and ATR through direct and indirect mechanisms. ATM and ATR directly phosphorylate p53 on Ser-15, which antagonizes interactions between p53 and the E3 ubiquitin ligase HDM2 (18,56). ATM and ATR indirectly promote p53 activation through phosphorylation of the CHK2 and CHK1 kinases, respectively, which, in turn, phosphorylate p53 on Ser-20 (37,57). ATR has previously been implicated in the regulation of p53 in response to IR, UV light, and hypoxic cell stress (24, 50, 58-59). Given the importance of ATR as a mediator of HU-induced responses, we used RNAi to test whether HU-induced accumulation of p53 in ML-1 cells was ATR dependent. Electroporation of ML-1 cells with an ATR-specific small interfering RNA (siRNA), but not a control siRNA, suppressed ATR expression and attenuated p53 induction by HU (Figure 4.5.B). In contrast, an ATM siRNA did not substantially inhibit the induction of p53 in response to HU (data not shown). This result suggests that ATR contributes to p53 induction in HU-treated ML-1 cells, most likely via direct phosphorylation of Ser-15.

The phosphorylation of p53 on Ser-20 by the CHK1 and CHK2 protein kinases is believed to contribute to p53 induction and activation in response to genotoxic stress (37,60). The differential induction of p53 between ML-1 and Molt-3 cells

could therefore reflect a difference in Ser-20 phosphorylation state. To explore this possibility, we measured the HU-induced phosphorylation of p53 on Ser-20 in both ML-1 and Molt-3 cells. ML-1 cells exhibited p53 Ser-20 phosphorylation within 1 h of HU treatment or 2 h after exposure to the radiomimetic drug zeocin, which induces DSBs (Figure 4.5.C). In contrast, HU-induced Ser-20 phosphorylation was not detected in Molt-3 cells, even though zeocin strongly induced both Ser-20 phosphorylation and p53 accumulation (Figure 4.5.C). To test whether the absence of p53 Ser-20 phosphorylation in HU-treated Molt-3 cells was caused by defective activation of the ATR-CHK1 pathway, we measured the ATR-dependent phosphorylation of CHK1 on Ser-317 following HU exposure (31,51). HU-treatment induced CHK1 phosphorylation in Molt-3 and ML-1 cells, indicating that the ATR-CHK1 pathway is activated in both cell lines. Interestingly, the levels of Ser-317-phosphorylated CHK1, total CHK1, and ATR were greatly reduced in ML cells relative to Molt-3 cells (Figure 4.5.D). The expression level of both proteins in ML-1 cells was also clearly reduced when compared to the ATR and CHK1 levels in a panel of human leukemic cell lines (Figure 4.7.). The importance of the reduced levels of ATR and CHK1 in the context of HU-hypersensitivity is uncertain. However the finding that CHK1 is strongly phosphorylated on Ser-317 in Molt-3 cells suggests that failure to induce p53 phosphorylation is not the result of a gross defect in the ATR-CHK1 pathway.

Nocodazole antagonizes p53 induction and PARP cleavage in HU-treated ML-1 cells. The above results demonstrated that differential of p53 between ML-1 and Molt-3 cells are largely responsible for their different sensitivities to HU. The findings also suggested that ATR activation *per se* was insufficient for p53 induction, and that a second signal is generated in ML-1 cells that potentiates p53 accumulation following HU treatment. One plausible explanation for the robust induction of p53 in response to HU was that stalled DNA replication forks in ML-1 cells are rapidly converted into cytotoxic DSBs, which strongly induce p53 (48). If this hypothesis is correct, then one should be able to detect DSBs prior to caspase activation and accumulation of apoptosis-related strand breaks. To explore this possibility, we examined the ATM/ATR-dependent phosphorylation of histone H2AX. The accumulation of phosphorylated histone H2AX (designated κ-H2AX) at foci of DNA damage provides an indirect measure of DSB formation in mammalian cells (61). In the absence of HU treatment, the nuclei of ML-1 cells demonstrated a weak and diffuse κ-H2AX immunostaining pattern, which was comparable to the pattern seen in untreated Molt-3 cells. Exposure to HU for 1 h induced similar levels of κ-H2AX immunostaining in ML-1 and Molt-3 cells (Figure 4.6.A), suggesting comparable levels of DSBs between the cell lines. However, at 4 h post-HU, approximately 50% of the κ-H2AX-positive ML-1 cells demonstrated an intense κ-H2AX staining pattern that was not observed in similarly treated Molt-3 cells (Figure 4.6.A, denoted by arrows). These cells often exhibited an abnormal nuclear morphology suggestive of

apoptosis. Caspase inhibitors inhibited HU-induced H2AX phosphorylation in immunoblotting experiments (Figure 4.6.B), suggesting that the κ-H2AX^{high} cells were actively undergoing apoptosis. This result is consistent with previous literature showing that apoptosis-dependent DSBs are potent inducers of H2AX phosphorylation (62). However, the finding that ML-1 and Molt-3 cell lines display comparable levels of κ-H2AX at early time points after HU exposure provides indirect evidence that these cell lines initially accumulate comparable levels of DSBs in response to DNA replication stress.

Microtubule inhibitors have been shown to antagonize topoisomerase poison-induced cell death and we wished to determine whether microtubules were important for apoptosis initiated by HU (63). To test this possibility, we treated ML-1 cells with the microtubule inhibitor nocodazole (NOC) 1 h prior to the addition of HU and then measured PARP cleavage 4 h later. HU-induced PARP cleavage was inhibited by NOC pre-exposure, though some cleavage was still observed (Figure 4.6.C). In addition, the reduction in PARP cleavage observed in HU- and NOC-treated cells was accompanied by a clear reduction in the level of p53 induction. At the cellular level, ML-1 cells treated with HU and NOC showed an approximately two-fold reduction in the hypodiploid fraction relative to cells treated with HU alone (Figure 4.6.D). Whereas the S phase population was essentially depleted in the HU-treated cells, ML-1 cells exhibiting S-phase DNA content were still observed following exposure to NOC and HU. Importantly,

NOC pretreatment did not reduce the fraction of ML-1 cells in S phase prior to HU exposure, ruling out the possibility that the protective effects of NOC were attributable to fewer HU-susceptible cells (data not shown). The finding that NOC delays apoptosis implies that mitosis or another microtubule-dependent process contributes to the initiation of apoptosis in ML-1 cells following HU treatment.

4.5. DISCUSSION

In this report we have investigated the mechanism of apoptosis induction by HU in ML-1 myeloid leukemia cells. We have shown that HU induces a remarkably rapid program of apoptosis in this cell line; HU exposures as short as 15-30 min are sufficient to induce cell death in approximately one third of S-phase cells, whereas exposures greater than 1 h effectively depleted the entire S phase population within 4-6 h. The inability of ML-1 cells to survive even relatively short pulses of HU or the DNA polymerase a inhibitor aphidicolin, when combined with the observation that these cells were relatively resistant to IR, implies that ML-1 harbors one or more defects in pathways that mediate resistance to DNA replication stress. We have therefore sought out to map the apoptosis pathways initiated following HU exposure, as well as to uncover potential defects responsible for HU hypersensitivity.

HU-induced a classical caspase-dependent apoptotic cell death in ML-1 cells characterized by cytoplasmic membrane blebbing, nuclear fragmentation, and caspase activation within 4 h. Given the rapidity of this response we were surprised to find that new protein synthesis was required for apoptosis induction. Nevertheless, the requirement for new protein synthesis is compatible with a role for a p53-dependent transcriptional program in the initiation of apoptosis and requirement for p53 in this process was directly established using RNAi (Figure 4.5.A). Although the contribution of p53 to replication inhibitor-induced apoptosis appears to be cell-type dependent, our findings are congruent with earlier work showing that p53 expression is positively correlated with HU sensitivity (6-7). Other studies have shown that p53 promotes apoptosis by trans-activating promoters of pro-apoptosis regulators including the BH3 domain containing proteins BAX, PUMA, and NOXA (55). Whereas the levels of BAX were constitutively high in ML-1 cells, PUMA was induced following HU treatment, suggesting that this p53 target gene contributes to apoptosis induction (Figure 4.4.C and data not shown). However, because 10 Gy of IR also strongly induced p53 in ML-1 cells, but elicited a lower level of cell death, p53-independent pathways must also contribute to apoptosis induction in this cell line.

The differential induction of p53 in ML-1 and Molt-3 cells appears to underlie their distinct sensitivities to DNA replication inhibitors and understanding the basis for this difference should illuminate the mechanism of HU-induced apoptosis. We

showed that the HU-induced accumulation of p53 required ATR and correlated with p53 phosphorylation on Ser-20, which is most likely carried out by the HU-inducible, ATR effector kinase, CHK1. Paradoxically, even though ATR is generally viewed as a determinant of cellular resistance to DNA replication stress, our results imply that ATR functions in a pro-apoptosis capacity following HU exposure—at least in the context of the acute response to this drug in ML-1 cells. Transfection of ATR siRNA did not suppress HU-induced PARP cleavage; however the efficacy of the electroporation-based ATR knock-down was relatively poor in ML-1 cells (Figure 4.8.) and residual p53 induction, either ATR-dependent or ATR-independent, was likely responsible for the observed cell death. Notably, a pro-apoptosis function of ATR was recently established in studies of HIV Vpr protein-induced apoptosis (64-65), suggesting that ATR is a cell type- and stimulus-dependent regulator of apoptosis in mammalian cells.

The ATR-CHK1 pathway was activated within minutes of HU exposure in both ML-1 and Molt-3 cells, however, the induction of p53, as well the phosphorylation of p53 on Ser-20, was much more robust in the ML-1 cells. The failure to induce p53 in HU-treated Molt-3 cells, despite robust CHK1 phosphorylation, implies that activation of the ATR-CHK1 pathway is insufficient for p53 induction and that a second signal generated in ML-1 cells promotes full activation of p53. Because prolonged exposures to HU induces DSBs in cultured mammalian cells (12-13), we initially hypothesized that ML-1 cells accumulate abnormally high levels of

cytotoxic DSBs in response to HU. However, ML-1 and Molt-3 cells exhibited qualitatively similar profiles of κ-H2AX staining when exposed to HU for 1 h or less, suggesting comparable levels of DSBs prior to the induction of apoptosis (Figure 4.6.A). Furthermore, HU-treated ML-1 cells did not exhibit hyperactivation of ATM, which is another sensitive marker for DSB formation (66). The available evidence therefore suggests that increased DSBs are not responsible for p53 accumulation or the inductive phase of apoptosis in ML-1 cells after brief exposures to HU. Although the source of the putative second signal for p53 induction is presently unclear, the finding that NOC partially suppressed p53 induction and PARP cleavage suggests a role for microtubules. A potential explanation for the protective effect of NOC is that mitotic events contribute to apoptosis induction. However, the CDK1-dependent phosphorylation of histone H3 on Ser-10 was downregulated in HU-treated ML-1 cells, suggesting that this aspect of the S-M checkpoint is intact (S. Kumar and R. Tibbetts, unpublished data). It is possible that ML-1 cells initiate lethal mitotic events independent of CDK1 activation or that the protective effect of NOC is unrelated to its effects on the mitotic spindle.

A recent study described reduced or undetectable expression of CHK1 in a subset of aggressive leukemias (46), and we showed here that ML-1 cells express low levels of ATR and CHK1. The significance of the reduced levels of these factors to the HU sensitivity of this cell line is uncertain; ML-1 cells are

refractory to stable transfection with ATR and CHK1 expression vectors and, for now, the link between reduced ATR and CHK1 expression and HU sensitivity is purely correlative. Nevertheless, given that CHK1 is haploinsufficient in mice (41), the reduced levels of CHK1 and its upstream kinase in ML-1 cells might be predicted to confer an HU sensitive phenotype. Although reduced, the levels of ATR in ML-1 cells are apparently sufficient to support p53 induction and subsequent apoptosis. Future experiments will be required to test whether ectopic expression of ATR or CHK1 can confer HU resistance to ML-1 cells, or if HU sensitivity in these cells is the result of additional defects in replication stress-response pathways.

4.6. REFERENCES

1. Kennedy BJ. The evolution of hydroxyurea therapy in chronic myelogenous leukemia. Seminar Oncol 1992; 19:21-26.

2. Elledge SJ, Zhou Z, Allen JB. Ribonucleotide reductase: regulation, regulation, regulation. Trends Biochem Sci 1992; 17:119-123.

3. Longley DB, Harkin DP, Johnston PG. 5-fluorouracil: mechanisms of action and clinical strategies. Nat Rev Cancer 2003; 3:330-8.

3. Plunkett W, Huang P, Searcy CE, Gandhi V. Gemcitabine: preclinical pharmacology and mechanisms of action. Seminar Oncol 1996; 23:3-15.

5. Sampath D, Rao VA, Plunkett W. Mechanisms of apoptosis induction by nucleoside analogs. Oncogene 2003; 22:9063-9074.

6. Palacios C, Gutierrez dA, Silva A, Collins MK. The role of p53 in death of IL-3-dependent cells in response to cytotoxic drugs. Oncogene 2000; 19:3556-3559.

7. Huyghe P, Dassonneville L, Fenaux P, Bailly C. Hydroxyurea-induced apoptosis in an EBV-immortalized lymphoblastoid cell line. Oncology Res 2005; 14:235-245.

8. Wu GS, el Deiry WS. Apoptotic death of tumor cells correlates with chemosensitivity, independent of p53 or bcl-2. Clin Cancer Res 1996; 2:623-633.

9. Kumari A, Schultz N, Helleday T. p53 protects from replication-associated DNA double-strand breaks in mammalian cells. Oncogene 2004; 23:2324-2329.

10. Gottifredi V, Shieh SY, Taya Y, Prives C. From the Cover: p53 accumulates but is functionally impaired when DNA synthesis is blocked. Proc Natl Acad Sci 2001; 98:1036-1041.

11. Nayak BK, Das GM. Stabilization of p53 and transactivation of its target genes in response to replication blockade. Oncogene 2002; 21:7226-9.

12. Saintigny Y, Delacote F, Vares G, Petitot F, Lambert S, Averbeck D, Lopez BS. Characterization of homologous recombination induced by replication inhibition in mammalian cells. EMBO J 2001; 20:3861-3870.

13. Lundin C, Erixon K, Arnaudeau C, Schultz N, Jenssen D, Meuth M, Helleday T. Different roles for nonhomologous end joining and homologous recombination following replication arrest in mammalian cells. Mol Cell Biol 2002; 22:5869-5878.

14. Ishii Y, Bender MA. Effects of inhibitors of DNA synthesis on spontaneous and ultraviolet light-induced sister-chromatid exchanges in Chinese hamster cells. Mutation Res 1980; 79:19-32.

15. Cox MM. Recombinational DNA repair of damaged replication forks in Escherichia coli: Questions. Ann Rev Genet; 2001; 35:53-82.

16. Sonoda E, Sasaki MS, Buerstedde JM, Bezzubova O, Shinohara A, Ogawa H, Takata M, Yamaguchi-Iwai Y, Takeda S. Rad51-deficient vertebrate cells accumulate chromosomal breaks prior to cell death. EMBO J 1998; 17:598-608.

17. Davies SL, North PS, Dart A, Lakin ND, Hickson ID. Phosphorylation of the Bloom's Syndrome Helicase and Its Role in Recovery from S-Phase Arrest. Mol Cell Biol 2004; 24:1279-1291.

18. Shiloh Y. ATM and related protein kinases: safeguarding genome integrity. Nat Rev Cancer 2003; 3:155-168.

19. Cliby WA, Roberts CJ, Cimprich KA, Stringer CM, Lamb JR, Schreiber SL, Friend SH. Overexpression of a kinase-inactive ATR protein causes sensitivity to DNA-damaging agents and defects in cell cycle checkpoints. EMBO J 1998; 17:159-169.

20. Cortez D, Guntuku S, Qin J, Elledge SJ. ATR and ATRIP: partners in checkpoint signaling. Science 2001; 294:1713-1716.

21. Brown EJ, Baltimore D. ATR disruption leads to chromosomal fragmentation and early embryonic lethality. Genes Dev 2000; 14:397-402.

22. de Klein A, Muijtjens M, van Os R, Verhoeven Y, Smit B, Carr AM, Lehmann AR, Hoeijmakers JHJ. Targeted disruption of the cell-cycle checkpoint gene ATR leads to early embryonic lethality in mice. Current Biol 2000; 10:479 - 482.

23. Casper AM, Nghiem P, Arlt MF, Glover TW. ATR regulates fragile site stability. Cell 2002; 111:779-789.

24. Brown EJ, Baltimore D. Essential and dispensable roles of ATR in cell cycle arrest and genome maintenance. Genes and Development 2003; 17:615-628.

25. Shechter D, Costanzo V, Gautier J. ATR and ATM regulate the timing of DNA replication origin firing. Nat Cell Biol 2004; 6:648-655.

26. Cliby WA, Lewis KA, Lilly KK, Kaufmann SH. S phase and G2 arrests induced by topoisomerase I poisons are dependent on ATR kinase function. J Biol Chem 2002; 277:1599-1606

27. Heffernan TP, Simpson DA, Frank AR, Heinloth AN, Paules RS, Cordeiro-Stone M, Kaufmann WK. An ATR- and Chk1-dependent S checkpoint inhibits replicon initiation following UVC-induced DNA damage. Mol Cell Biol 2002; 22:8552-8561.

28. Guo ZJ, Kumagai A, Wang SX, Dunphy WG. Requirement for Atr in phosphorylation of Chk1 and cell cycle regulation in response to DNA replication blocks and UV-damaged DNA in Xenopus egg extracts. Genes Dev 2000; 14:2745 -2756.

29. Nghiem P, Park PK, Kim Y, Vaziri C, Schreiber SL. ATR inhibition selectively sensitizes G1 checkpoint-deficient cells to lethal premature chromatin condensation. Proc Natl Acad Sci USA 2001; 98:9092-9097.

30. Liu Q, Guntuku S, Cui XS, Matsuoka S, Cortez D, Tamai K, Luo G, Carattini-Rivera S, DeMayo F, Bradley A, Donehower LA, Elledge SJ. Chk1 is an essential kinase that is regulated by Atr and required for the G(2)/M DNA damage checkpoint. Genes Dev 2000; 14:1448-1459.

31. Zhao H, Piwnica-Worms H. ATR-mediated checkpoint pathways regulate phosphorylation and activation of human Chk1. Mol Cell Biol 2001; 21:4129-4139.

32. Gatei M, Sloper K, Sorensen C, Syljuasen R, Falck J, Hobson K, Savage K, Lukas J, Zhou BB, Bartek J, Khanna KK. Ataxia-telangiectasia-mutated (ATM) and NBS1-dependent phosphorylation of Chk1 on Ser-317 in response to ionizing radiation. J Biol Chem 2003; 278:14806-14811.

33. Busino L, Chiesa M, Draetta GF, Donzelli M. Cdc25A phosphatase: combinatorial phosphorylation, ubiquitylation and proteolysis. Oncogene 2004; 23:2050-2056.

34. Peng CY, Graves PR, Thoma RS, Wu Z, Shaw AS, Piwnica-Worms H. Mitotic and G2 checkpoint control: regulation of 14-3-3 protein binding by phosphorylation of Cdc25C on serine-216. Science 1997; 277:1501-1505.

35. Sanchez Y, Wong C, Thoma RS, Richman R, Wu Z, Piwnica-Worms H, Elledge SJ. Conservation of the Chk1 checkpoint pathway in mammals: linkage of DNA damage to Cdk regulation through Cdc25. Science 1997; 277:1497-1501.

36. Donzelli M, Draetta GF. Regulating mammalian checkpoints through Cdc25 inactivation. EMBO Rep 2003; 4:671-7.

37. Shieh SY, Ahn J, Tamai K, Taya Y, Prives C. The human homologs of checkpoint kinases Chk1 and Cds1 (Chk2) phosphorylate p53 at multiple DNA damage-inducible sites. Genes Dev 2000; 14:289 -300.

38. Zachos G, Rainey MD, Gillespie DAF. Chk1-Dependent S-M Checkpoint Delay in Vertebrate Cells Is Linked to Maintenance of Viable Replication Structures. Mol Cell Biol 2005; 25:563-574.

39. Takai H, Tominaga K, Motoyama N, Minamishima YA, Nagahama H, Tsukiyama T, Ikeda K, Nakayama K, Nakanishi M, Nakayama K. Aberrant cell cycle checkpoint function and early embryonic death in Chk1(-/-) mice. Genes Dev 2000; 14:1439-1447.

40. Kumagai A, Guo Z, Emami KH, Wang SX, Dunphy WG. The Xenopus Chk1 Protein Kinase Mediates a Caffeine-sensitive Pathway of Checkpoint Control in Cell-free Extracts. J Cell Biol 1998; 142:1559-1569.

41. Lam MH, Liu Q, Elledge SJ, Rosen JM. Chk1 is haploinsufficient for multiple functions critical to tumor suppression. Cancer Cell 2004; 6:45-59.

42. Feijoo C, Hall-Jackson C, Wu R, Jenkins D, Leitch J, Gilbert DM, Smythe C. Activation of mammalian Chk1 during DNA replication arrest: a role for Chk1 in the intra-S phase checkpoint monitoring replication origin firing. J Cell Biol 2001 154:913-23.

43. Xiao Z, Xue J, Sowin TJ, Rosenberg SH, Zhang H. A novel mechanism of checkpoint abrogation conferred by Chk1 downregulation. Oncogene 2004; 24:1403-1411.

44. Cho SH, Toouli CD, Fujii GH, Crain C, Parry D. Chk1 is essential for tumor cell viability following activation of the replication checkpoint. Cell Cycle 2005; 4:131-139.

45. Sorensen CS, Hansen LT, Dziegielewski J, Syljuasen RG, Lundin C, Bartek J, Helleday T. The cell-cycle checkpoint kinase Chk1 is required for mammalian homologous recombination repair. Nat Cell Biol 2005; 7:195-201.

45. Tort F, Hernandez S, Bea S, Camacho E, Fernandez V, Esteller M, Fraga MF, Burek C, Rosenwald A, Hernandez L, Campo E. Checkpoint kinase 1 (CHK1) protein and mRNA expression is downregulated in aggressive variants of human lymphoid neoplasms. Leukemia 2004; 19:112-117.

47 Ohyashiki K, Ohyashiki JH, Sandberg AA. Cytogenetic characterization of putative human myeloblastic leukemia cell lines (ML-1, -2, and -3): origin of the cells. Cancer Res 1986; 46:3642-3647.

48. Nelson WG, Kastan MB. DNA strand breaks: the DNA template alterations that trigger p53-dependent DNA damage response pathways. Mol Cell Biol 1994; 14:1815-1823.

49.. Sampath D, Shi Z, Plunkett W. Inhibition of Cyclin-Dependent Kinase 2 by the Chk1-Cdc25A Pathway during the S-Phase Checkpoint Activated by Fludarabine: Dysregulation by 7-Hydroxystaurosporine. Mol Pharmacol 2002; 62:680-688.

50. Tibbetts RS, Brumbaugh KM, Williams JM, Sarkaria JN, Cliby WA, Shieh SY, Taya Y, Prives C, Abraham RT. A role for ATR in the DNA damage-induced phosphorylation of p53. Genes Dev 1999; 13:152-157.

51. Dodson GE, Shi Y, Tibbetts RS. DNA Replication Defects, Spontaneous DNA Damage, and ATM-dependent Checkpoint Activation in Replication Protein A-deficient Cells. J Biol Chem 2004; 279:34010-34014.

52. Sampath D, Plunkett W. The Role of c-jun Kinase in the Apoptotic Response to Nucleoside Analogue-induced DNA Damage. Cancer Res 2000; 60:6408-6415.

53. Kastan MB, Onyekwere O, Sidransky D, Vogelstein B, Craig RW. Participation of p53 protein in the cellular response to DNA damage. Cancer Res 1991; 51:6304-6311.

54. Kaufmann SH, Desnoyers S, Ottaviano Y, Davidson NE, Poirier GG. Specific proteolytic cleavage of poly(ADP-ribose) polymerase: an early marker of chemotherapy-induced apoptosis. Cancer Research 1993; 53:3976-3985.

55. Vousden KH, Lu X. Live or let die: the cell's response to p53. Nat Rev Cancer 2002; 2:594-604.

56. Shieh SY, Ikeda M, Taya Y, Prives C. DNA damage-induced phospho rylation of p53 alleviates inhibition by MDM2. Cell 1997; 91:325-334.

57. Chehab NH, Malikzay A, Stavridi ES, Halazonetis TD. Phosphorylation of Ser-20 mediates stabilization of human p53 in response to DNA damage. Proc Natl Acad Sci 1999; 96:13777-13782.
58. Lakin ND, Hann BC, Jackson SP. The ataxia-telangiectasia related protein ATR mediates DNA-dependent phosphorylation of p53. Oncogene 1999; 18:3989-3995.

59. Hammond EM, Denko NC, Dorie MJ, Abraham RT, Giaccia AJ. Hypoxia Links ATR and p53 through Replication Arrest. Mol Cell Biol 2002; 22:1834-1843.

60. Chehab NH, Malikzay A, Appel M, Halazonetis TD. Chk2/hCds1 functions as a DNA damage checkpoint in G(1) by stabilizing p53. Genes Dev 2000 14:278 -288.

61. Rogakou EP, Boon C, Redon C, Bonner WM. Megabase chromatin domains involved in DNA double-strand breaks in vivo. J Cell Biol 1999; 146:905-916.

62. Rogakou EP, Nieves-Neira W, Boon C, Pommier Y, Bonner WM. Initiation of DNA fragmentation during apoptosis induces phosphorylation of H2AX histone at serine 139. J Biol Chem 2000; 275:9390 -9395.

63. Akimitsu N, Kamura K, Tone S, Sakaguchi A, Kikuchi A, Hamamoto H, Sekimizu K. Induction of apoptosis by depletion of DNA topoisomerase II[alpha] in mammalian cells. Biochem Biophys Res Comm 2003; 30:301-307.

64. Andersen JL, Zimmerman ES, DeHart JL, Murala S, Ardon O, Blackett J, Chen J, Planelles V. ATR and GADD45[alpha] mediate HIV-1 Vpr-induced apoptosis. Cell Death Diff 2005; 12:326-334.

65. Stewart SA, Poon B, Jowett JBM, Xie Y, Chen ISY. Lentiviral delivery of HIV-1 Vpr protein induces apoptosis in transformed cells. Proc Natl Acad Sci 1999; 96:12039-12043

66. Bakkenist CJ, Kastan MB. DNA damage activates ATM through intermolecular autophosphorylation and dimer dissociation. Nature 2003; 421:499-506.

4.7. Figure legends

Figure 4.1. ML-1 myeloid leukemia cells are hypersensitive to HU. (**A,B**) ML-1 cells were either left untreated or treated with 3 mM HU for the indicated times. (**A**) The cells were stained with annexin V-FITC and PI and analyzed by flow cytometry. The percentages of annexin-positive cells are displayed in each panel. (**B**) The cells were fixed in ethanol, stained with PI, and analyzed by flow cytometry to measure DNA content. The percentage of cells exhibiting a sub-2N DNA content is shown in each panel. (**C**) Apoptotic morphology of HU-treated ML-1 cells. ML-1 cells were allowed to adhere for an hour to poly-lysine coated glass bottom dishes. Subsequently, cells were either left untreated or treated with 3 mM HU for 4 h and then stained with Hoecsht 33342 to visualize cell nuclei. Cells displaying an apoptotic, budded morphology are denoted by arrows.

FIGURE 4.1.

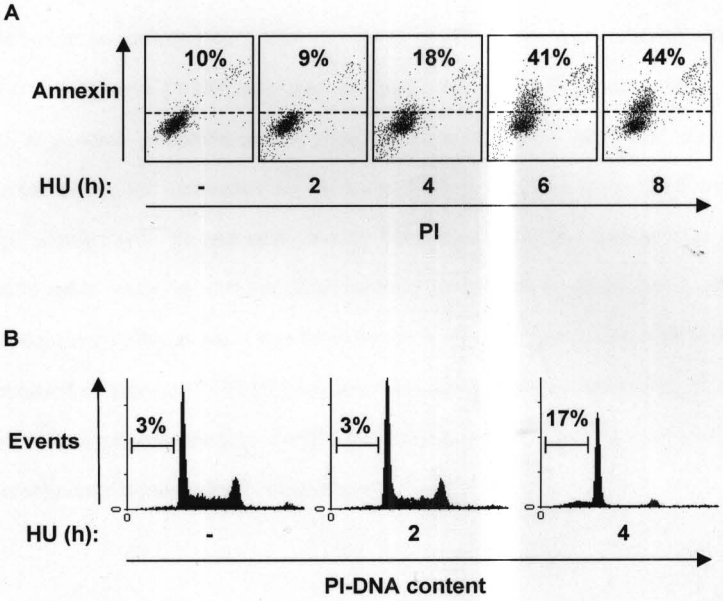
A
Annexin
10%
9%
18%
41%
44%
HU (h):
-
2
4
6
8
PI
B
Events
3%
3%
17%
HU (h):
-
2
4
PI-DNA content
C
Untreated
HU treated

Figure 4.2. Differential sensitivities of ML-1 and Molt-3 cells to HU and IR. (**A**) Exponentially growing K562, Jurkat, Molt-3, and ML-1 cells were either left untreated or exposed to 3 mM HU for 6 h. The cells were stained with annexin V-FITC and PI and analyzed by flow cytometry. The percentage of annexin V-positive, apoptotic cells is shown in each panel. (**B**) ML-1 and Molt-3 cells were either left untreated or HU-treated for 4 h. Cells were fixed with ethanol, stained with PI and analyzed by flow cytometry. The percentage of apoptotic cells showing sub-2N DNA content is shown in each panel. (**C**) Differential sensitivities of ML-1 and Molt-3 cells to IR. ML-1 or Molt-3 cells were left untreated or exposed to IR (10 Gy) and harvested at the indicated times. The cells were stained with annexin V-FITC and PI and analyzed by flow cytometry. Cell viability data is presented in each panel.

FIGURE 4.2.

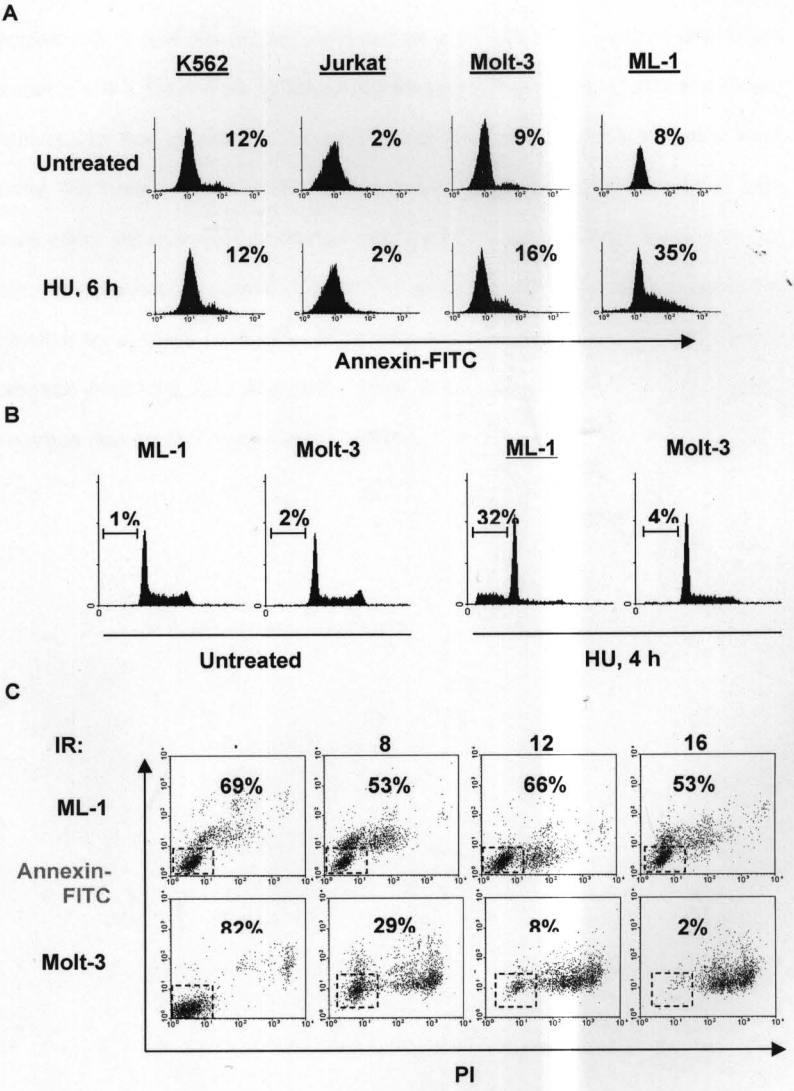
A
K562
Jurkat
Molt-3
ML-1
Untreated
12%
2%
9%
8%
HU, 6 h
12%
2%
16%
35%
Annexin-FITC
B
ML-1
Molt-3
ML-1
Molt-3
1%
2%
32%
4%
Untreated
HU, 4 h
C
IR:
8
12
16
ML-1
69%
53%
66%
53%
Annexin-FITC
Molt-3
82%
29%
8%
2%
PI

Figure 4.3. Characterization of HU-induced apoptosis. (**A**) Induction of apoptosis by pulse exposures to HU. ML-1 cells were either left untreated or treated with 3 mM HU for the indicated times. Cells were washed and left to recover for 4 h. Cells were subsequently stained with annexin V-FITC and PI and analyzed by flow cytometry. The percentage of apoptotic cells is shown in each panel. (**B**) Time course of PARP cleavage following exposure to HU. ML-1 cells were either left untreated or treated with 3 mM HU for the indicated times. Cell extracts were immunoblotted with a-PARP antibody. (**C**) HU-induced apoptosis is inhibited by caspase inhibitors. ML-1 cells were preincubated with a mixture of caspase inhibitors *(see Methods)* prior to exposure to HU for 4 h. PARP cleavage was measured by immunoblotting.

FIGURE 4.3.

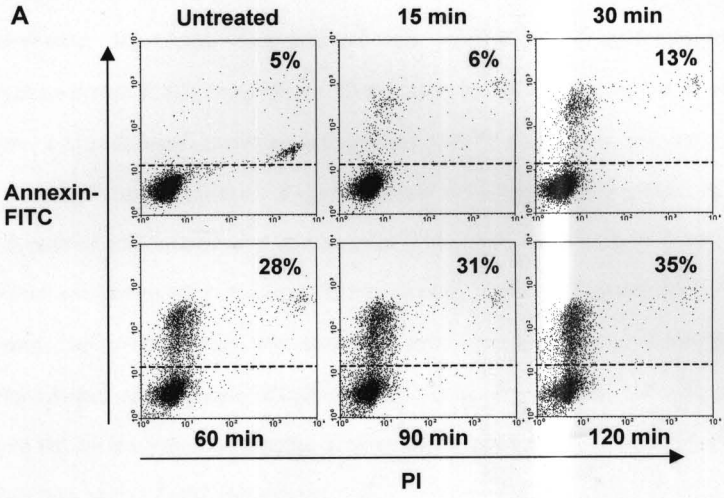
A
Untreated
15 min
30 min
5%
6%
13%
Annexin-FITC
28%
31%
35%
60 min
90 min
120 min
PI
B
HU
time (h): - 0.5 1 2 4
PARP
Full-length
Cleaved
C
Z-VAD-fmk
HU: - + - +
PARP

Figure 4.4. Differential p53 induction correlates with the HU sensitivities of ML-1 and Molt-3 cells. (**A**) HU-induced apoptosis required new protein synthesis. ML-1 cells were preincubated with the protein synthesis inhibitor cycloheximide (CHX, 5 μg/ml) for 30 min prior to the addition of HU or vehicle. After 4 h, cells were co-stained with annexin V-FITC and PI and analyzed by flow cytometry. The percentages of apoptotic cells are shown in each panel. (**B**) Time courses of p53 induction in response to HU or IR. ML-1 or Molt-3 cells were either left untreated or exposed to HU (3 mM) or IR (10 Gy) for the indicated times. Cell extracts were immunoblotted with κ-p53 or κ-tubulin antibodies. (**C**) HU-induced accumulation of PUMA in ML-1 cells. ML-1 cells were exposed to 3 mM HU for the indicated lengths of time. Cell extracts were immunoblotted with κ-PUMA and κ-PARP antibodies.

FIGURE 4.4.

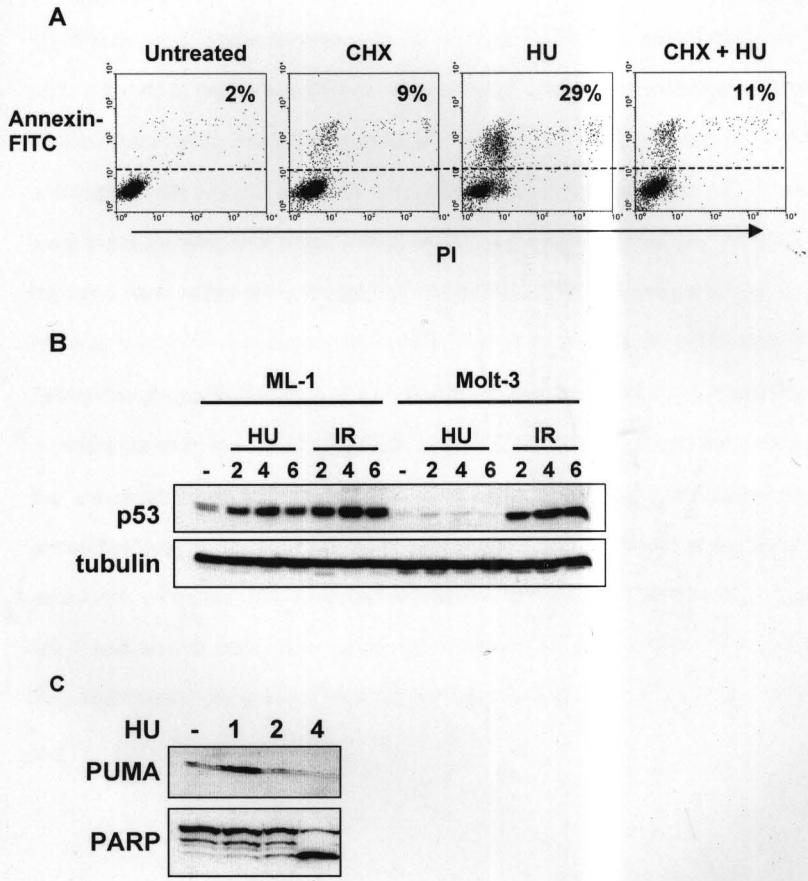
A
Untreated
CHX
HU
CHX + HU
2%
9%
29%
11%
Annexin-FITC
PI
B
ML-1
Molt-3
HU
IR
HU
IR
- 2 4 6 2 4 6 - 2 4 6 2 4 6
p53
tubulin
C
HU - 1 2 4
PUMA
PARP

Figure 4.5. ATR-dependent accumulation of p53 is required for optimal HU-induced apoptosis. (**A**) p53 is required for HU-induced PARP cleavage. ML-1 cells were electroporated with either control siRNA or siRNA targeted to p53. After 48 h, the cells were treated with HU or vehicle for the indicated times. Cell extracts were then immunoblotted with κ-p53, κ-PARP and κ-RPA32 antibodies. (**B**) HU-induced p53 accumulation is ATR-dependent. ML-1 cells were electroporated with either control siRNA or ATR-specific siRNA. After 48 h, the cells were either left untreated or HU-treated for the indicated times. Cell extracts were immunoblotted with κ-ATR, κ-p53 and κ-tubulin antibodies. (**C**) Differential phosphorylation of p53 on Ser-20 in response to HU. ML-1 and Molt-3 cells were exposed to HU (3 mM) or zeocin (Zeo, 0.5 μg/ml) and harvested at the indicated times after treatment. Cell extracts were immunoblotted with antibodies specific for p53, Ser-20-phosphorylated p53 (p53-pS20), and RPA32 as a loading control. **(D)** Reduced expression of ATR and CHK1 in ML-1 cells. ML-1 and Molt-3 cells were either left untreated or treated with HU for the indicated times. Cell extracts were immunoblotted with κ-CHK1-pS317, κ-CHK1, κ-ATR, and κ-tubulin antibodies.

FIGURE 4.5.

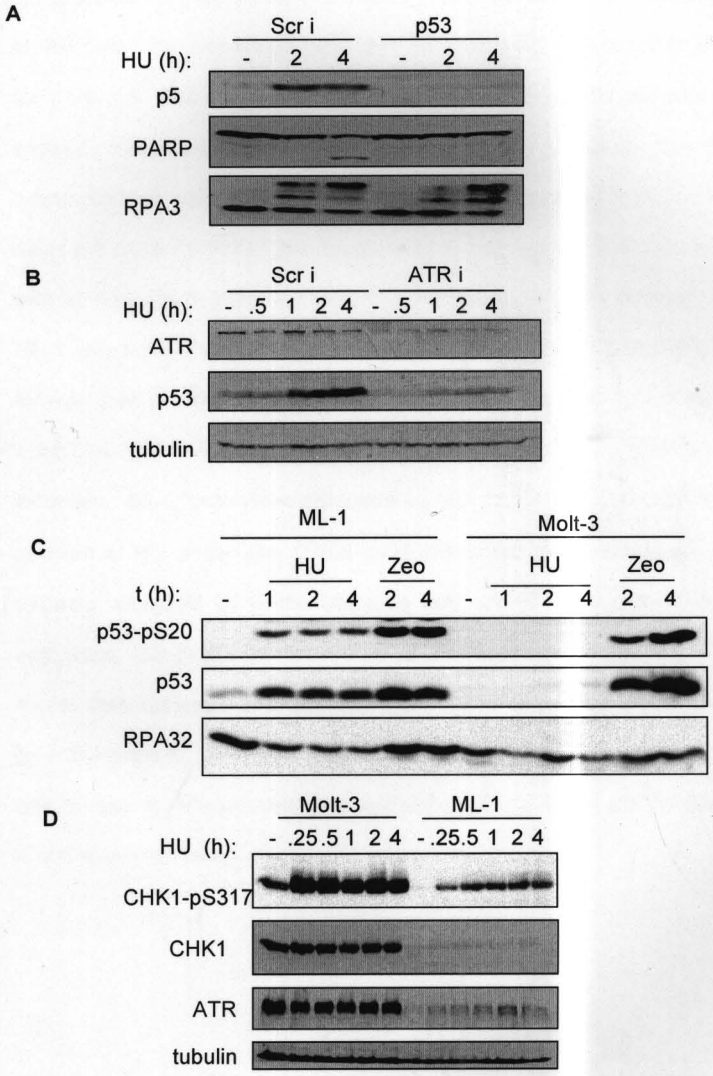
A
Scr i
p53
HU (h):
- 2 4 - 2 4
p5
PARP
RPA3
B
Scr i
ATR i
HU (h):
- .5 1 2 4 - .5 1 2 4
ATR
p53
tubulin
C
ML-1
Molt-3
HU
Zeo
HU
Zeo
t (h):
- 1 2 4 2 4 - 1 2 4 2 4
p53-pS20
p53
RPA32
D
Molt-3
ML-1
HU (h):
- .25 .5 1 2 4 - .25 .5 1 2 4
CHK1-pS317
CHK1
ATR
tubulin

Figure 4.6. Suppression of HU-induced apoptosis by nocodazole. (**A**)[166] Comparison of histone H2AX phosphorylation between HU treated ML-1 and Molt-3 cells. ML-1 or Molt-3 cells were left untreated or exposed to HU (3 mM) for 1 h or 4 h. The cells were cytospun onto glass slides, stained with κ-κ-H2AX antibody followed by a FITC-conjugated secondary antibody. The cells were counterstained with DAPI to visualize nuclei. Digital images of representative fields are shown (100X). The locations of two apoptotic ML-1 cells are marked with arrows. (**B**) Suppression of H2AX phosphorylation by caspase inhibitors. ML-1 cells were pretreated with a caspase inhibitor cocktail prior to HU exposure for 4 h. Cell extracts were then prepared and analyzed by immunoblotting with κ-κ-H2AX. (**C**) Nocodazole (NOC) inhibits HU-induced PARP cleavage and p53 induction. ML-1 cells were preincubated with NOC (0.5 μg/ml) for 1 h prior to addition of HU or vehicle. Cells were harvested at the indicated times and extracts analyzed by immunoblotting with κ-PARP, κ-p53, and κ-tubulin antibodies. (**D**) NOC inhibits hypodiploid DNA formation in response to HU. ML-1 cells were cultured with or without NOC 1 h prior to addition of HU or vehicle for an additional 4 h. Cells were fixed with ethanol, stained with PI and analyzed by flow cytometry. The percentage of apoptotic cells exhibiting sub-2N DNA content is shown in each panel.

FIGURE 4.6.

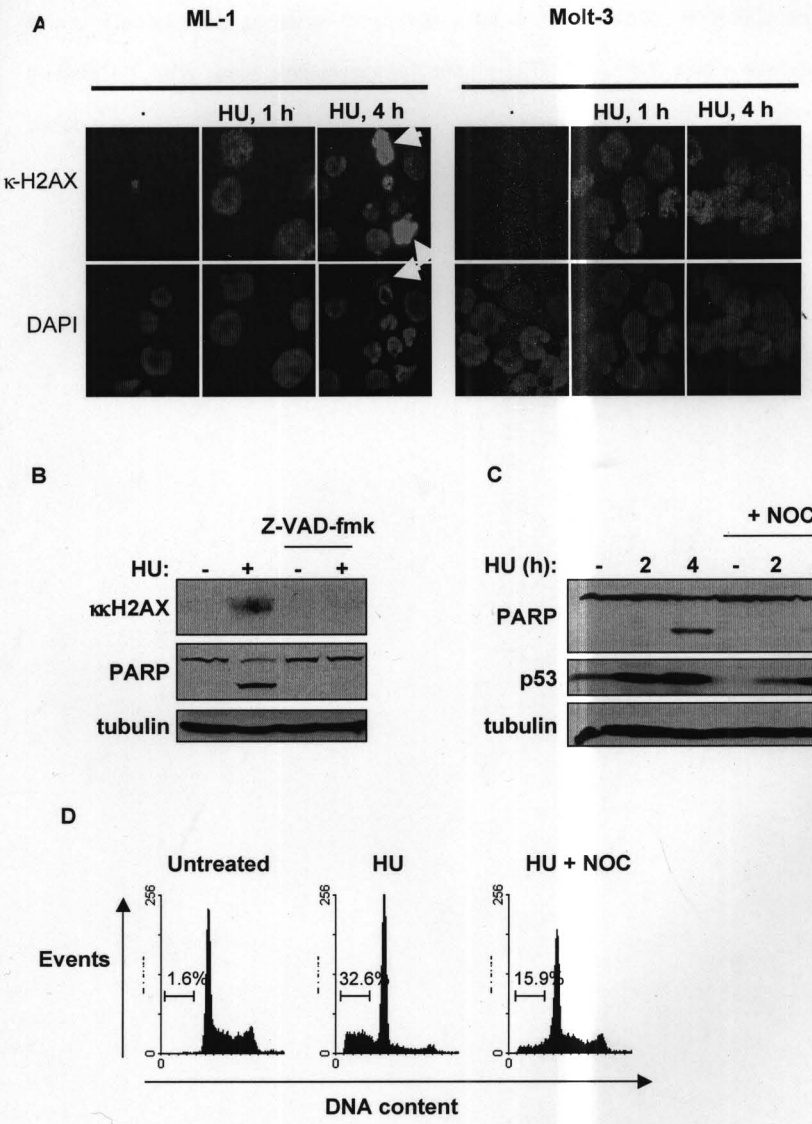
A
ML-1
Molt-3
-
HU, 1 h
HU, 4 h
-
HU, 1 h
HU, 4 h
κ-H2AX
DAPI
B
Z-VAD-fmk
HU: - + - +
κH2AX
PARP
tubulin
C
+ NOC
HU (h): - 2 4 - 2 4
PARP
p53
tubulin
D
Untreated
HU
HU + NOC
Events
256
0
1.6%
32.6%
15.9%
DNA content

Figure 4.7. Comparison of ATR and CHK1 levels between leukemia cell lines[168]. Cell extracts prepared from Molt-3, ML-1, HL60, K562, HPB-ALL and Karpus 45 cells were immunoblotted with κ-ATR, κ-CHK1, and κ-tubulin antibodies.

Figure 4.7.

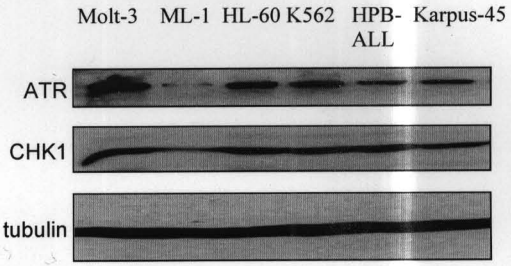

Figure 4.8. Effects of ATR siRNA transfection on HU-induced p53[170] expression and PARP cleavage in ML-1 cells. ML-1 cells were electroporated with scrambled (Scr i) or ATR (ATR i)-specific siRNAs and then exposed to HU or mock treated 48 h later. p53 induction and PARP cleavage were assessed using the appropriate antibodies.

Figure 4.8.

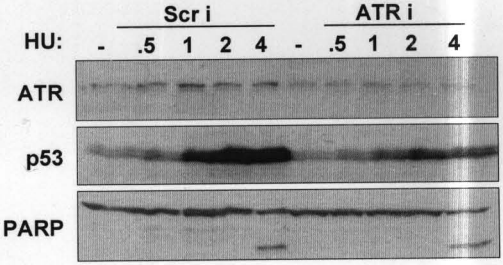

CHAPTER 5

Discussion and Future Directions

In our first publication we provided evidence for a stress-induced signaling[173] link between ATM and CREB (1). Our findings indicated that ATM regulated CREB via a non-canonical, Ser-133 phosphorylation-independent mechanism involving the direct phosphorylation of three closely-spaced amino acids (Thr-100, Ser-111, and Ser-121) located within the KID of CREB. Our data also suggested that the ATM sites are modified in a processive manner, i.e., phosphorylation of Ser-111 was required for the DNA damage-inducible phosphorylation of Ser-121 (1). Given that the ATM phosphorylation sites are clustered, and that phosphorylation of at least two of the sites (Ser-111 and Ser-121) is induced by a wide variety of stress stimuli, we collectively refer to Thr-100/Ser-111/Ser-121 as a stress-inducible domain (SID) (1,2). What is the biochemical function of SID domain ? One possibility is that the phosphorylation of SID alters the phosphorylation of the transcriptionally active Ser-133 site on CREB. Our preliminary findings did not support this idea, as both overexpression of $CREB^{WT}$ or a non-phosphorylatable $CREB^{3A}$ mutant showed no effect on Ser-133 phosphorylation as detected by immunoblotting. A second possibility is that phosphorylation of SID modifies the affinity of CREB for DNA. Our previous unpublished findings using electrophoretic mobility shift assays did not reveal a role for the ATM phosphorylation sites in altering DNA binding activity of CREB. However these experiments utilized a synthetic 3XCRE as probe, which may not recapitulate CREB binding to chromatin. It is fully possible that the impact of the ATM phosphorylation sites on CREB DNA binding may not be adequately modeled by generic CRE probes, but instead may be gene and promoter

context-dependent. To fully address this hypothesis, promoter microarrays[174] need to be performed to determine if CREB occupancy is altered after exposure to genotoxic stimuli and if this effect is dependent on the ATM phosphorylation sites. A third possibility is that ATM-mediated phosphorylation of CREB recruits co-factors that modify CREB-dependent gene expression. This hypothesis can be addressed in two ways. It is likely that phosphorylation of CREB recruits proteins that are known to bind CREB including PP1 or HDAC1 (3). Both of these proteins fit a model for a repressive function for the ATM-CREB pathway as PP1 is known to be a negative regulator of CREB function (4), and HDAC1 is a transcriptional repressor. These possibilities can be easily addressed by using standard immunoprecipitation techniques. To cast a wider net, we can also perform comparative yeast two-hybrid analysis using a phosphomimetic CREB3E mutant containing glutamic acid substitutions in all three ATM phosphorylation sites and non-phosphorylatable CREB3A mutant. Previous studies in our lab show that a CREB3D mutant with aspartic acid substitutions at the ATM phosphorylation sites does not function as a phosphomimetic mutant. Such a case has been previously reported in the literature. Whereas a CREBSer-133E mutant functions as a phosphomimetic, a CREBSer-133D mutant does not (5). The possibility that the phosphorylation of the ATM sites on CREB may cause a structural change in the KID domain cannot be ruled out. This option can be assessed by comparing the crystal structure of unphosphorylated and phosphorylated forms of CREB.

We have previously shown that IR-induced phosphorylation of SID correlated[175] with a decrease in CREB trans-activation potential using a synthetic CRE promoter construct (1). We have also validated these results using promoter constructs of known CREB target genes including CyclinA, Cyclin D and DNA polymerase beta (S.Kumar & R.Tibbetts, unpublished). Our findings revealed that ATM-mediated phosphorylation of CREB decreased CREB transcriptional activity by reducing the interaction of CREB with its transcriptional co-activator, CBP. The decrease in CREB-CBP interaction after exposure to genotoxic stimuli can be a result of at least two possible events. One possibility is that upon phosphorylation of CREB by ATM, CREB interacts with other transcriptional co-factors such as ACT or FHL, which are known transcriptional co-activators that bind and mediate CREB-dependent gene expression in a Ser-133 phosphorylation-independent manner. Another possibility is that, in response to stress stimuli, other transcription factors compete with CREB for binding CBP. For instance, p53 levels are upregulated in cells after IR treatment and it is possible that p53 and CREB compete for the same pool of CBP. Whatever the biochemical function of these ATM target sites on CREB, it is clear from our initial findings that there exists an ATM-CREB pathway linking genome surveillance apparatus to a regulator of gene expression and cellular survival. As an obvious next step, we sought to determine the gene(s) that may be regulated by this pathway.

A comprehensive scan of the human genome revealed 10,447 full CRE sites[176] and more than 700,000 half-CRE sites, all of which mapped to promoter regions. Global analysis of CREB occupancy (using ChIP on Chip) showed that greater than 3000 promoters were bound by CREB, which accounts for approximately 20% of all protein coding genes (6). In HEK293T cells, CREB occupied the promoters of approximately 5000 genes, of which interestingly, only 2% were cAMP-responsive (6). So far, more than 100 well characterized CREB target genes have been reported. Our gene chip array analysis revealed that the expression of over 7000 genes was altered (at least two fold) by decreasing CREB levels in cells using RNA interference (S.Kumar & R.Tibbetts, unpublished). Although CREB function stretches far and wide in regulation of genes involved in neurotransmission, metabolism, cell cycle, DNA repair, growth factors, transcription factors, cell survival and immune regulation, the mechanisms by which CREB drives signal-specific expression of its target genes is not fully understood.

Given that CREB can be activated in response to a variety of stimuli and mediate the expression of several genes, it is not unreasonable to suggest that signal-specific post-translational modifications on CREB impart some specificity for CREB-dependent gene expression. These modifications may modulate the affinity of CREB for a target promoter, or provide a docking site for binding specific factors that can impact gene expression. In addition, it is also conceivable that, modulating CREB-CBP binding affinity may alter the repertoire

of CREB target genes expressed. Recently, Montminy group proposed that[177] CREB-dependent gene expression may be regulated at the level of the target gene promoter (7). For instance, they showed that the PKA pathway preferentially activated CRE-containing promoters which possess a TATA box (7).

We initially proposed that CREB target genes with documented functions in regulation of cell cycle, oxidative stress responses and apoptosis - cellular processes in which ATM has well established roles - may be logical candidate genes for regulation by the ATM-CREB pathway. For instance, promoters of anti-oxidant defense enzymes including MnSOD and HO-1, which are known to be up-regulated in brains of ATM-/- mice (8), contained binding sites for CREB. This prompted us to examine if these genes were regulated by IR treatment in an ATM and CREB-dependent manner. Our preliminary findings revealed no role for these enzymes, at least in cellular context we examined. The observation that anti-apoptotic gene MCL-1 (Myeloid Cell Leukemia – 1) was regulated in response to genotoxic stress stimuli (9), prompted us to examine if it was a potential target for the ATM-CREB pathway. Though the expression of this gene was entirely CREB-dependent, its regulation in response to stress stimuli did not require ATM (data not shown). Interestingly, several members of the DNA damage response pathways including ATM had binding sites for CREB in their promoters. However, our preliminary findings suggested no role for ATM-CREB pathway in the regulation of those genes. The list of genes that we examined

included cell cycle regulators (PCNA, Cyclin D, Cyclin A, MCM3, RPA),[178] Checkpoint Kinases (CHK1,CHK2), Cell survival regulators (BCL-2, MCL-1), Antioxidant defense enzymes (HO-1, MnSOD), and transcriptional regulators (c-fos and ICER). In summary, our logical albeit biased approach failed to reveal a CREB target gene that may be regulated by the ATM-CREB pathway.

To cast a broader net, we utilized gene chip array analysis to examine ATM and CREB-dependent changes in global gene expression in response to IR treatment. We obtained several targets that showed differential expression upon IR treatment in an ATM and CREB-dependent manner (Table 3.1.). One of these, HOXB13 has been validated by Real Time PCR analysis (Figure 3.2.). In the absence of any DNA damage, reducing the levels of CREB in cells using RNA interference resulted in a slight decrease (~30%) in HOXB13 expression (Figure 3.2.), suggesting that other transcription factors are required for basal expression of HOXB13. However, it is clear from our data that the IR-induced repression of HOXB13 is mediated through ATM and CREB, suggesting that HOXB13 may be one downstream target regulated by the ATM-CREB pathway (Figure 3.2.). The mechanism by which ATM-CREB pathway may contribute to HOXB13 repression is presently unclear. One possibility is that ATM-mediated phosphorylation of CREB recruits a co-repressor, which inhibits the expression of HOXB13. For instance, ATM target sites on CREB may recruit a Histone Deacetylase (HDAC) that can cause transcriptional repression. It has been previously shown that CREB can bind to class I HDAC and this interaction

required at least one of the two glutamine rich regions (Q1 or Q2) in CREB[179] (3). Another possibility is that upon phosphorylation of ATM sites in CREB, the affinity of CREB to bind the HOXB13 promoter may be decreased. Careful examination of HOXB13 promoter region reveals a single half-CRE binding site for CREB. CREB has been shown to occupy half-CRE sites with lower affinity. Our previous unpublished findings using electrophoretic mobility shift assays did not reveal a role for the ATM phosphorylation sites in altering DNA binding activity of CREB. However these experiments utilized a synthetic 3XCRE as probe, which may not recapitulate CREB binding to chromatin. It is fully possible that the impact of the ATM phosphorylation sites on CREB DNA binding may not be adequately modeled by generic CRE probes, but instead may be gene and promoter context-dependent. In the future, chromatin immunoprecipitation assays will be performed to determine if CREB directly binds to the HOXB13 promoter and if this binding is altered by IR treatment.

The magnitude of the effect of HOXB13 repression upon exposure to stress stimuli varies in different cell lines. Whereas in HEK293T cells, IR induces repression if HOXB13 by 2-fold (Figure 3.2.), in CEMT cells we observe greater than a 100-fold repression (Figure 3.3.). The IR-induced decrease in HOXB13 occurs at very low doses of IR and within 1 hour of treatment (Figure 3.3.). HOXB13 contains a very long 3' untranslated region that harbors several motifs that may decrease its RNA stability. The magnitude of HOXB13 repression may also be one way to explain differential sensitivities of these cells to IR. HEK293T

are more resistant to killing by IR than CEM T cells. It is also important to monitor changes in protein levels of HOXB13 in response to genotoxic stimuli. We are unable to address this at the present time due to the unavailability of a commercially available HOXB13 antibody.

Previous studies have shown that overexpression of HOXB13 in cancer cells results in decreased cell proliferation and increased apoptosis (10). Conversely, a small interfering RNA targeted specifically towards HOXB13 in cells resulted in increased proliferation and decreased apoptosis in prostrate cancer cells (10). Given that CREB3A has shown increased transcriptional activity and increased binding to CBP (1), we hypothesize that $CREB^{3A}$ transfected cells may display increased HOXB13 expression. We predict that our inability to generate $CREB^{3A}$ stable cell lines may be a result of decreased cell proliferation and increased apoptosis resulting from increased HOXB13 expression. HOXB13 target genes that mediate its functions in cell growth and survival are currently unknown. Further studies to identify HOXB13 target genes using microarray analysis will help understand HOXB13-mediated gene expression. In addition, a promoter microarray to determine the occupancy of HOXB13 on its target genes can be performed. HOXB13 is implicated as a tumor suppressor in various cancers including renal, prostrate and skin (11). Considering that HOXB13 contains a consensus ATM phosphorylation site, it will be interesting to determine if HOXB13 can also be directly regulated by ATM.

In response to genotoxic stimuli, ATM activates transcription factors that are[181] implicated in both pro-apoptotic and anti-apoptotic endpoints. For example, in response to DNA damage, ATM causes p53 accumulation and activation of pro-apoptotic p53 target genes (12). Parallely, ATM also upregulates pro-survival pathways through direct activation of transcription factor NFκB (13). Our findings demonstrate yet another putative anti-apoptotic pathway initiated by ATM through the direct phopshorylation of CREB (1). We propose that the pro-survival functions of the ATM-CREB pathway may be mediated through the repression of HOXB13. Since cells activate both pro- and anti-apoptotic pathways in response to IR, it is reasonable to suggest that the ultimate fate of the DNA-damaged cell will depend on the relative balance of ATM-regulated death and survival pathways.

Finally, given that CREB is a neuron survival factor (14), it is attractive to speculate that ATM-CREB pathway regulates neuron homeostasis and/or apoptosis. It has been previously reported that the cerebellar granule neurons (CGNs) and purkinje cells are most severely affected in A-T (15). As a first step, we examined if ATM-CREB pathway was activated in primary mice CGNs in response to genotoxic stimuli. Consistent with a neuronal function for the ATM-CREB pathway, we found that ATM phosphorylated CREB in neurons exposed to IR in a dose- and time-dependent manner (Figure 2.5. and data not shown) (1). We also showed that IR-induced CREB phosphorylation was ATM-dependent (Figure 2.5.) (1). The effects of the ATM-CREB pathway in neurons

can be more directly addressed by the generation of a gene targeted knock-in[182] mouse with alanine substitutions in ATM phosphorylation sites ($mCREB^{3A}$). *In vitro* CGN cultures of $mCREB^{WT}$ and $mCREB^{3A}$ mice can be compared for their ability to survive after exposure to stress stimuli. Since it has been reported that ATM is required for dendritogenesis (16), we can also compare the ability of the $mCREB^{WT}$ and $mCREB^{3A}$ neurons to generate dendrites in culture. If the ATM-CREB pathway contributes to pro-survival functions in neurons, we would expect that the $mCREB^{3A}$ mouse present with an overt cerebellar phenotype. Therefore, histologic examination of the brains of the $mCREB^{WT}$ and $mCREB^{3A}$ mice should also be performed. ***Our current working hypothesis (Figure 5.1.) is that in response to DNA damage, the ATM-CREB pathway functions in pro-survival capacity by repressing HOXB13 function and that deregulation of the ATM-CREB-HOXB13 pathway may contribute to neuropathogenesis in A-T.***

References :

1. Shi Y, Venkataraman SL, Dodson GE, Mabb AM, LeBlanc S, Tibbetts RS. (2004) Direct regulation of CREB transcriptional activity by ATM in response to genotoxic stress.Proc Natl Acad Sci U S A. 101(16):5898-903.

2. Dodson GE, Tibbetts RS. DNA replication stress-induced phosphorylation of cyclic AMP response element-binding protein mediated by ATM. J Biol Chem. 2006 Jan 20;281(3):1692-7.

3. Canettieri G, Morantte I, Guzman E, Asahara H, Herzig S, Anderson SD, Yates JR 3rd, Montminy M. Attenuation of a phosphorylation-dependent activator by an HDAC-PP1 complex. Nat Struct Biol. 2003 Mar;10(3):175-81.

4. Wadzinski BE, Wheat WH, Jaspers S, Peruski LF Jr, Lickteig RL, Johnson GL, Klemm DJ.(1993) Nuclear protein phosphatase 2A dephosphorylates protein kinase A-phosphorylated CREB and regulates CREB transcriptional stimulation.Mol Cell Biol. 13(5):2822-34.

5. Gonzalez, G. A. & Montminy, M. R. (1989) Cyclic AMP stimulates somatostatin gene transcription by phosphorylation of CREB at serine 133. Cell. 59, 675-680.

6. Zhang X, Odom DT, Koo SH, Conkright MD, Canettieri G, Best J, Chen H, Jenner R, Herbolsheimer E, Jacobsen E, Kadam S, Ecker JR, Emerson B, Hogenesch JB, Unterman T, Young RA, Montminy M. (2005) Genome-wide analysis of cAMP-response element binding protein occupancy, phosphorylation, and target gene activation in human tissues.Proc Natl Acad Sci U S A. 102(12):4459-64.

7. Conkright MD, Canettieri G, Screaton R, Guzman E, Miraglia L, Hogenesch JB, Montminy M. (2003) TORCs: transducers of regulated CREB activity.Mol Cell. 12(2):413-23.

8. Barlow, C., Dennery, P. A., Shigenaga, M. K., Smith, M. A., Morrow, J. D., Roberts, L. J., Wynshaw-Boris, A. & Levine, R. L. (1999) Loss of the ataxia-telangiectasia gene product causes oxidative damage in target organs. Proc.Natl.Acad.Sci. 96, 9915-9919.

9. Nijhawan D, Fang M, Traer E, Zhong Q, Gao W, Du F, Wang X. Elimination of Mcl-1 is required for the initiation of apoptosis following ultraviolet irradiation.Genes Dev. 2003 Jun 15;17(12):1475-86.

10. Jung C, Kim RS, Lee SJ, Wang C, Jeng MH (2004) HOXB13 homeodomain protein suppresses the growth of prostate cancer cells by the negative regulation of T-cell factor 4. Cancer Res. 64(9):3046-51

11. Okuda H, Toyota M, Ishida W, Furihata M, Tsuchiya M, Kamada M, Tokino T, Shuin T (2005) Epigenetic inactivation of the candidate tumor suppressor gene HOXB13 in human renal cell carcinoma. Oncogene. 1-10.

12. Schuler M, Green DR.(2001) Mechanisms of p53-dependent apoptosis. Biochem Soc Trans. 29(Pt 6):684-8. Review.

13. Lee SJ, Dimtchev A, Lavin MF, Dritschilo A, Jung M.(1998) A novel ionizing radiation-induced signaling pathway that activates the transcription factor NF-kappaB.Oncogene. 17(14):1821-6.

14. Lonze, B. E. & Ginty, D. D. (2002) Function and regulation of CREB family transcription factors in the nervous system.Neuron. 35, 605-623.

15. Becker-Catania, S. G. & Gatti, R. A. (2001) Ataxia-telangiectasia. Adv.Exp.Med.Biol. 495, 191-198.

16. Chen P, Peng C, Luff J, Spring K, Watters D, Bottle S, Furuya S, Lavin MF. Oxidative stress is responsible for deficient survival and dendritogenesis in purkinje neurons from ataxia-telangiectasia mutated mutant mice.J Neurosci. 2003 Dec 10;23(36):11453-60.

Figure 5.1. ATM-CREB-HOXB13 pathway may function in pro-survival capacity. In response to genotoxic stimuli, ATM phosphorylates CREB in vivo. ATM-mediated phosphorylation of CREB inhibits CREB transcriptional activity by altering CREB-CBP interaction. One outcome of the ATM-CREB pathway may be the repression of HOXB13 expression. We propose that the deregulation of ATM-CREB-HOXB13 pathway contributes to neuropathogenesis in A-T.

Figure 5.1.

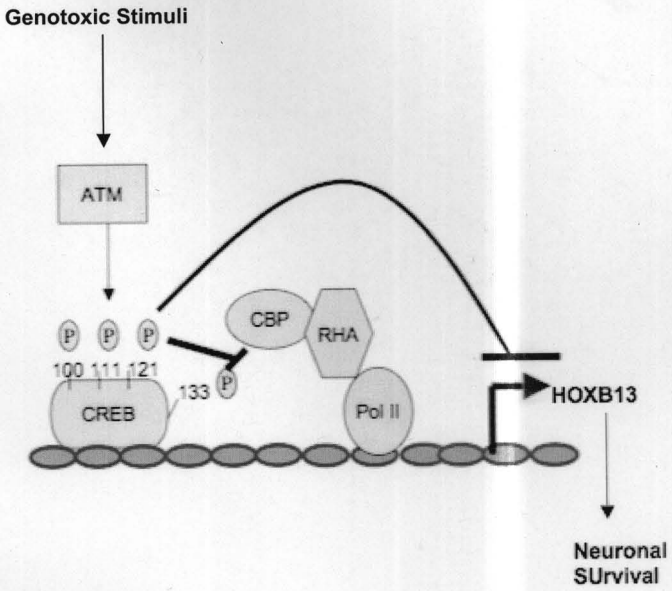
Genotoxic Stimuli
ATM
P
P
P
100 111 121
CREB
133
P
CBP
RHA
Pol II
HOXB13
Neuronal
SUrvival